

NACA RM L56D18

REF ID: A62-63861

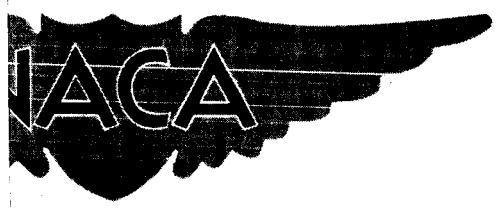
Copy 343  
RM L56D18

GPO PRICE \$ \_\_\_\_\_

OTS PRICE(S) \$ \_\_\_\_\_

Hard copy (HC) 3.00

Microfiche (MF) .75



# RESEARCH MEMORANDUM

1821-X

FULL-SCALE WIND-TUNNEL TESTS OF A 35° SWEEP-WING  
FIGHTER AIRPLANE WITH A SPOILER-SLOT-DEFLECTOR

LATERAL CONTROL SYSTEM

By William I. Scallion

Langley Aeronautical Laboratory  
Langley Field, Va.

DECLASSIFIED - EFFECTIVE 1-25-64  
Authority: Memo Geo. Drobka NASA HQ.  
Code ATSS-A Dtd. 3-12-64 Subj: Change  
in Security Classification Marking.

CAT-02



NATIONAL ADVISORY COMMITTEE  
FOR AERONAUTICS

WASHINGTON

October 26, 1956

CATEGORY



N 5-12716

(THRU)

(CODE)

(CATEGORY)

(ACCESSION NUMBER)

(PAGES)

(NASA CR OR TMX OR AD NUMBER)

FAILITY FORM 66

REF ID: A60118

NATIONAL ADVISORY COMMITTEE FOR AERONAUTICS

RESEARCH MEMORANDUM

FULL-SCALE WIND-TUNNEL TESTS OF A 35° SWEEP-WING  
FIGHTER AIRPLANE WITH A SPOILER-SLOT-DEFLECTOR

LATERAL CONTROL SYSTEM<sup>1</sup>

By William I. Scallion

SUMMARY

An investigation was made in the Langley full-scale tunnel to determine the low-speed aerodynamic characteristics of a 35° swept-wing fighter airplane with a segmented spoiler-slot-deflector lateral control system installed ahead of the conventional ailerons and operated as individual units and as combined segments. The longitudinal characteristics of the airplane and spoiler-slot-deflector effectiveness data were obtained through the complete angle-of-attack range with the ailerons neutral and with the ailerons drooped in conjunction with the normal flaps. Spoiler-deflector hinge-moment data were also obtained for a number of spoiler-deflector combinations. The test Reynolds number was  $5 \times 10^6$  and the Mach number was 0.10.

With the ailerons neutral, better spoiler effectiveness and greater rolling-moment coefficients were obtained with the spoiler-slot-deflector combinations in the mutual-motion arrangement (deflected in unison) than in differential motion (each spanwise segment deflected at a different rate). With the ailerons drooped, the greatest spoiler-slot-deflector effectiveness was obtained when the ailerons maintained a high aerodynamic loading. This was accomplished by modifying the original aileron nose radius and adding shrouds to eliminate the aileron stalled flow which was detrimental to the spoiler performance. For the highly loaded condition, small deflections of the mutual-motion arrangement caused abrupt separation on the aileron, resulting in very high spoiler effectiveness at these small deflections at low angles of attack. An almost linear variation of rolling-moment coefficient with spoiler deflection was obtained, however, with the spoiler-deflector combinations arranged in differential motion.

<sup>1</sup>The information presented herein was previously made available to the U. S. military air services.

DECLASSIFIED - EFFECTIVE 1-15-64  
Authority: Memo Geo. Drobka NASA HQ.  
Code ATSS-A Dtd. 3-12-64 Subj: Change  
in Security Classification Marking

12716

*Author*

## INTRODUCTION

An investigation has been conducted in the Langley full-scale tunnel to evaluate the effectiveness of a spoiler-slot-deflector lateral control system on a  $35^\circ$  swept-wing fighter airplane. This system was selected on the basis of data reported in references 1 to 3, which indicated that adequate control effectiveness and possible reductions in control forces could be obtained by suitably linking the spoiler-deflector segments.

In view of the lack of data on swept wings with flaps directly behind the spoilers, the main emphasis of the investigation was concentrated on the configuration with the conventional ailerons drooped as flaps in conjunction with the inboard flaps. The program also included investigation of the spoiler-deflector characteristics with the conventional ailerons neutral for several spoiler-deflector configurations.

Aerodynamic forces and moments, as well as spoiler-deflector hinge-moment data, were obtained in the angle-of-attack range of  $-1.7^\circ$  to the angle required for maximum lift at zero sideslip. The test Reynolds number was  $5 \times 10^6$  and the Mach number was 0.10.

## COEFFICIENTS AND SYMBOLS

All results are presented in standard form of coefficients and moments. The wing moments are referred to the stability axes originating at the projection of the quarter-point of the mean aerodynamic chord on the plane of symmetry (fig. 1). The coefficients and symbols are defined as follows:

$C_L$  lift coefficient,  $\frac{F_L}{qS}$

$C_D'$  drag coefficient,  $\frac{F_D'}{qS}$

$C_Y$  side-force coefficient,  $\frac{F_Y}{qS}$

$C_m$  pitching-moment coefficient,  $\frac{M_Y}{qS\bar{c}}$

$C_n$  yawing-moment coefficient,  $\frac{M_Z}{qS\bar{r}}$

$C_L$	rolling-moment coefficient, $\frac{M_X}{qSb}$
$C_h$	hinge-moment coefficient, $\frac{H}{2Qq}$
$F_L$	lift, lb
$F_D'$	drag, lb
$F_Y$	side force, lb
$M_Y$	pitching moment, ft-lb
$M_Z$	yawing moment, ft-lb
$M_X$	rolling moment, ft-lb
$H$	hinge moment (positive for a closing load), ft-lb
$S$	total wing area, sq ft
$Q$	moment of area of control surface about hinge line, ft <sup>3</sup>
$C$	local wing chord, ft
$\bar{c}$	wing mean aerodynamic chord, ft
$b$	wing span, ft
$\beta$	angle of sideslip, deg
$\frac{pb}{2V}$	rolling angular-velocity parameter, radians
$C_{L_p}$	damping-in-roll parameter, $\frac{\partial C_L}{\partial \frac{pb}{2V}}$

CONFIDENTIAL



$\alpha$  angle of attack of fuselage center line, deg  
 $\delta$  control deflection (negative when opening), deg  
 $i_t$  horizontal tail incidence, deg

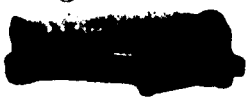
Subscripts:

f flap  
sc center spoiler  
max maximum  
t total

MODEL

The model used in this investigation was a  $35^\circ$  swept-wing fighter airplane modified by an installation of a spoiler-slot-deflector control system ahead of the conventional ailerons on the outboard wing panels. For the test installation, the normal ailerons were inoperative, but could be set at angles of  $0^\circ$ ,  $30^\circ$ , and  $45^\circ$  (by changing support brackets) to represent a flap behind the spoiler-slot-deflector control system. A three-view sketch of the airplane is shown in figure 2 and the airplane geometric characteristics are given in table I. Sketches of the spoiler-slot-deflector arrangement for the ailerons-neutral and the ailerons-deflected conditions are shown in figure 3 and sketches of the spoiler and deflector surfaces are given in figure 4. Photographs of the airplane and control details for the various configurations are given in figure 5.

The spoilers and deflectors of the control system were each composed of spanwise segments (designated inboard, center, and outboard spoilers and deflectors). Each spoiler segment was interconnected to its corresponding deflector segment to provide a ratio of movement of 2 to 1 between spoiler and deflector. Two types of spoiler-deflector operation could be obtained through suitable linkage changes in the system. These arrangements will be designated as mutual- and differential-motion operation in this paper. Mutual-motion operation produced equal deflections in all the spoiler-deflector segments with deflector movement one-half the spoiler deflection (figs. 5(b) and 5(c)). Differential motion produced full deflection in the center spoiler-deflector segment, while the inboard and outboard segments were deflected through reduced ranges. (See fig. 5(d).) Figures 6 and 7 show the rates of deflection of the various spoiler and deflector segments as a function of center spoiler



deflection for differential and mutual motion with the ailerons neutral and the ailerons deflected.

Figure 8 shows the percent wing chord projection of the spoilers and deflectors as a function of control deflection in degrees.

The maximum deflection ranges of the spoilers and deflectors were  $0^\circ$  to  $-70^\circ$  and  $0^\circ$  to  $-35^\circ$ , respectively, for the ailerons-neutral configuration. For the drooped aileron configuration the deflection range of the spoilers was  $-5^\circ$  to  $-45^\circ$  and the deflection range of the deflectors was  $-15^\circ$  to  $-35^\circ$ . When the conventional ailerons were deflected as flaps, the spoilers and deflectors were given initial openings of  $-5^\circ$  and  $-15^\circ$ , respectively, to provide a slot at the nose of the aileron so as to have, in effect, a slotted flap. This initial opening was considered as zero deflection of the spoiler-deflector combinations for the drooped aileron configuration, and the ratio of movement between the spoilers and deflectors was still approximately two to one.

The airplane was mounted for tests on the six-component balance system in the Langley full-scale tunnel. The engine air-intake duct at the nose of the airplane was faired and sealed by a metal fairing as shown in figure 2 for all tests.

The tests included measurement of the static longitudinal and lateral stability and control characteristics of the airplane through the angle-of-attack range from  $-1.7^\circ$  to stall. Spoiler and deflector hinge moments were measured from strain gages mounted on special control actuating rods designed for high sensitivity for the low-speed tunnel tests to replace the normal flight test actuating rods.

Although the test program was primarily devoted to studies of the high-lift configuration, data were also obtained for the normal flight configuration.

The longitudinal tests were made principally to determine the lift effectiveness of the airplane configuration with the conventional ailerons drooped as flaps along with the normal inboard flaps. Various modifications were tried for the purpose of improving the lift effectiveness of the drooped ailerons; these modifications, however, were limited in scope because of the nature of the wing and aileron structure. The modifications that were tried included addition of curved shrouds to the trailing edges of the spoilers to extend the spoiler exit slot over the nose of the aileron in order to aid in turning the flow around the rather small nose radius of the ailerons. (See fig. 3.) Additionally, tests were made in which the aileron nose and upper surface contours were modified (as shown in fig. 3) to increase the nose radius of the  $30^\circ$

drooped ailerons. In order to maintain a reasonable slot gap at the spoiler trailing edges, the original shrouds were bent to maintain a 5/8-inch exit slot for both the 45° and 30° drooped aileron configurations. In the case of the modified 30° ailerons,  $1\frac{1}{4}$  inches of the trailing edges of the original shrouds were cut off to maintain this slot (redesignated as modified shrouds in this case).

Limited stabilizer effectiveness tests were made to obtain trim data for the drooped aileron configurations. Spoiler-slot-deflector effectiveness tests were made for the normal flight configuration (ailerons neutral) and for the most pertinent of the high-lift configurations (ailerons drooped). The spoiler-slot-deflector effectiveness tests were made for both the differential- and mutual-motion configurations in order to provide data for varying degrees of effectiveness. Tests were also made with the inboard and center spoiler-deflector combination and with the center and outboard spoiler-deflector segments tied together, while the remaining segments in each case were closed and sealed so as to indicate the effect of spanwise location on control effectiveness.

Limited data on the effects of the conventional flaps and slats on the control effectiveness of the spoiler-deflectors were obtained for the normal flight configuration.

Spoiler-deflector hinge-moment data were recorded for the aforementioned tests. It should be noted that some of the data contain inaccuracies because of the presence of friction in the hinges and linkages, as would be expected for a system designed for complete boost control and high-speed operation. Attempts were made to reduce the friction to acceptable tolerances and this was accomplished for the drooped aileron configurations. For the neutral aileron configuration the deflectors continued to possess large amounts of friction at small deflections (0° to -10°) as will be noted in the subsequent discussion.

All tests were conducted at a Reynolds number of  $5 \times 10^6$  and a Mach number of 0.10. The force data have been corrected for stream misalignment and tunnel jet-boundary corrections have been applied to the angle of attack, drag coefficient, and pitching-moment coefficient. The drag data have also been corrected for tunnel buoyancy effects. No corrections have been made for support-strut interference effects; however, it is believed that they are small.

## PRESENTATION OF RESULTS

The results of this investigation are presented in the following figures:

	Figures
Longitudinal characteristics . . . . .	9 to 12
Spoiler-deflector characteristics, ailerons neutral . . . . .	13 to 17
Spoiler-deflector characteristics, ailerons drooped . . . . .	18 to 24
Hinge-moment characteristics, ailerons neutral . . . . .	25 to 30
Hinge-moment characteristics, ailerons drooped . . . . .	31 to 35

## RESULTS AND DISCUSSION

## Longitudinal Characteristics

Ailerons neutral.- The basic airplane with ailerons neutral and with flaps and slats retracted (fig. 9) attained a maximum lift coefficient of 1.03 at  $\alpha = 17.1^\circ$  and was longitudinally stable through stall. For the normal landing configuration, flaps  $45^\circ$  and leading-edge slats extended, lift coefficients were generally increased by approximately 0.4 throughout the lift range, giving a  $C_{L_{\max}}$  of 1.41 at an  $\alpha$  of about  $17^\circ$  for this configuration. Longitudinal stability was not appreciably affected by flap deflection although a small positive moment shift was indicated throughout the lift range.

Ailerons drooped  $45^\circ$ .- Drooping the ailerons  $45^\circ$  with the basic spoiler set to provide a slotted flap effect produced a lift increment of approximately 0.21 at zero angle of attack but an increment of only 0.08 at  $C_{L_{\max}}$  (fig. 10). Tuft observations showed the ailerons to be stalled throughout the  $\alpha$  range with little or no slotted flap effect provided by the initial spoiler and deflector openings of  $-5^\circ$  and  $-15^\circ$ , respectively (termed the basic spoiler-slot arrangement for the drooped aileron configurations). This was expected because of the restricted slot entrance (the initial  $-15^\circ$  opening of the deflector was insufficient because of the shape of the deflector) and the sharp aileron nose radius condition existing for this design (fig. 3).

A curved shroud in the form of an extension to the spoiler was installed. This addition produced some improvement in the flow on the ailerons and increased the increment in  $C_L$  to approximately 0.30 at  $\alpha = 0^\circ$  and 0.13 at  $C_{L_{\max}}$  (fig. 10). It was determined by tuft

observations that the flow over the ailerons was still far from optimum. In view of the importance of the aileron loading on the ultimate effectiveness of the spoilers, several attempts were made to improve the aileron loading by eliminating a nonuniform slot exit gap formed by the original shroud, and by providing additional droop to the outboard deflector segments to eliminate the restricted slot entrance condition outboard. These and other modifications had little or no effect on the lift values, and the maximum lift coefficient obtained with this configuration was 1.54 at an angle of attack of  $16^\circ$ .

Ailerons drooped  $30^\circ$ .- Initial tests with the basic spoiler configuration and with the ailerons drooped  $30^\circ$  showed that undesirable flow conditions existed over the ailerons, and lift-coefficient increments of only 0.16 and 0.06 at zero angle of attack and  $C_{L_{\max}}$  conditions, respectively, were obtained (fig. 11(a)). As was done for the  $45^\circ$  aileron configuration, an attempt was made to achieve unseparated flow on the  $30^\circ$  drooped ailerons. The modified spoiler shrouds (fig. 3) were added and the upper surfaces of the ailerons were refaired to give as much relief as possible to the very sharp nose radius of the ailerons. This could be done only by external fairing on this design due to the limitations imposed by the spoiler-aileron geometries and the nature of construction of the ailerons. For this test configuration the results showed a lift-coefficient increase of 0.24 at  $\alpha = 0^\circ$  and an increase of 0.11 at  $C_{L_{\max}}$  (fig. 11(a)). Flow observations indicated that the modified ailerons were essentially unstalled through most of the angle-of-attack range. The  $C_{L_{\max}}$  value (untrimmed) for this configuration was 1.52 as compared to 1.54 for the best  $45^\circ$  aileron configuration. The sharp loss in drooped aileron effectiveness at high lift coefficients is felt to be a result of inadequate leading-edge flow control coupled with a mild flow deterioration on the aileron with increasing  $\alpha$ , but further modifications were not attempted as the test program was set up with emphasis on spoiler control configuration evaluation.

Trim characteristics.- Drooping the ailerons resulted in a large negative shift in pitching-moment coefficient (figs. 10 and 11(a)); however, the stabilizer effectiveness plot (fig. 11(c)) shows that the stabilizer had adequate power to trim out these moments.

The maximum trim lift coefficient of the basic airplane with flaps deflected, slats extended, and with ailerons neutral was 1.30 (fig. 12). The gains in maximum trim lift coefficients produced by drooping the ailerons and adding shrouds to the spoiler trailing edges were 0.12 and 0.10 for the  $45^\circ$  ailerons and the  $30^\circ$  modified ailerons, respectively.

### Spoiler-Deflector Characteristics

Ailerons neutral.- Although the emphasis of this investigation was placed on the spoiler-deflector characteristics on the high lift configuration (ailerons drooped, flaps and slats deflected), the data on the normal flight configuration (ailerons neutral) were obtained to give a more complete coverage of the spoiler-slot-deflector system.

The spoiler-deflector combinations with differential motion on the normal flight configuration were relatively ineffective at low spoiler deflections as can be seen by the rather flat portions of the  $C_l$  against  $\delta_{sc}$  curves in figure 13(a). An increase in the slope of the curves occurred at higher spoiler deflections. The insensitivity of the controls at low deflections would not be considered a desirable flight characteristic, inasmuch as large deflections would be required before any appreciable response could be obtained from the controls. The maximum rolling-moment coefficients produced by this control configuration increased somewhat with angle of attack (from 0.019 at  $\alpha = -0.5^\circ$  to 0.026 at  $\alpha = 13.5^\circ$ ) as might be expected inasmuch as the loading on the wing would increase with  $\alpha$  until stall.

The spoiler-deflector combinations with mutual motion were more effective than the differential-motion combinations at low deflections (fig. 14), and the maximum rolling-moment coefficients produced by this configuration were somewhat greater, and, for these reasons would be considered a better flight control arrangement than the differential-motion configuration. The increase in effectiveness of the mutual-motion configuration was primarily due to the increase in spoiler-deflector projected area per degree deflection.

In order to obtain the characteristics of a plain flap-type spoiler with a deflector, and to determine the effectiveness of the clearance gap between the leading edge of the spoiler and the wing, the spoiler leading-edge clearance gaps were sealed on the mutual-motion configuration. The maximum rolling-moment coefficients obtained (fig. 15) were slightly higher than those of the comparable mutual-motion configuration of figure 14(a), but the elimination of the gap resulted in reduced effectiveness at small deflections in the intermediate  $\alpha$  range. Different spanwise locations of the mutual-motion spoiler-deflector configuration (fig. 16) indicated that there was only a small difference in the effectiveness of an inboard spoiler-deflector combination (combination of inboard and center spoilers and deflectors) and an outboard spoiler-deflector combination (combination of center and outboard spoilers and deflectors). The effectiveness and maximum rolling-moment coefficients produced in either case were of approximately the same magnitude as the differential-motion configuration of figure 13.

The characteristics of the spoiler-slot-deflector combinations for the differential-motion configuration on a high-lift version of the neutral aileron configuration (with the normal flaps and slats deflected) are given in figure 17. The effectiveness of the spoiler-deflector combinations was increased by deflection of the flaps and slats as can be seen by comparison with figure 13. This increase in effectiveness can be attributed to an increase in loading on the wing produced by deflection of the flaps and the delay of separation on the outboard portion of the wing by the extended slats.

Ailerons drooped  $45^\circ$ . The basic spoiler-slot-deflector configuration in differential motion with the ailerons drooped  $45^\circ$  and the flaps and slats deflected (fig. 18) produced maximum rolling-moment coefficients varying from 0.019 to 0.017 throughout the angle-of-attack range. The effectiveness and control characteristics of the spoiler-slot-deflector configuration in this case were about the same as those of the comparable configuration with ailerons neutral for the same deflection range. (See fig. 17.) An increase in effectiveness might have been expected from the spoiler-deflectors with the aileron drooped as a slotted flap (as is the case for the unswept wing with a slotted flap of ref. 4). As previously mentioned, however, the drooped aileron was stalled at all angles of attack, resulting in a spoiler control system of low effectiveness. The addition of the curved shrouds (intended to provide a direct guide of air flow around the sharp corner of the flap leading edge) produced some improvement in the flow over the aileron and the spoiler characteristics were slightly improved (fig. 19(a)). It should also be noted that a portion of this increase in effectiveness must be attributed to the shrouds' increasing the projected height of the spoilers.

Ailerons drooped  $30^\circ$ . Flow observations on the ailerons with the droop reduced to  $30^\circ$  indicated that although the original shrouds improved the flow characteristics over the ailerons to some extent, rough spanwise flow still existed, which indicated that the ailerons did not develop as high an aerodynamic loading as might be obtained.

As one of the main objectives of the program was to determine spoiler characteristics for a condition representing a spoiler ahead of a highly loaded flap, further modifications to the aileron upper surface contour and shrouds (previously discussed under lift characteristics) were carried out prior to further control evaluation. Control data for the best aileron shroud combination obtained are presented in figures 20 through 23.

For this flap condition ( $\delta_a = 30^\circ$ ,  $\delta_f = 45^\circ$ , slats extended), the spoiler-deflector control effectiveness for the differential motion configuration (fig. 20(a)) was increased, especially in the low-deflection range as would be anticipated. The rolling-moment-coefficient curves


were nearly linear over the deflection range and maximum  $C_l$  values for full deflection varied from 0.036 at low angles of attack to 0.022 for an angle of attack of  $20.2^\circ$ . A brief check of the effects of slat retraction on the control characteristics (fig. 21) showed only an expected loss in effectiveness at high angles of attack resulting from wing leading-edge stall over the outboard wing sections.

Data obtained with the spoiler-deflector combinations operating in mutual motion (fig. 22(a)) for this modified aileron configuration show an average increase of approximately 0.01 in maximum rolling-moment coefficients at full deflection over those obtained for the differential-motion arrangement (fig. 20(a)). For the mutual-motion arrangement, however, the simultaneous opening of all spoiler segments along the drooped aileron caused abrupt separation on the aileron, and, in the first few degrees of spoiler deflection, a very high effectiveness was produced.

From comparison of these results for the  $30^\circ$  modified aileron with a high aerodynamic loading with those from the  $45^\circ$  aileron configuration which should be considered essentially as a plain or split flap, it appears that the gearing system employed for a spoiler located ahead of a trailing-edge flap will depend on the nature of the flap loading. The spoiler located ahead of a plain or split flap with separated flow existing will require larger deflections to obtain its effectiveness than the same spoiler ahead of a flap developing an appreciable upper surface loading which may have large effectiveness at very small deflections (resulting from an abrupt separation on the flap).

Comparison with conventional ailerons.— A limited comparison of the rolling-effectiveness parameter  $\frac{pb}{2V}$  of the spoiler-slot-deflector arrangement considered to be optimum for the drooped aileron configuration (fig. 22) with that of a similar airplane (from ref. 5) with conventional ailerons is shown in figure 24. The values of  $\frac{pb}{2V}$  for the model were calculated by using a  $C_{lp}$  value of -0.35 per radian as obtained from unpublished data for the clean airplane. At a trim lift coefficient of 0.72 the rolling effectiveness of the spoiler system was about the same as that of the conventional ailerons. At maximum lift the spoiler system had somewhat greater rolling effectiveness than the conventional ailerons.

Effect on yawing moment.— The yawing-moment coefficients produced by deflecting the spoiler-deflector combinations on the right wing with the ailerons neutral were generally positive and the maximum value of  $C_n$  ranged from 0.015 to 0.0095 with the spoiler-deflector combinations in the mutual-motion arrangement (fig. 15).





The yawing-moment coefficients produced by deflecting the spoiler-deflector combinations with the ailerons drooped were also positive, with the exception of the differential-motion arrangement at an angle of attack of  $12.5^\circ$  on the modified  $30^\circ$  aileron configuration (fig. 21). The values of  $C_n$  were small for all the drooped aileron configurations.

Effect on pitching-moment coefficient.- The pitching-moment increments produced by deflection of the spoiler-deflector combinations were positive in all cases.

The maximum effect on  $C_m$  was produced by the mutual-motion spoiler-deflector combinations with the  $30^\circ$  aileron upper surface contour modified. Maximum deflection of the spoiler-deflector combinations in this case produced increments in  $C_m$  ranging from 0.085 to 0.04 through the lift range (fig. 22(b)).


### Hinge-Moment Characteristics

As previously stated the hinge-moment data for the ailerons-neutral configuration was subject to inaccuracies due to the presence of friction in the deflector hinges. The friction band was calibrated and applied to the data and it is believed that the general trends of the hinge-moment characteristics are fairly represented.

Ailerons neutral.- With the ailerons neutral, the spoiler-deflector hinge-moment coefficients were generally opposite in sign and magnitude. (See figs. 25 to 28.) Under these conditions some reduction in the control forces might be expected by allowing the deflector hinge moments to oppose the spoiler hinge moments through a linkage. As an example, the spoiler and deflector hinge-moment coefficients of figure 26 (mutual-motion configuration) were combined into total resultant hinge-moment coefficients in figure 30. As can be seen from this figure, there was a considerable reduction in the total hinge-moment coefficients throughout most of the angle-of-attack range.

Ailerons deflected.- With the ailerons deflected, the spoiler hinge-moment coefficients generally varied positively with spoiler deflection; however, the hinge-moment coefficient values were negative (opening load) through a large portion of the spoiler deflection range. (See figs. 31 to 34.)

The deflector hinge-moment coefficients were much smaller than the spoiler hinge-moment coefficients and as they varied erratically with deflection no definite trend of variation could be established. It is apparent from the character and magnitude of the deflector hinge moments that they would not contribute as much toward balancing the spoiler hinge moments as in the case of the neutral aileron configuration.



This is illustrated in figure 35 where the spoiler and deflector hinge-moment coefficients of figure 34 ( $30^\circ$  modified aileron, mutual-motion configuration) are combined into total resultant hinge-moment coefficients.

#### SUMMARY OF RESULTS

The results of a low-speed investigation of the aerodynamic characteristics of a  $35^\circ$  swept-wing fighter airplane with a spoiler-slot-deflector lateral control system installed ahead of the conventional ailerons and with the ailerons neutral and drooped as flaps are summarized as follows:

1. The original ailerons when drooped  $45^\circ$  and  $30^\circ$  with the spoiler-deflector combinations set at initial openings were essentially stalled. The characteristics of the  $30^\circ$  ailerons modified to increase the nose radius and with the shrouds installed more nearly approached those of a highly loaded flap and the lift increment was essentially the same as that of the original  $45^\circ$  ailerons with shrouds.
2. The increments in maximum trim lift coefficient (over that of the basic airplane high-lift configuration) produced by drooping the aileron were 0.12 for the  $45^\circ$  ailerons and 0.10 for the modified ailerons deflected  $30^\circ$ .
3. The spoiler-slot-deflector combinations produced greater effectiveness and higher maximum rolling-moment coefficients for the mutual-motion case (controls deflected in unison) than for differential motion (each spanwise segment deflected at a different rate) with the normal flight configuration (ailerons neutral).
4. With the ailerons drooped, the greatest spoiler-slot-deflector effectiveness was obtained when the ailerons maintained a high aerodynamic loading. This loading was accomplished by modifying the original aileron nose radius and adding shrouds to the spoiler trailing edges to eliminate the aileron stalled flow which was detrimental to spoiler performance.
5. The spoiler-slot-deflector combinations arranged in differential motion on the best high-lift configuration investigated ( $30^\circ$  drooped ailerons with modified nose radius) produced an almost linear variation in rolling-moment coefficient with deflection. The mutual-motion arrangement on this configuration produced larger maximum rolling-moment coefficients; however, abrupt separation on the aileron at small spoiler deflections produced high effectiveness at low angles of attack.
6. The calculated rolling effectiveness of the spoiler-slot-deflector combinations (differential motion case) on the high-lift

configuration (with the ailerons modified and drooped  $30^{\circ}$ ) was about the same as conventional ailerons on a similar airplane at a lift coefficient of 0.72 and was somewhat greater at maximum lift.

7. The yawing moments produced by deflection of the spoiler-deflector combinations were generally positive and positive pitching-moment increments were produced in all cases.

8. The deflector hinge moments considerably reduced the control hinge moments when linked together with the spoilers on the normal flight configuration, but they contributed little toward reducing the spoiler hinge moments on the drooped aileron high-lift configurations.

Langley Aeronautical Laboratory,  
National Advisory Committee for Aeronautics,  
Langley Field, Va., April 9, 1956.

#### REFERENCES

1. Vogler, Raymond D.: Wind-Tunnel Investigation at High Subsonic Speeds of a Spoiler-Slot-Deflector Combination on an NACA 65A006 Wing With Quarter-Chord Line Swept Back  $32.6^{\circ}$ . NACA RM L53D17, 1953.
2. Watson, James M.: Low-Speed Lateral-Control Investigation of a Flap-Type Spoiler Aileron With and Without a Deflector and Slot on a 6-Percent-Thick, Tapered,  $45^{\circ}$  Sweptback Wing of Aspect Ratio 4. NACA RM L52G10, 1952.
3. Lowry, John G.: Data on Spoiler-Type Ailerons. NACA RM L53I24a, 1953.
4. Wenzinger, Carl J., and Rogallo, Francis M.: Wind-Tunnel Investigation of Spoiler, Deflector, and Slot Lateral-Control Devices on Wings With Full-Span Split and Slotted Flaps. NACA Rep. 706, 1941.
5. Magruder, William M., and Everest, Frank K., Jr.: Phase IV Flight Test of the North American F-86E Airplane USAF No. 50-582. Memo. Rep. No. FTD 51-19, Air Res. and Dev. Command, U. S. Air Force, Aug. 1952.

TABLE I.- GEOMETRIC CHARACTERISTICS

## Wing:

Area, sq ft . . . . .	287.9
Span, ft . . . . .	37.12
Aspect ratio . . . . .	4.785
Taper ratio . . . . .	0.5131
Sweepback of 0.25-chord line, deg . . . . .	35.23
Dihedral, deg . . . . .	3
Root airfoil section (normal to 0.25-chord line) . . .	NACA 0012-64 (modified)
Tip airfoil section (normal to 0.25-chord line) . . .	NACA 0011-64 (modified)

## Horizontal tail:

Area, sq ft . . . . .	47.18
Span, ft . . . . .	15.08
Aspect ratio . . . . .	4.82
Taper ratio . . . . .	0.447
Sweepback of 0.25-chord line, deg . . . . .	35
Ratio of tail area to wing area . . . . .	0.1639

## Vertical tail:

Area, sq ft . . . . .	35.09
Span, ft . . . . .	7.40
Aspect ratio . . . . .	1.724
Taper ratio . . . . .	0.365
Sweepback of 0.25-chord line, deg . . . . .	35
Ratio of vertical tail area to wing area . . . . .	0.1104

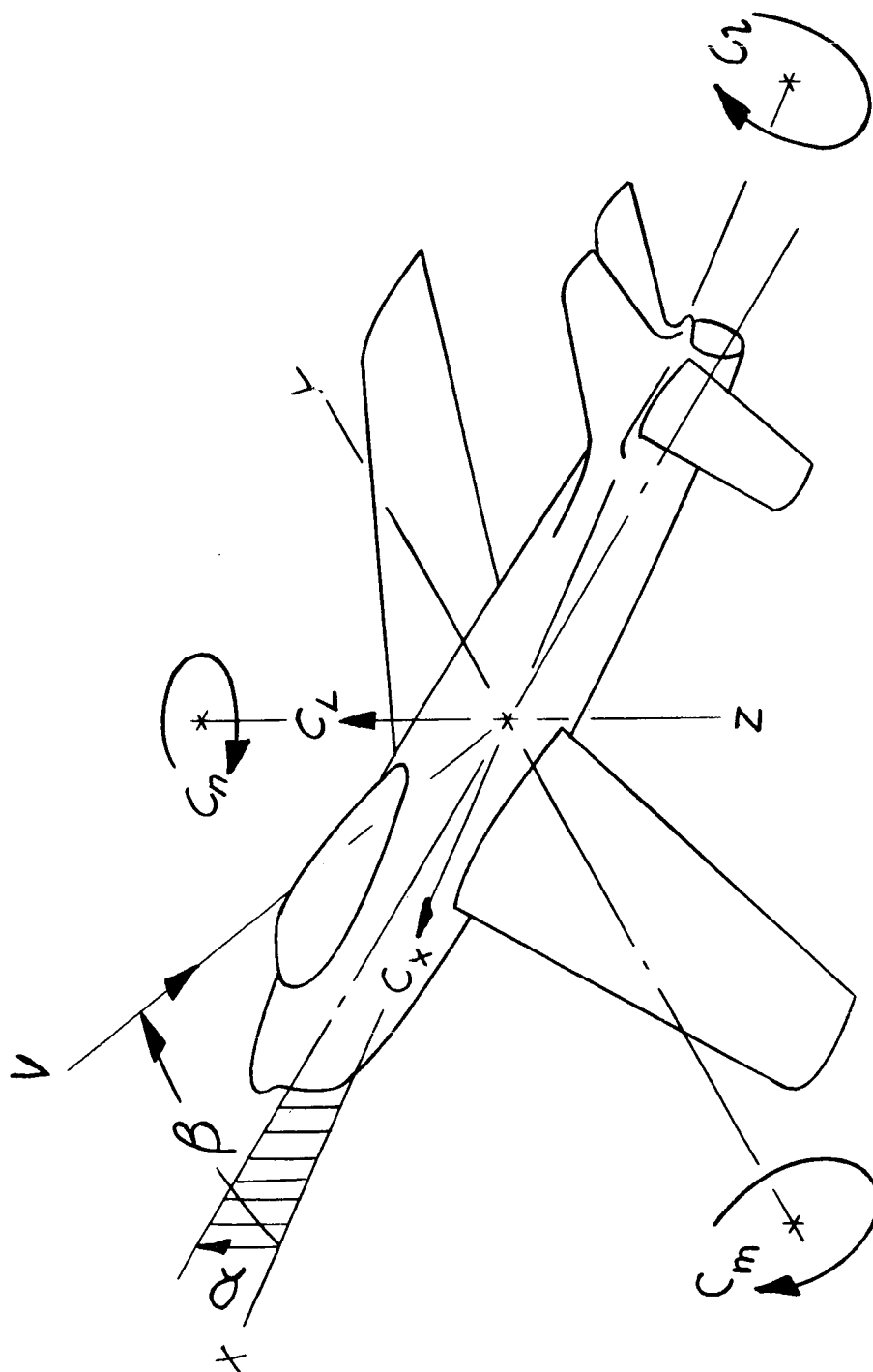


Figure 1.- System of axes used. Arrows indicate positive direction of forces and moments.

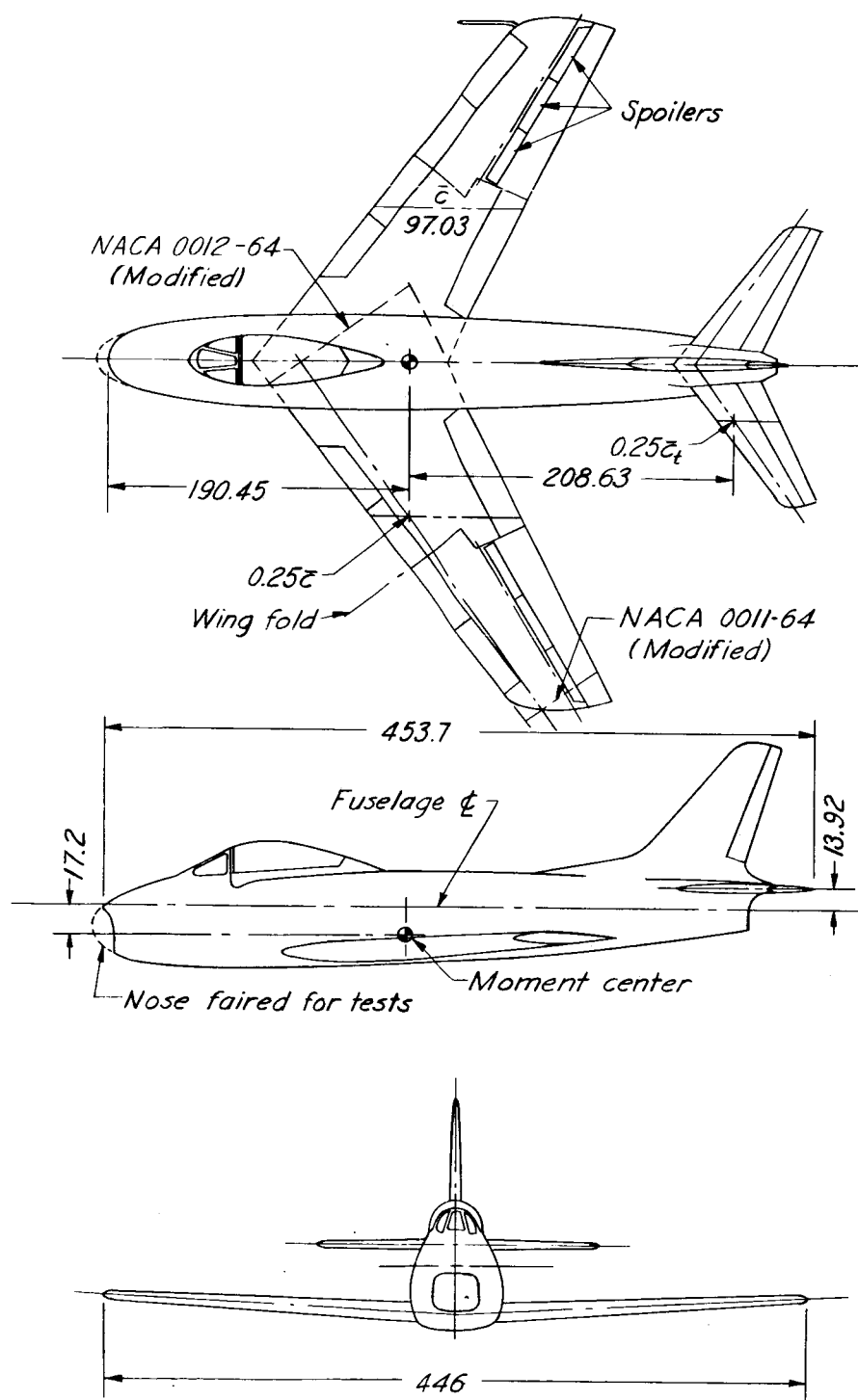


Figure 2.- Principal dimensions of the  $35^\circ$  swept-wing fighter airplane.  
All dimensions are given in inches unless otherwise noted.

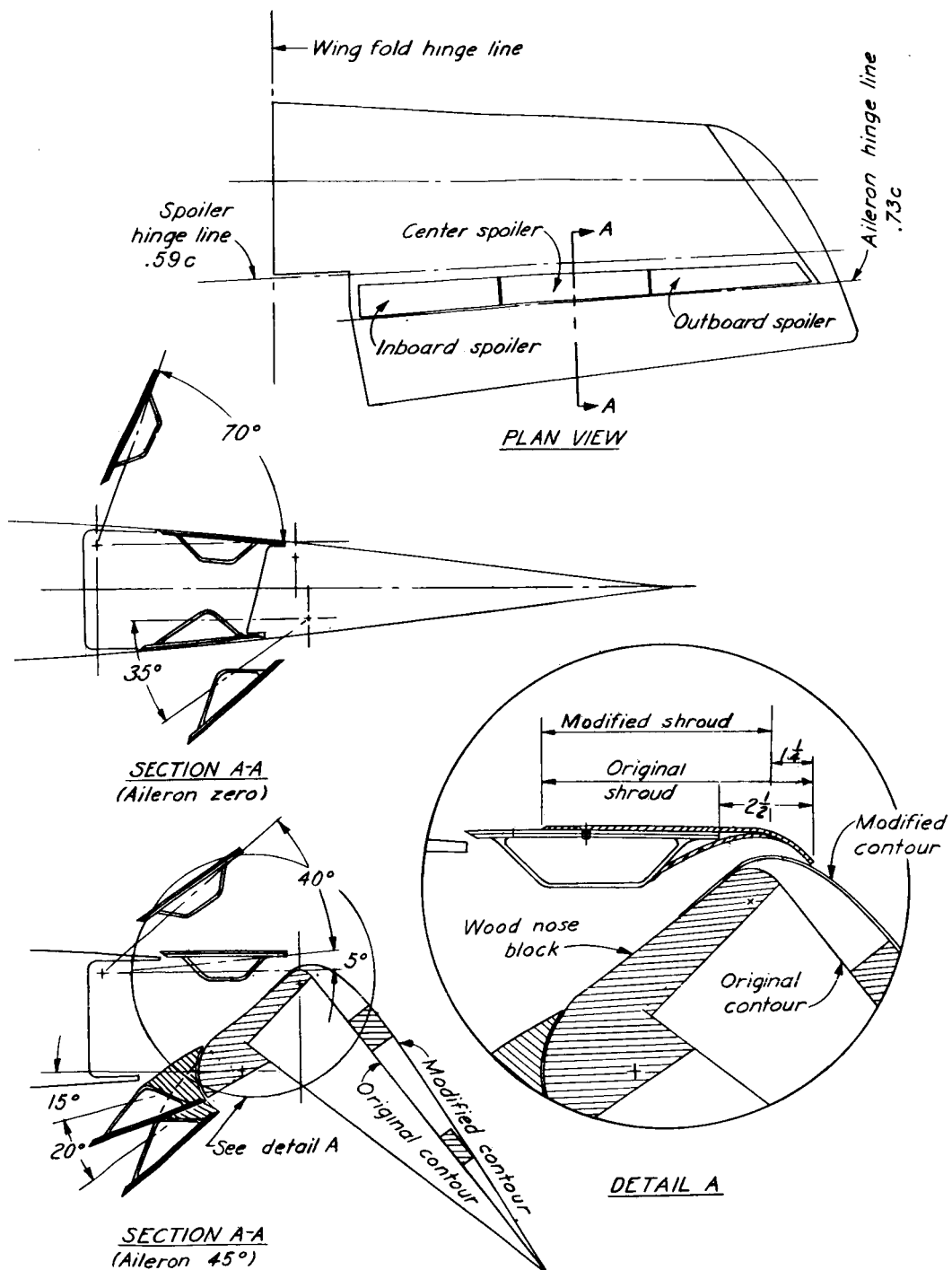


Figure 3.- Spoiler and aileron details. All dimensions are given in inches unless otherwise noted.

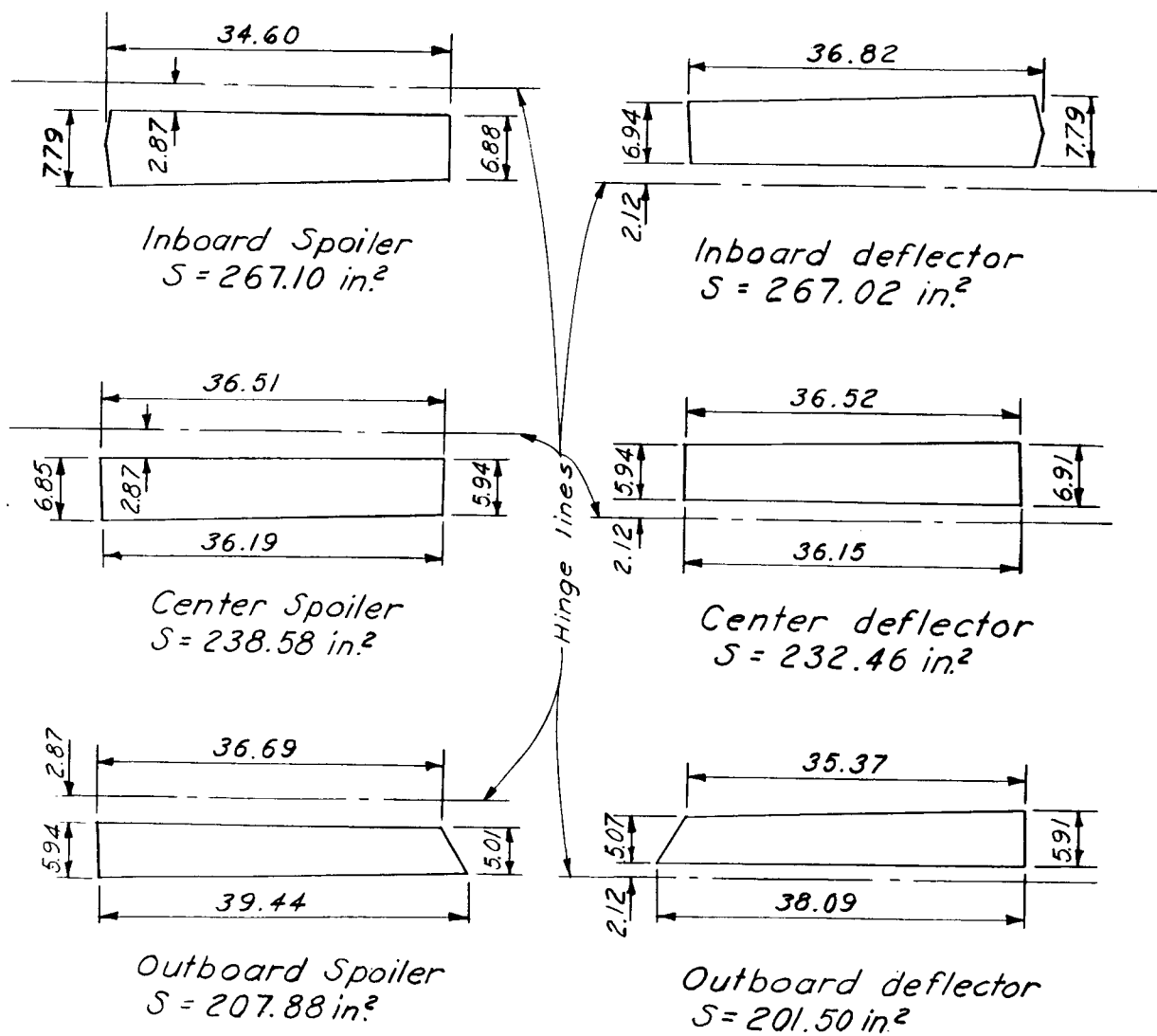
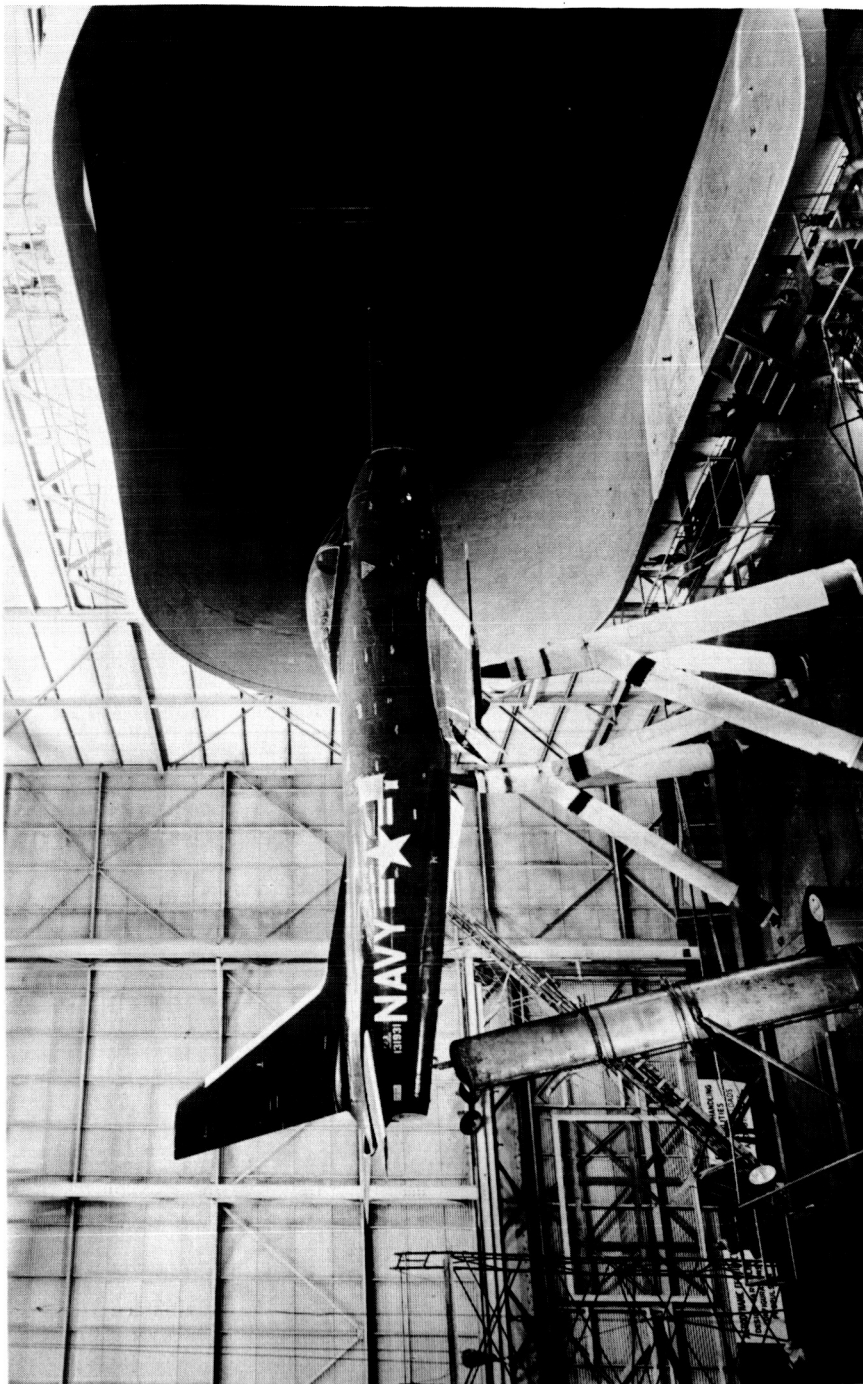


Figure 4.- Principal spoiler and deflector dimensions. All dimensions are given in inches unless otherwise noted.

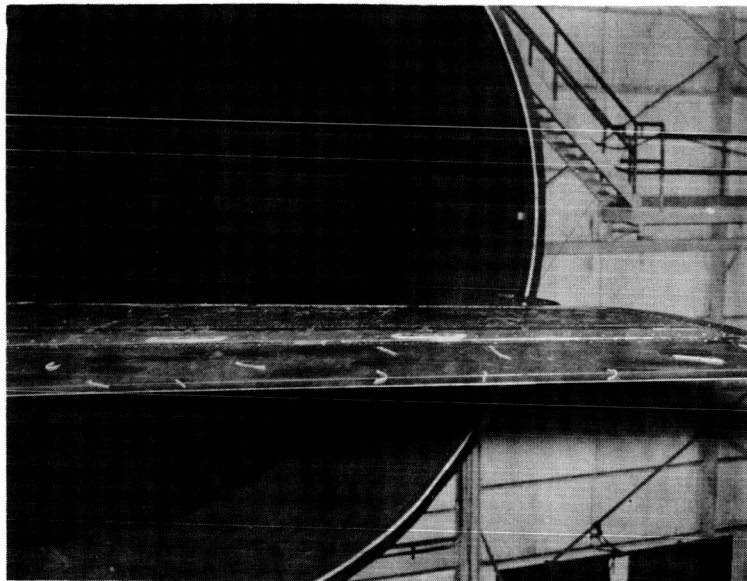




L-86089

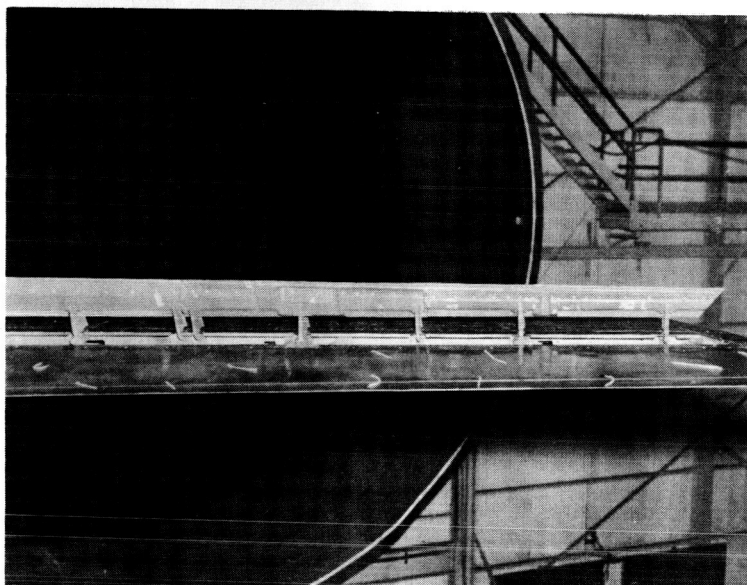
(a) General view of the airplane with flaps deflected  $45^\circ$  and ailerons drooped  $45^\circ$ .

Figure 5.- Photographs of the  $35^\circ$  swept-wing fighter airplane and spoiler-deflector configurations.



Spoilers closed, mutual motion

L-86187



Spoilers open, mutual motion

L-86188

(b) Normal flight configuration.

Figure 5.- Continued.





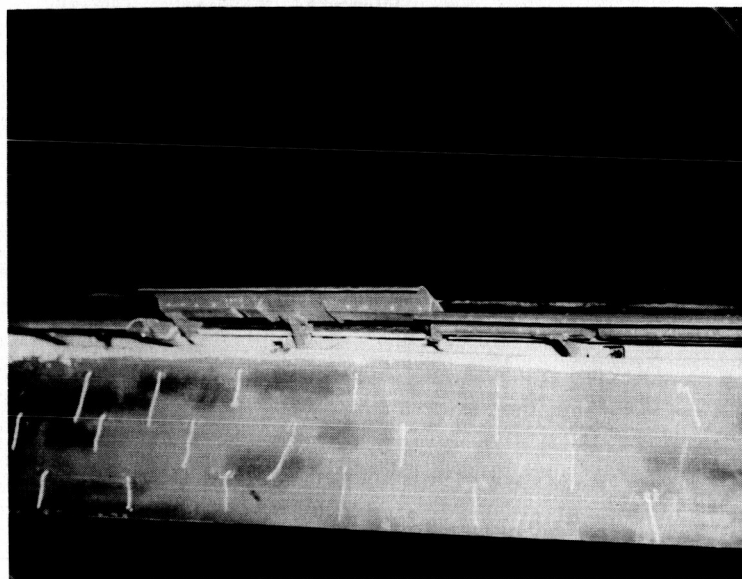
Deflectors closed, mutual motion L-86193



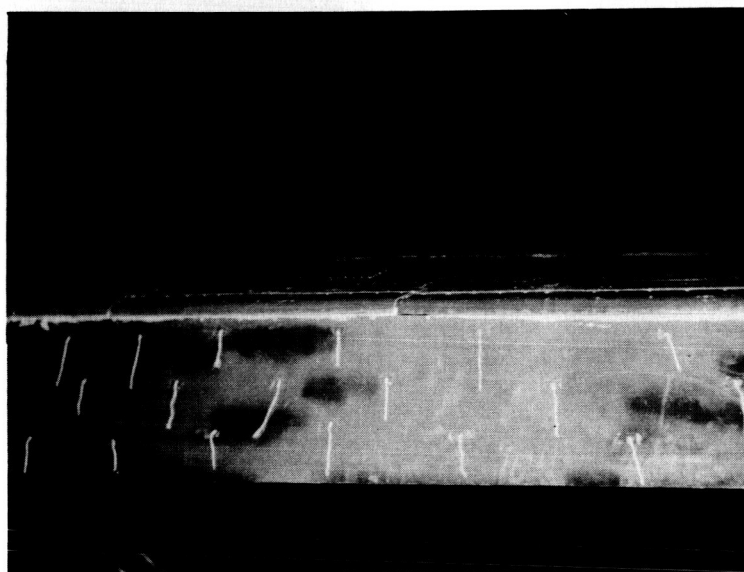
Deflectors open, mutual motion L-86194

(c) Normal flight configuration.

Figure 5.- Continued.



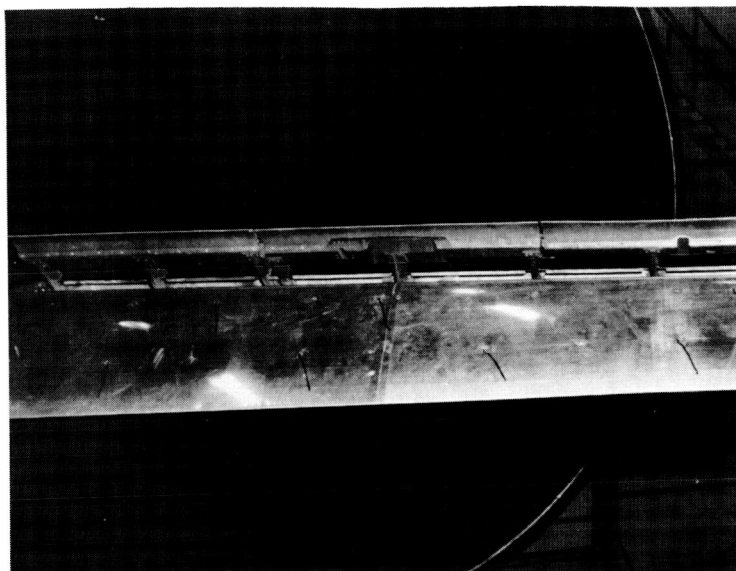
Spoilers open, differential motion L-86083



Spoilers closed, differential motion L-86084

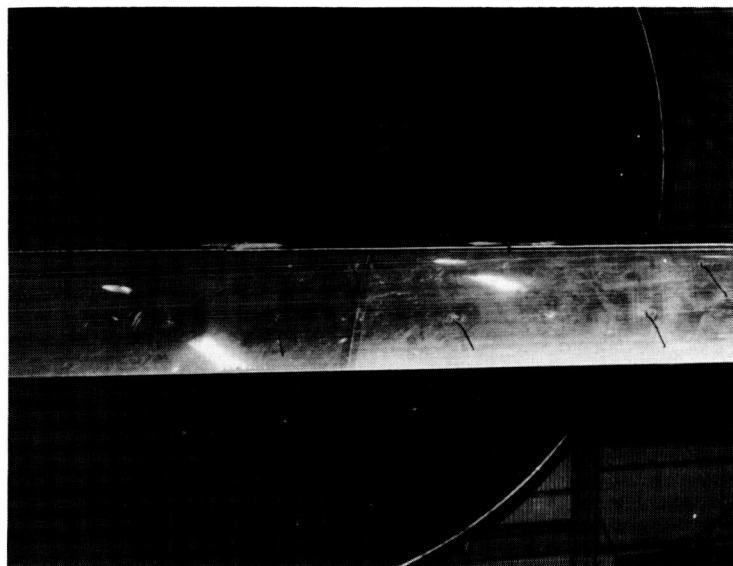
(d) Original shrouds installed, ailerons drooped  $45^\circ$ .

Figure 5.- Continued.



Spoilers open, mutual motion

L-86135



Spoilers closed, mutual motion

L-86136

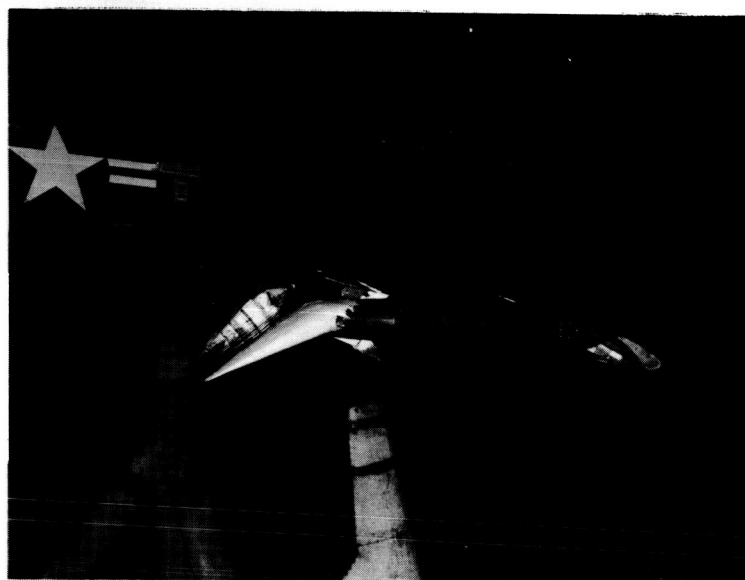
(e) Modified shrouds installed, modified ailerons drooped  $30^{\circ}$ .

Figure 5.- Continued.



Spoilers closed, mutual motion

L-86138

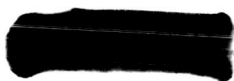


Spoilers partly open, mutual motion

L-86144

(f) Modified shrouds installed, modified aileron drooped  $30^{\circ}$ .

Figure 5.- Concluded.



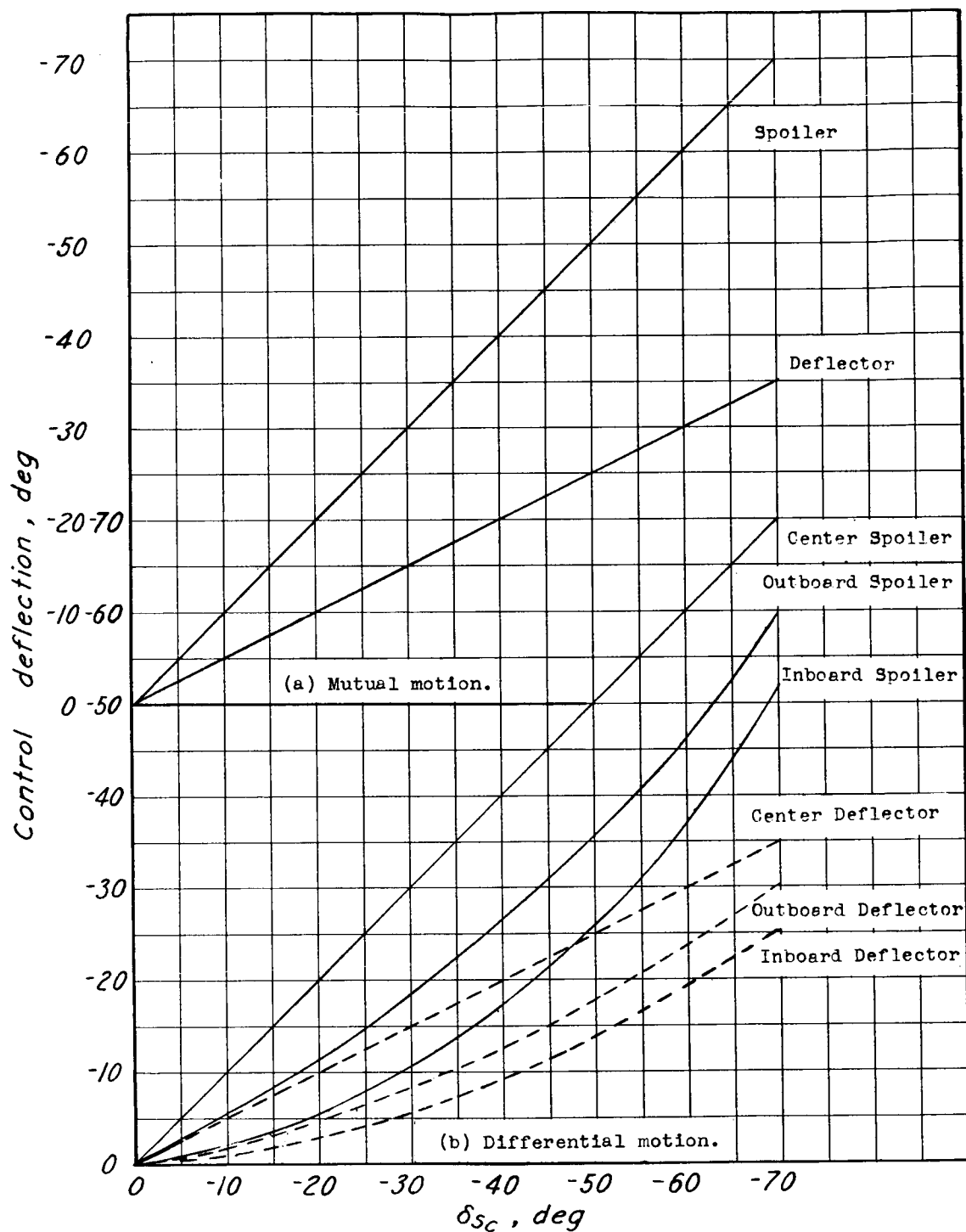
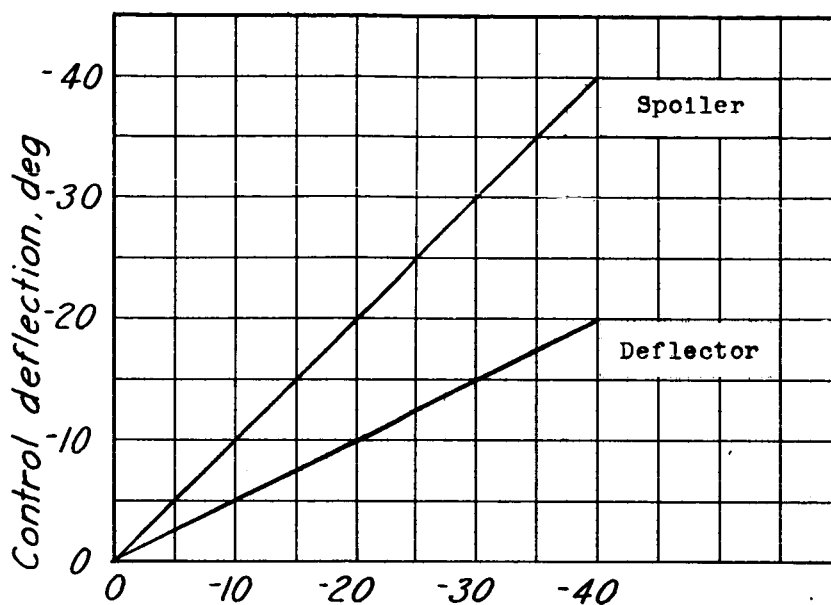
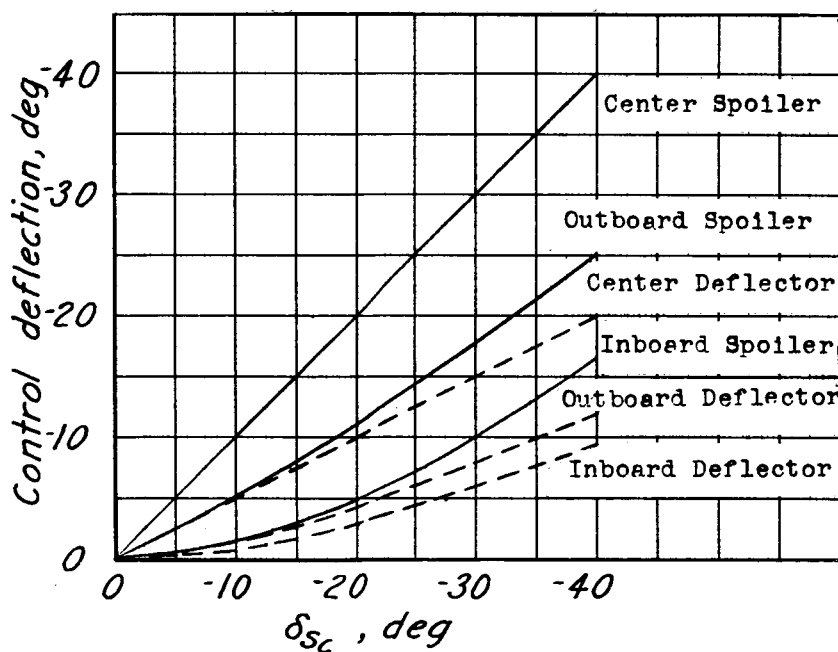


Figure 6.- Variation of spoiler and deflector motion with center spoiler deflection. Ailerons neutral.



(a) Mutual motion.



(b) Differential motion.

Figure 7.- Variation of spoiler and deflector motion with center spoiler deflection. Ailerons deflected.



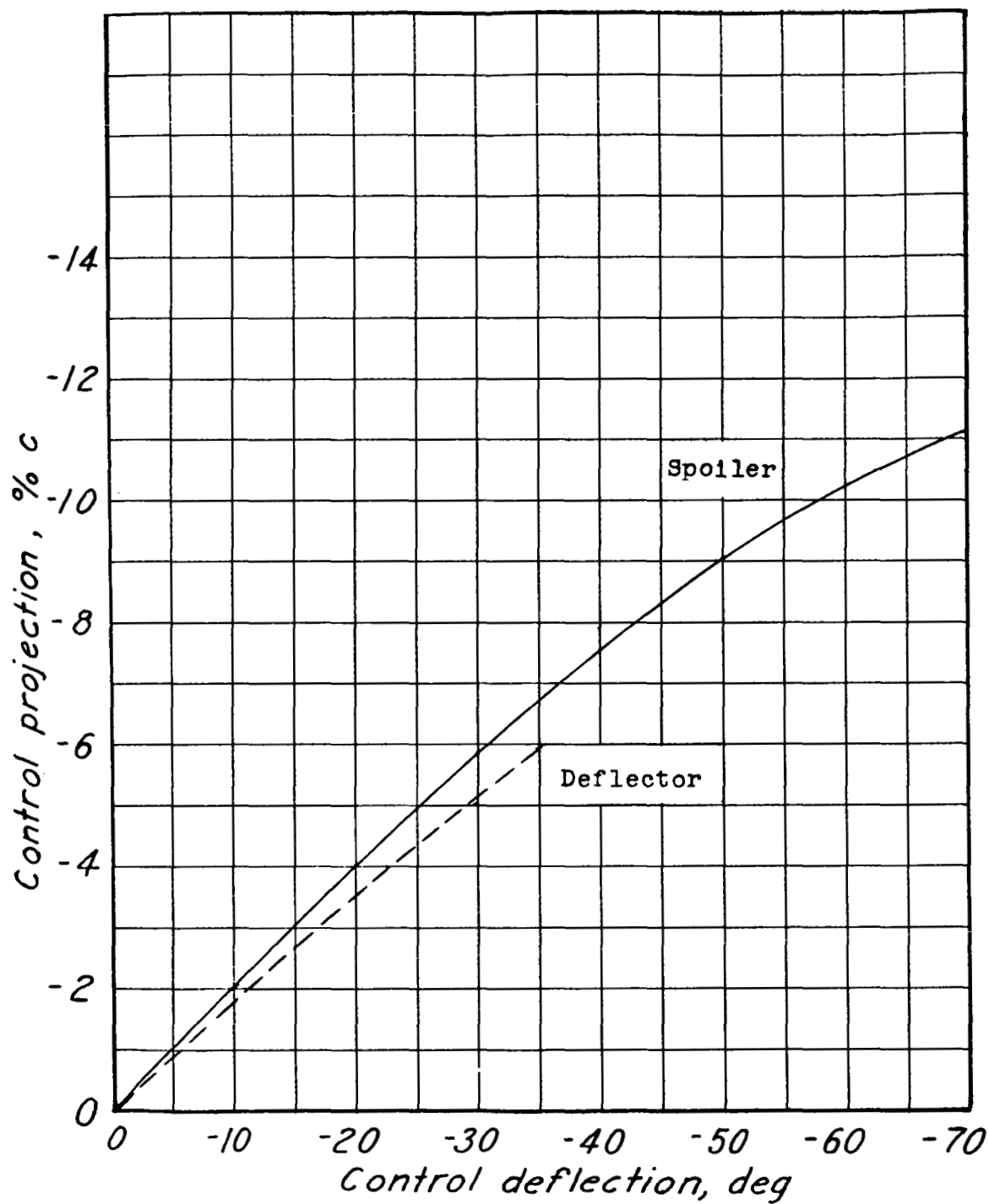


Figure 8.- Variation of control projection (percent c) with control deflection in degrees for the spoilers and deflectors.

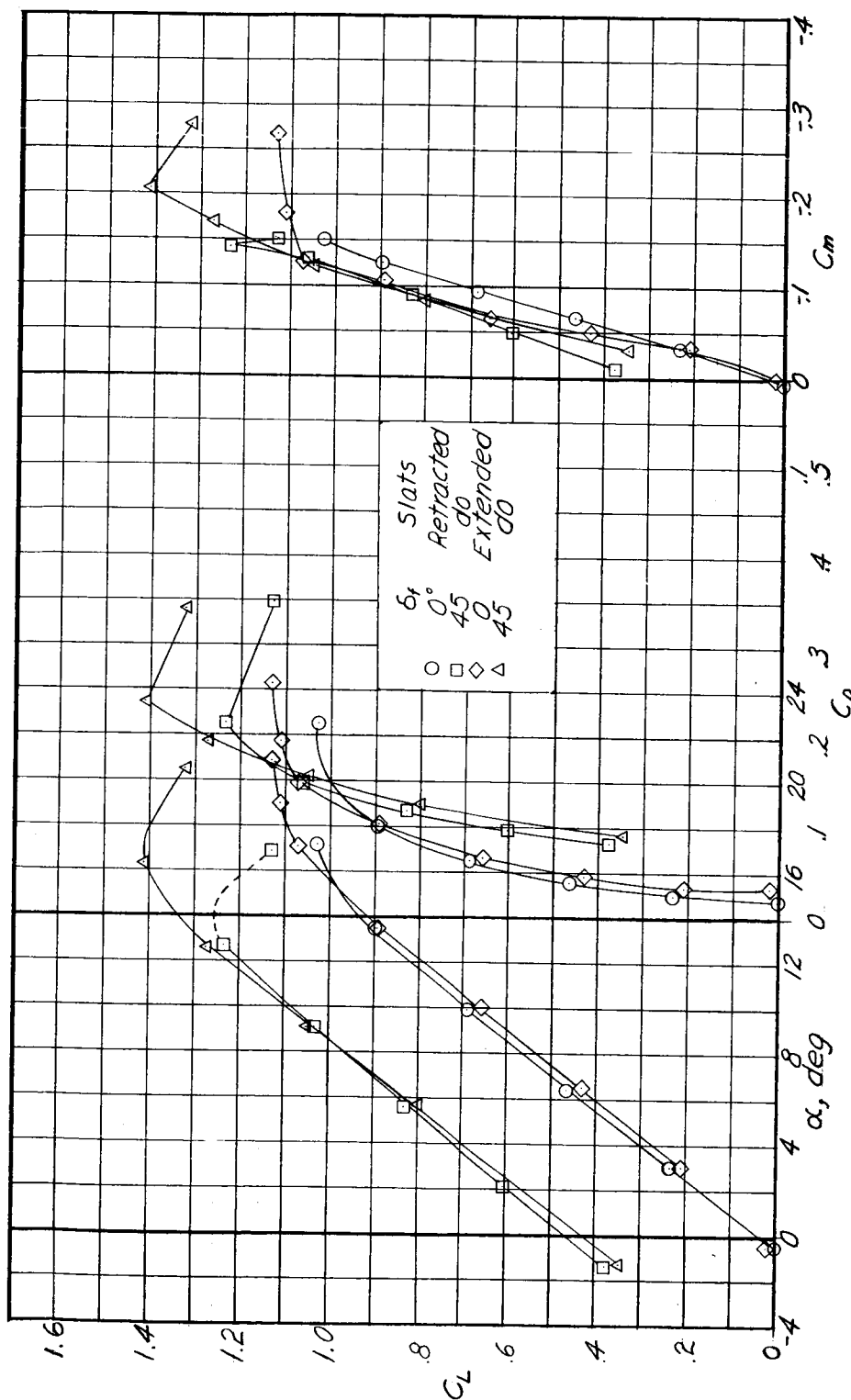


Figure 9.- Aerodynamic characteristics of the 35° swept-wing fighter airplane with ailerons neutral.  $i_t = 0^\circ$ ;  $R = 5 \times 10^6$ .

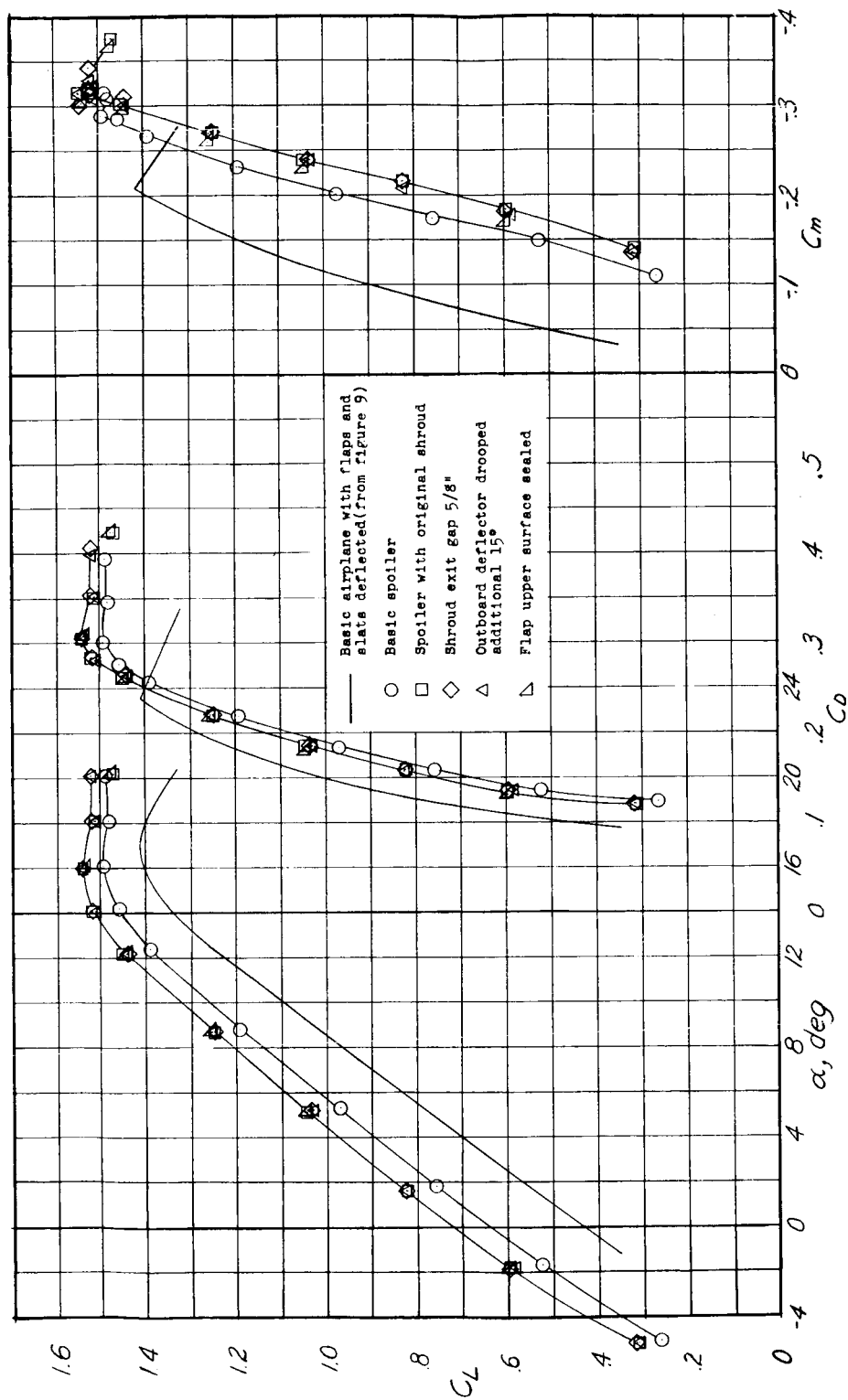
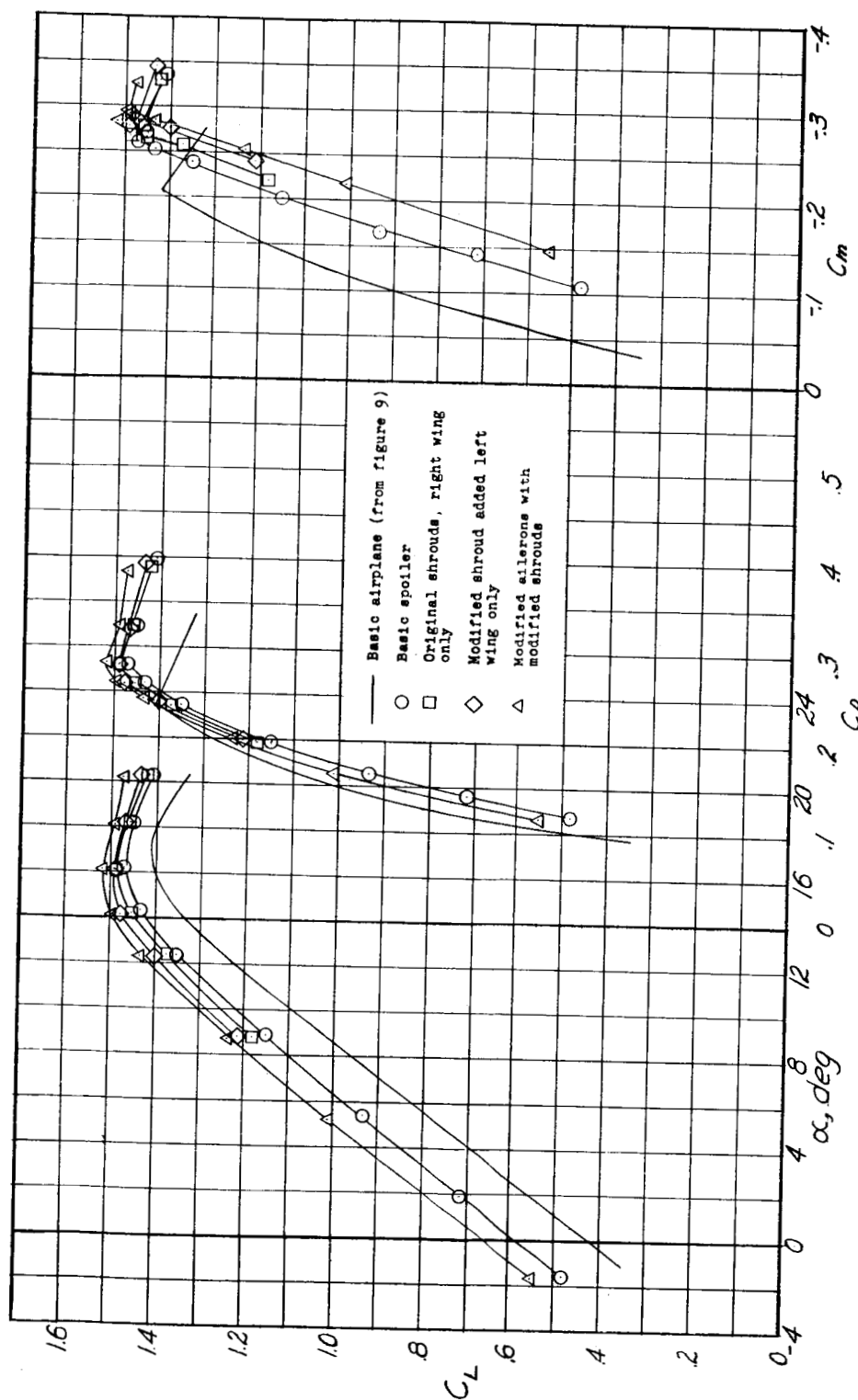
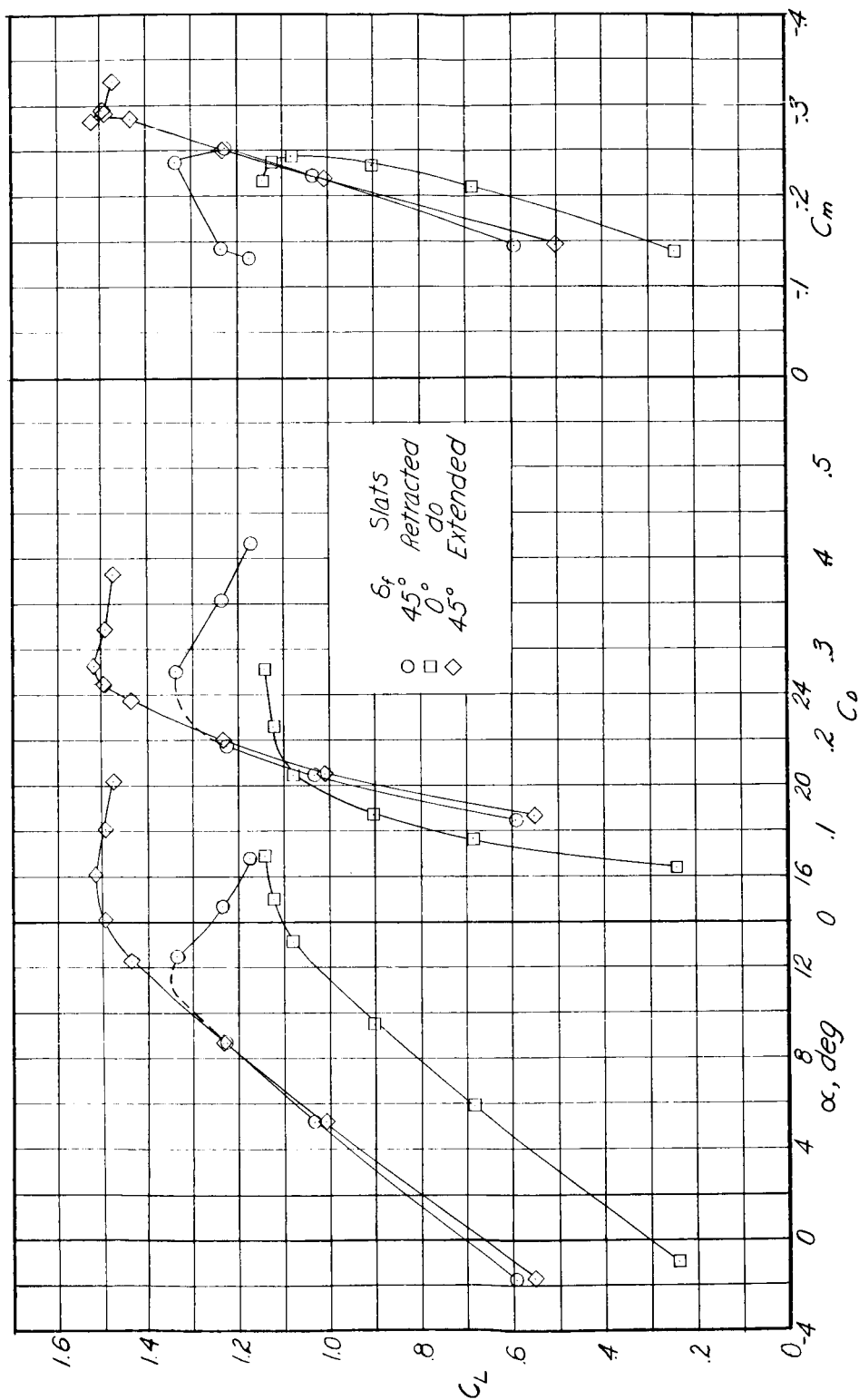


Figure 10.- Aerodynamic characteristics of the 35° swept-wing fighter airplane with ailerons drooped 45°.  $\delta_f = 45^\circ$ ; slats extended;  $i_t = 0^\circ$ ;  $R = 5 \times 10^6$ .



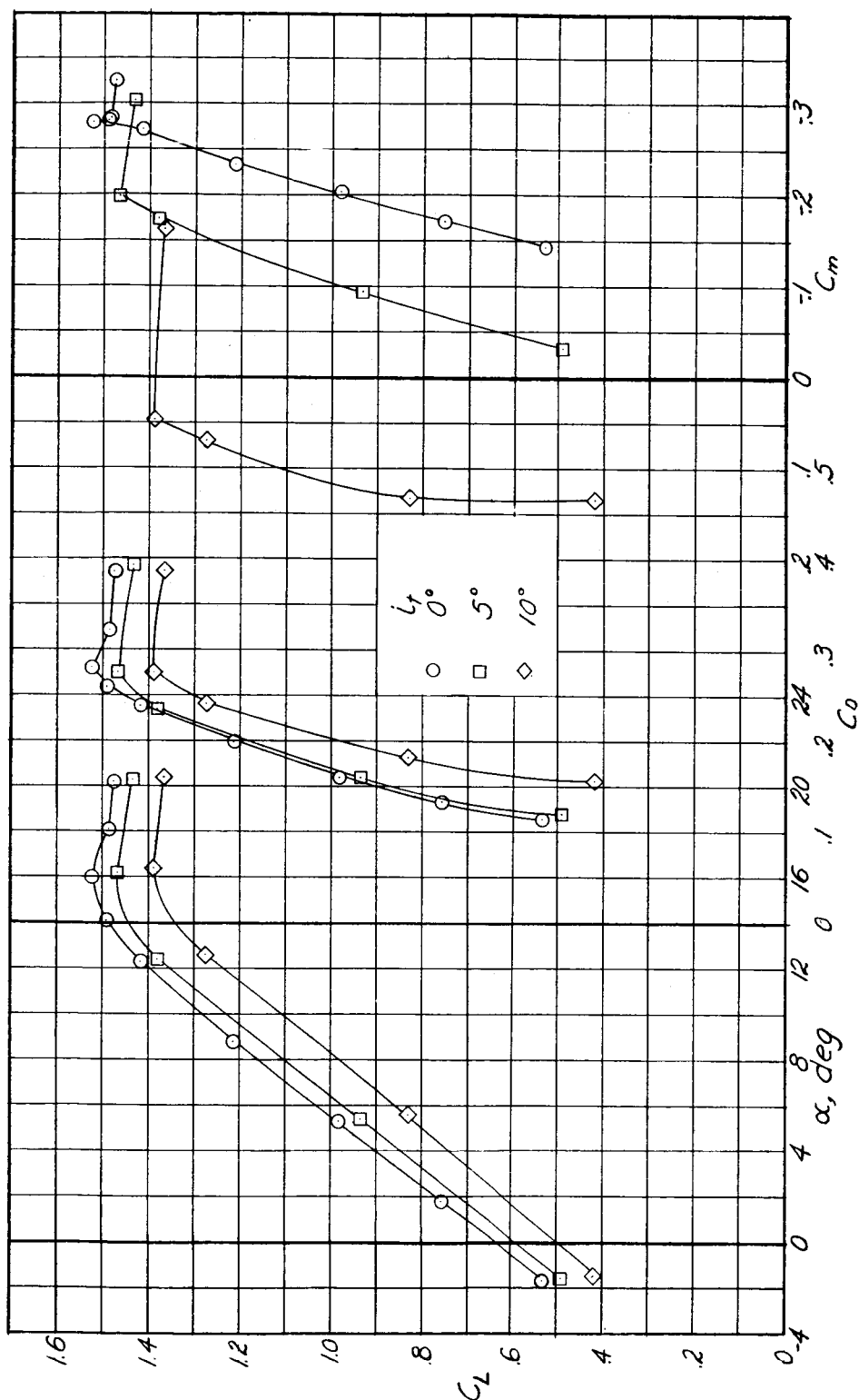
(a) Effect of shroud and aileron modification.  $\delta_f = 45^\circ$ ; slats extended.

Figure 11.- Aerodynamic characteristics of the 350 swept-wing fighter airplane with ailerons drooped 30°.  $i_t = 0^\circ$ ;  $R = 5 \times 10^6$ .



(b) Effect of flap and slat deflection. Modified aileron installed.

Figure 11.- Continued.



(c) Effect of stabilizer deflection. Modified aileron installed.  $\delta_f = 45^\circ$ ; slats extended;  $R = 5 \times 10^6$ ;  $\delta_a = 30^\circ$ .

Figure 11.- Concluded.

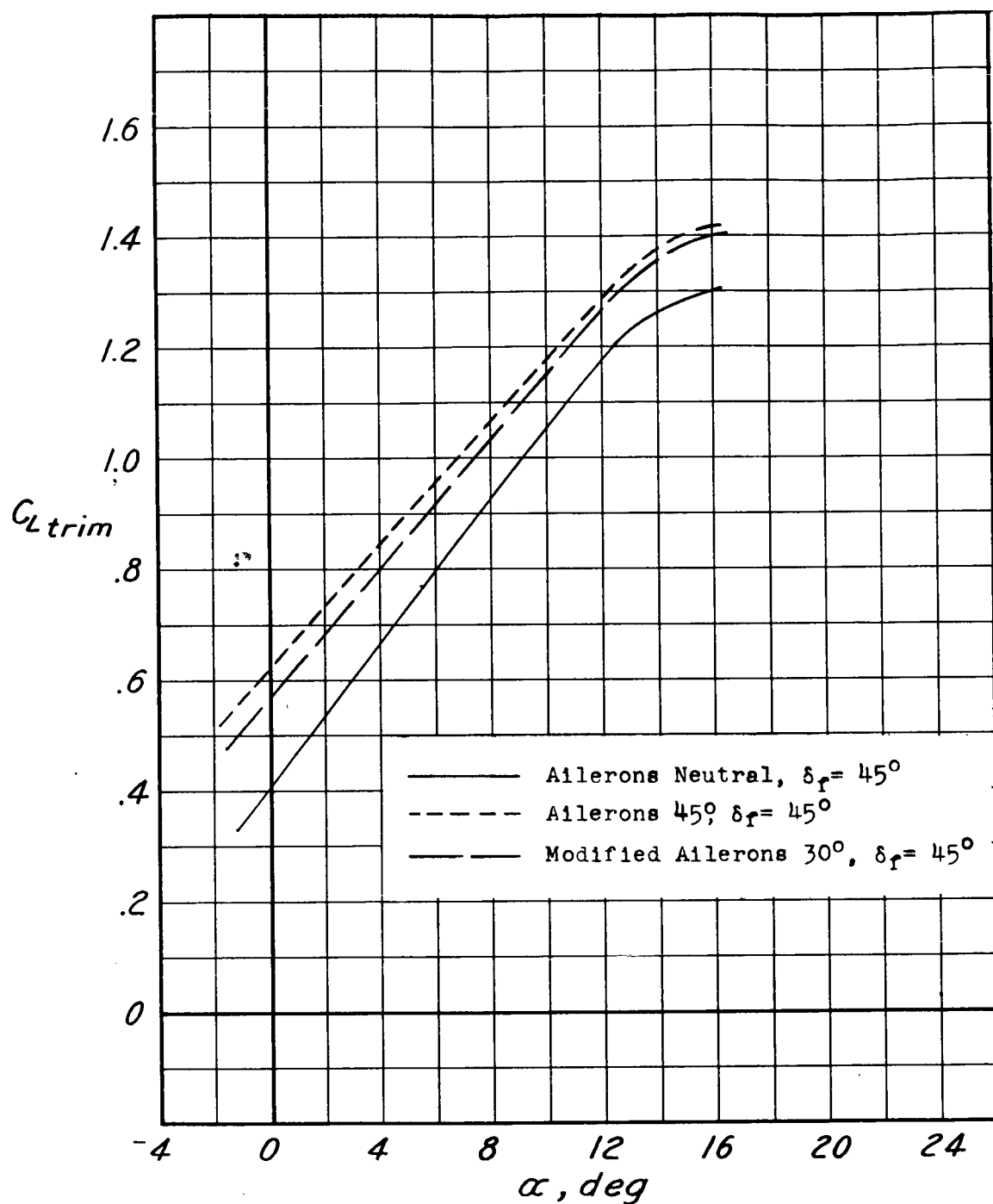
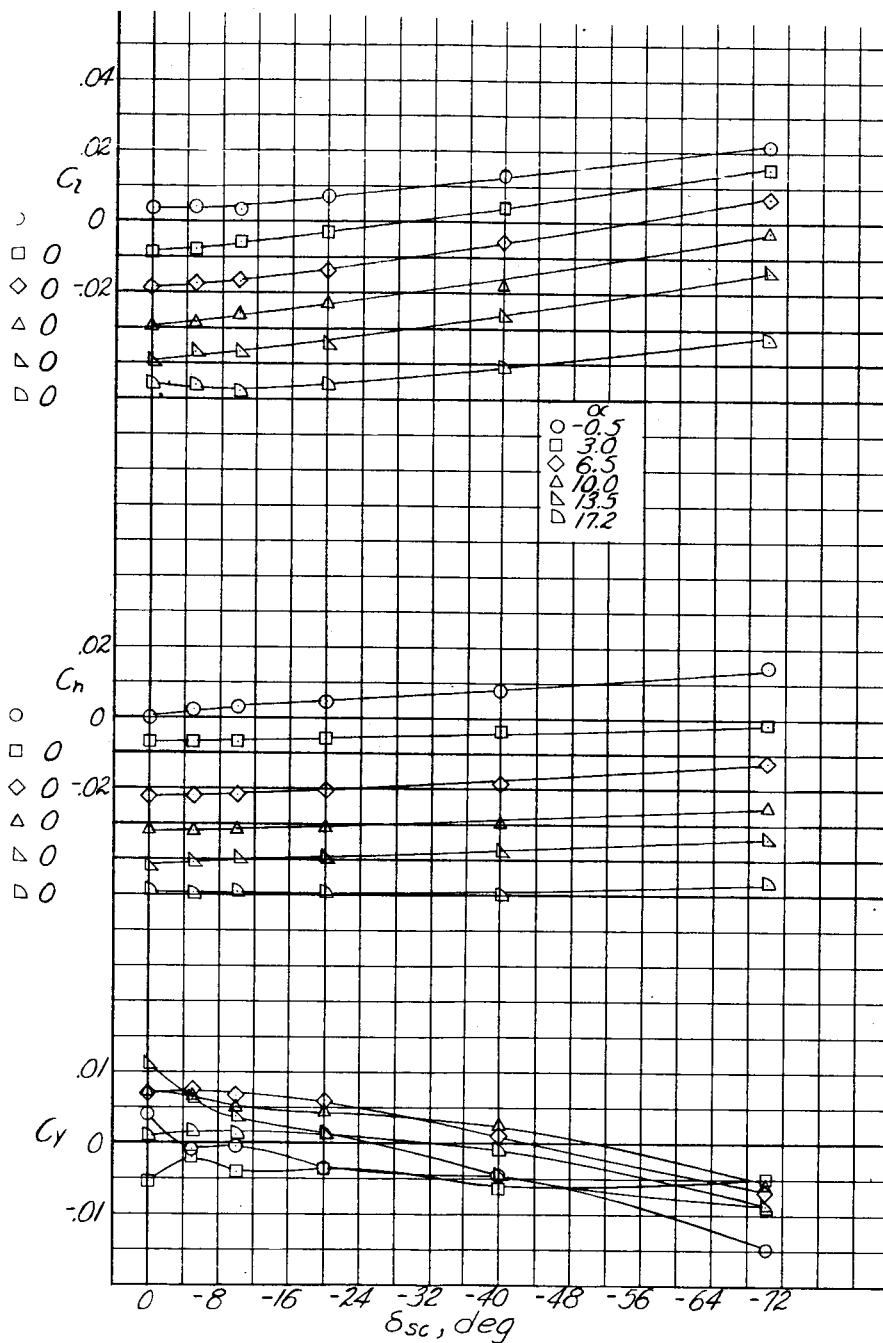


Figure 12.- Variation of trim lift coefficient with angle of attack for the  $35^\circ$  swept-wing fighter airplane. Slats extended.

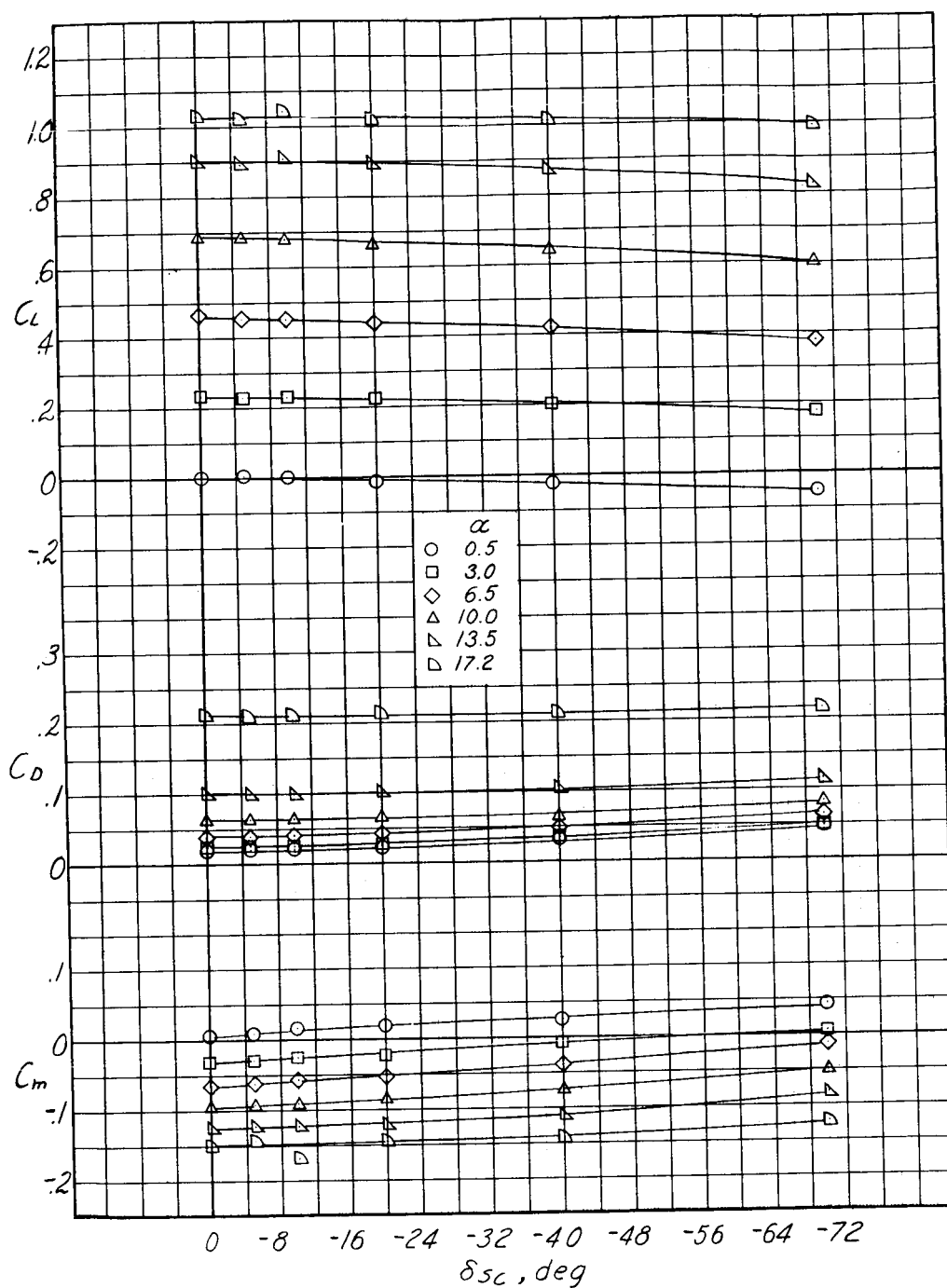


(a) Lateral characteristics.

Figure 13.- Effect of spoiler-deflector deflection on the lateral and longitudinal characteristics with the ailerons neutral. Basic spoiler; differential motion;  $\delta_f = 0^\circ$ ; slats retracted.

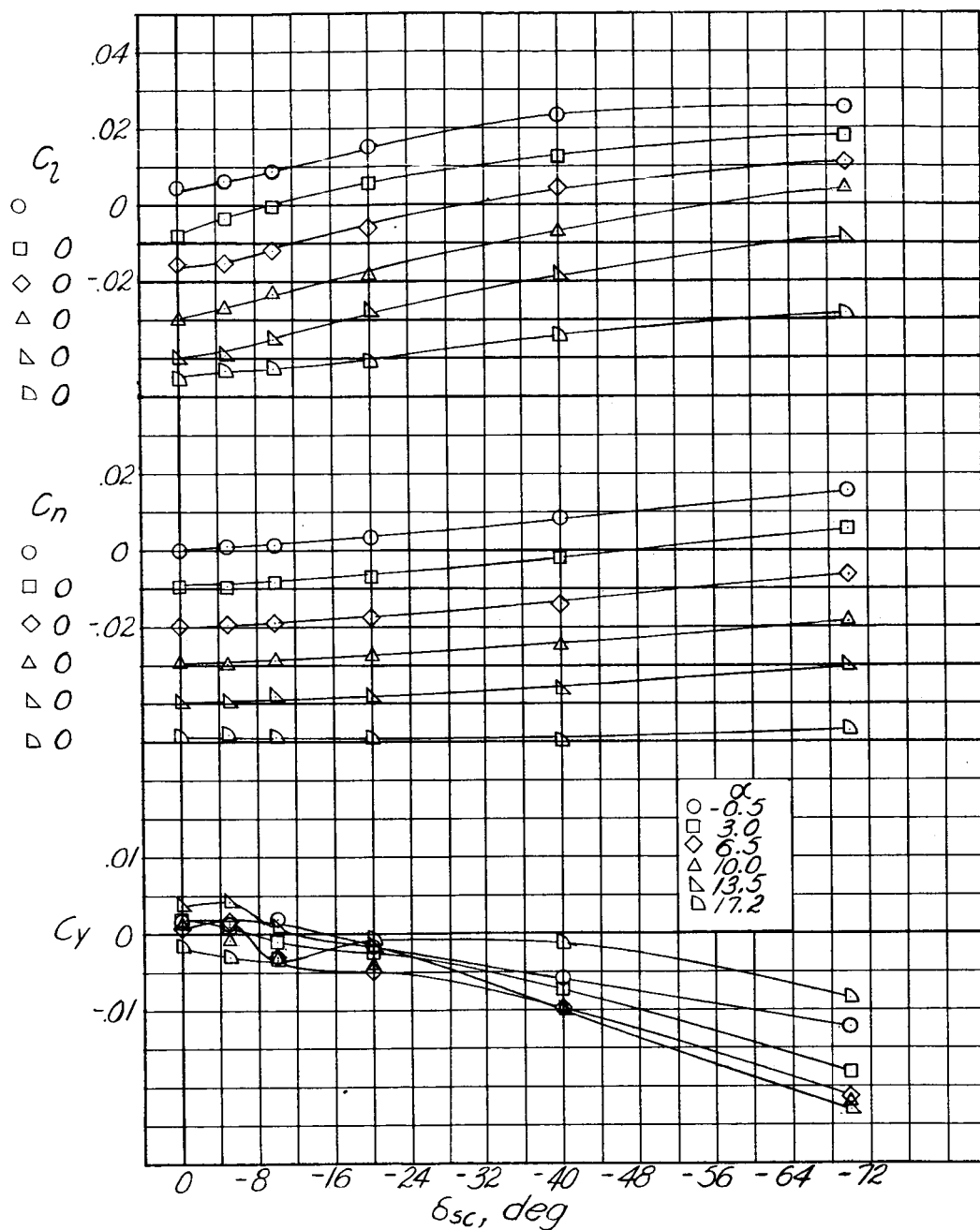






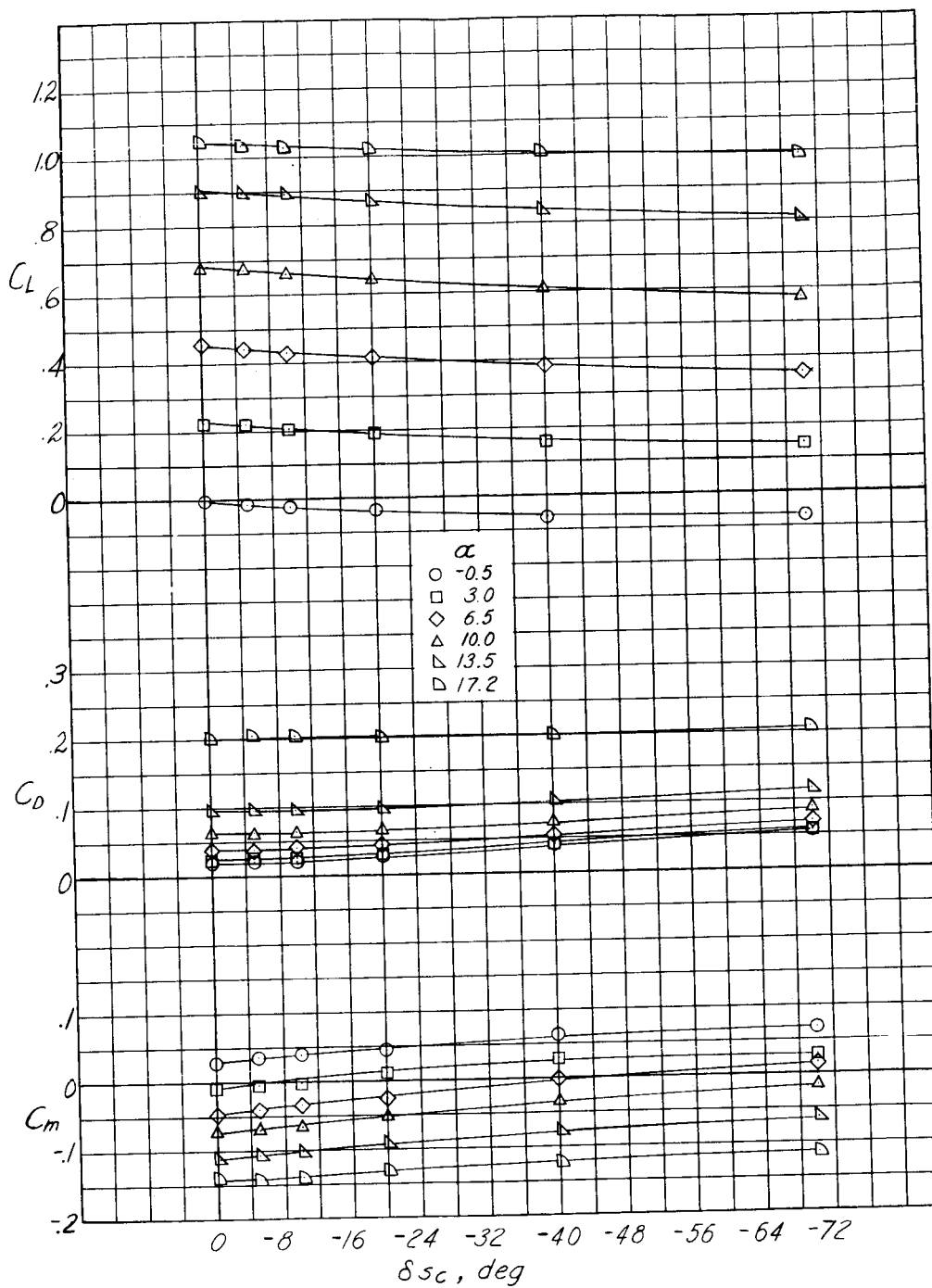
(b) Longitudinal characteristics.

Figure 13.- Concluded.



(a) Lateral characteristics.

Figure 14.- Effect of spoiler-deflector deflection on the lateral and longitudinal characteristics with the ailerons neutral. Basic spoiler; mutual motion;  $\delta_F = 0^\circ$ ; slats retracted.



(b) Longitudinal characteristics.

Figure 14.- Concluded.

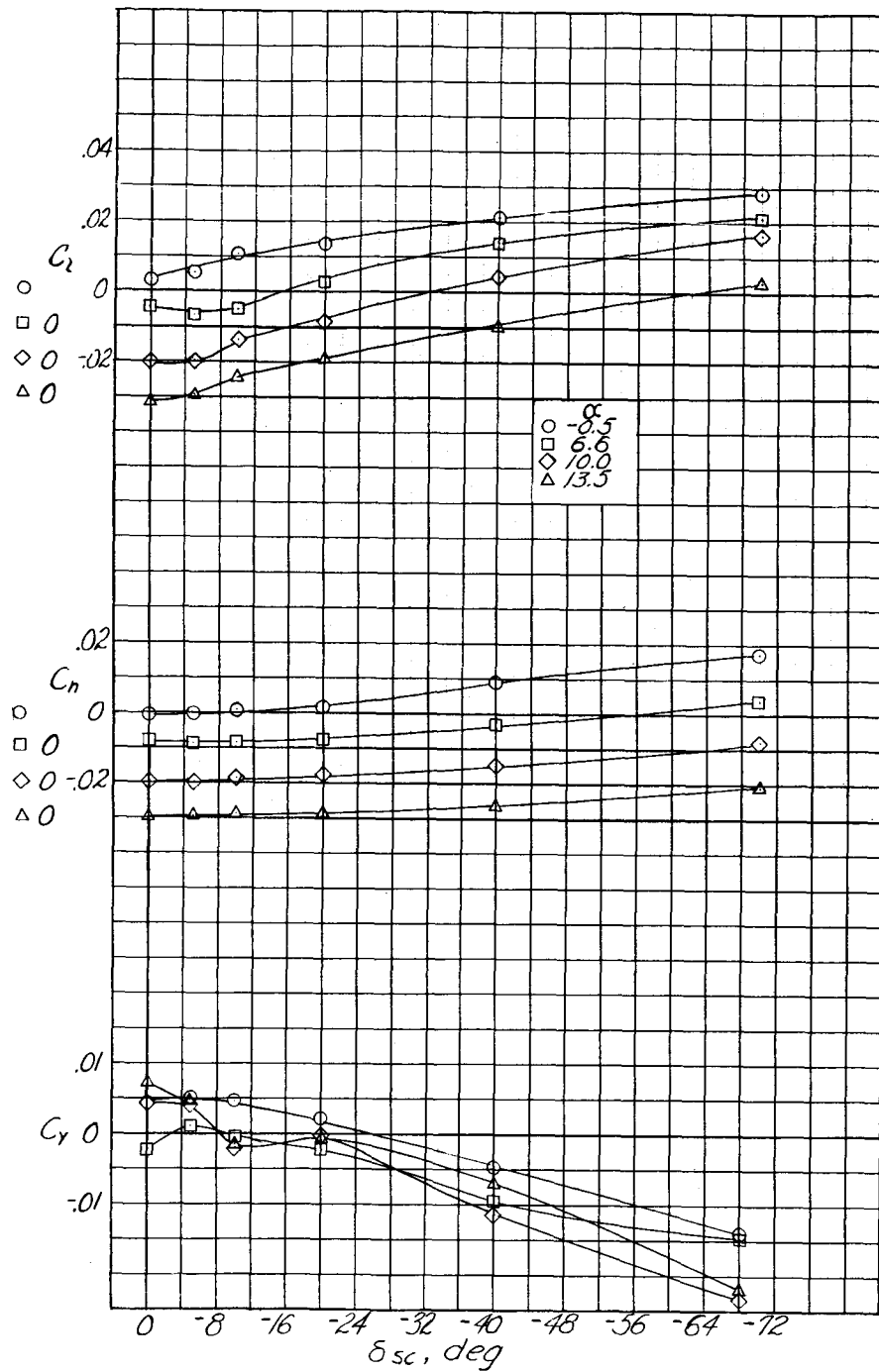


Figure 15.- Effect of spoiler-deflector deflection on the lateral characteristics with the spoiler hinge gaps sealed. Aileron neutral; mutual motion;  $\delta_f = 0^\circ$ ; slats retracted.

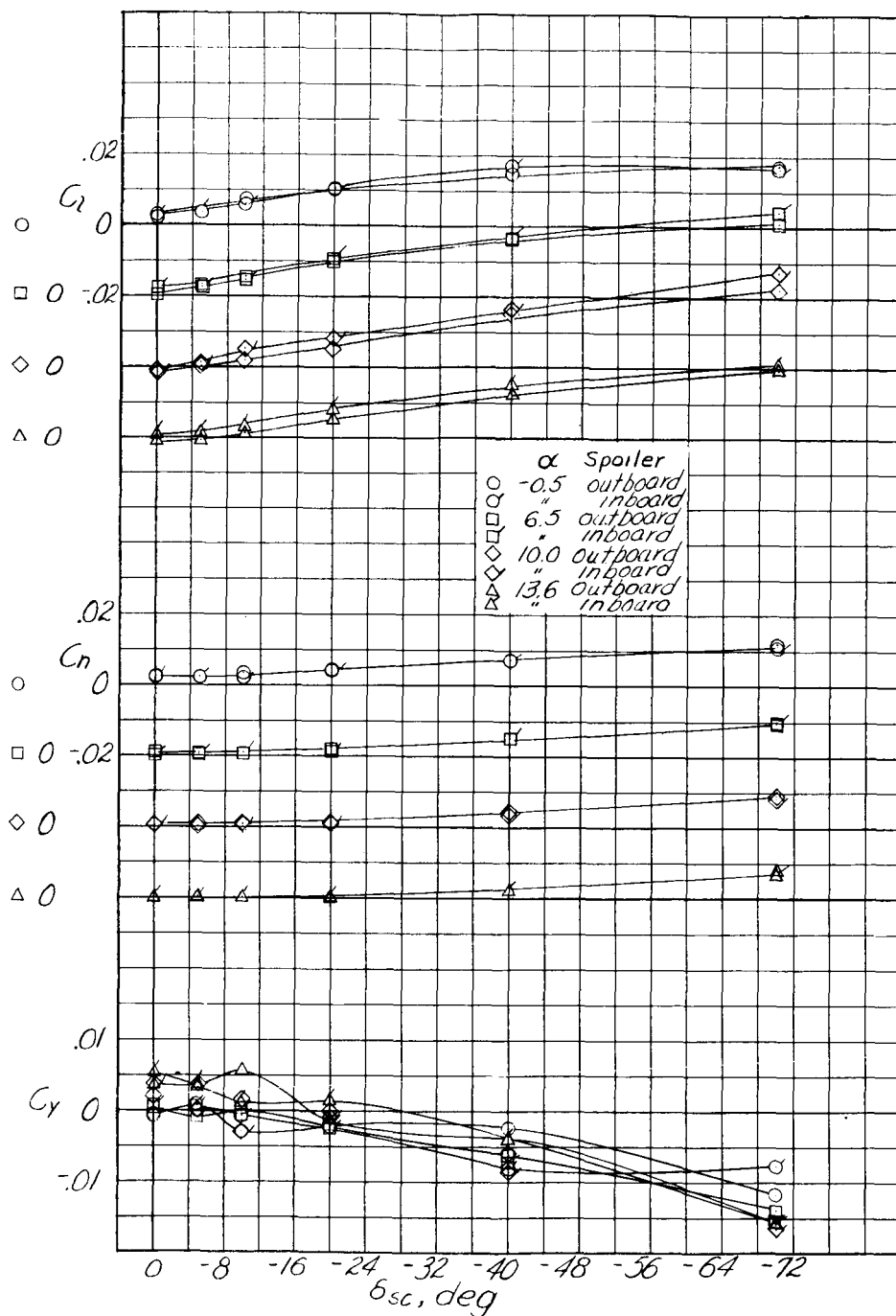


Figure 16.- Effect of spoiler-deflector deflection on the lateral characteristics at two spanwise spoiler-deflector locations with the ailerons neutral. Basic spoiler; mutual motion;  $\delta_f = 0^\circ$ ; slats retracted.

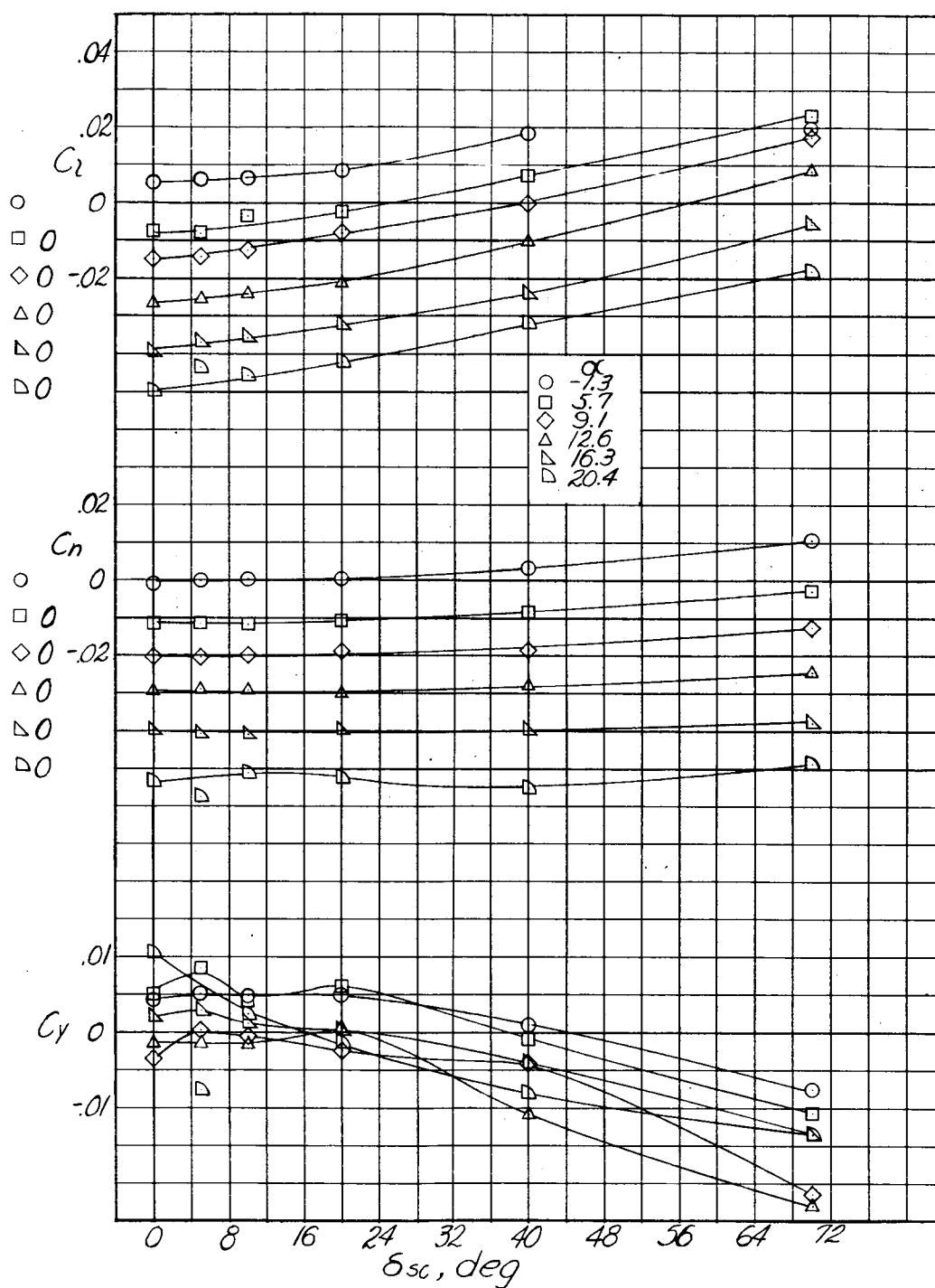


Figure 17.- Effect of spoiler-deflector deflection on the lateral characteristics with the ailerons neutral. Basic spoiler; differential motion;  $\delta_f = 45^\circ$ ; slats extended.

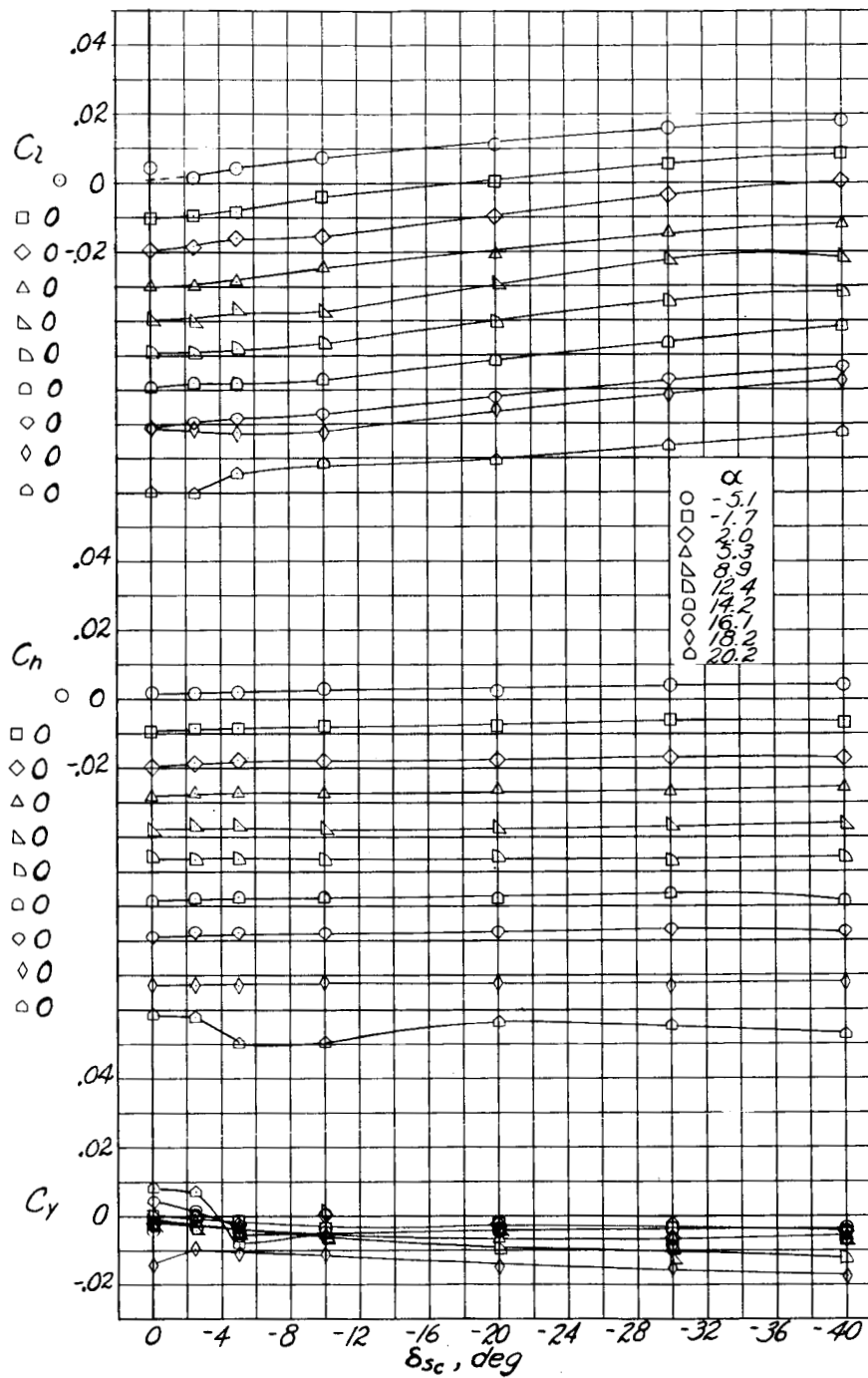


Figure 18.- Effect of spoiler-deflector deflection on the lateral characteristics. Basic spoiler without shroud; differential motion;  $\delta_f = 45^\circ$ ;  $\delta_a = 45^\circ$ ; slats extended.

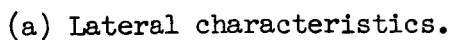
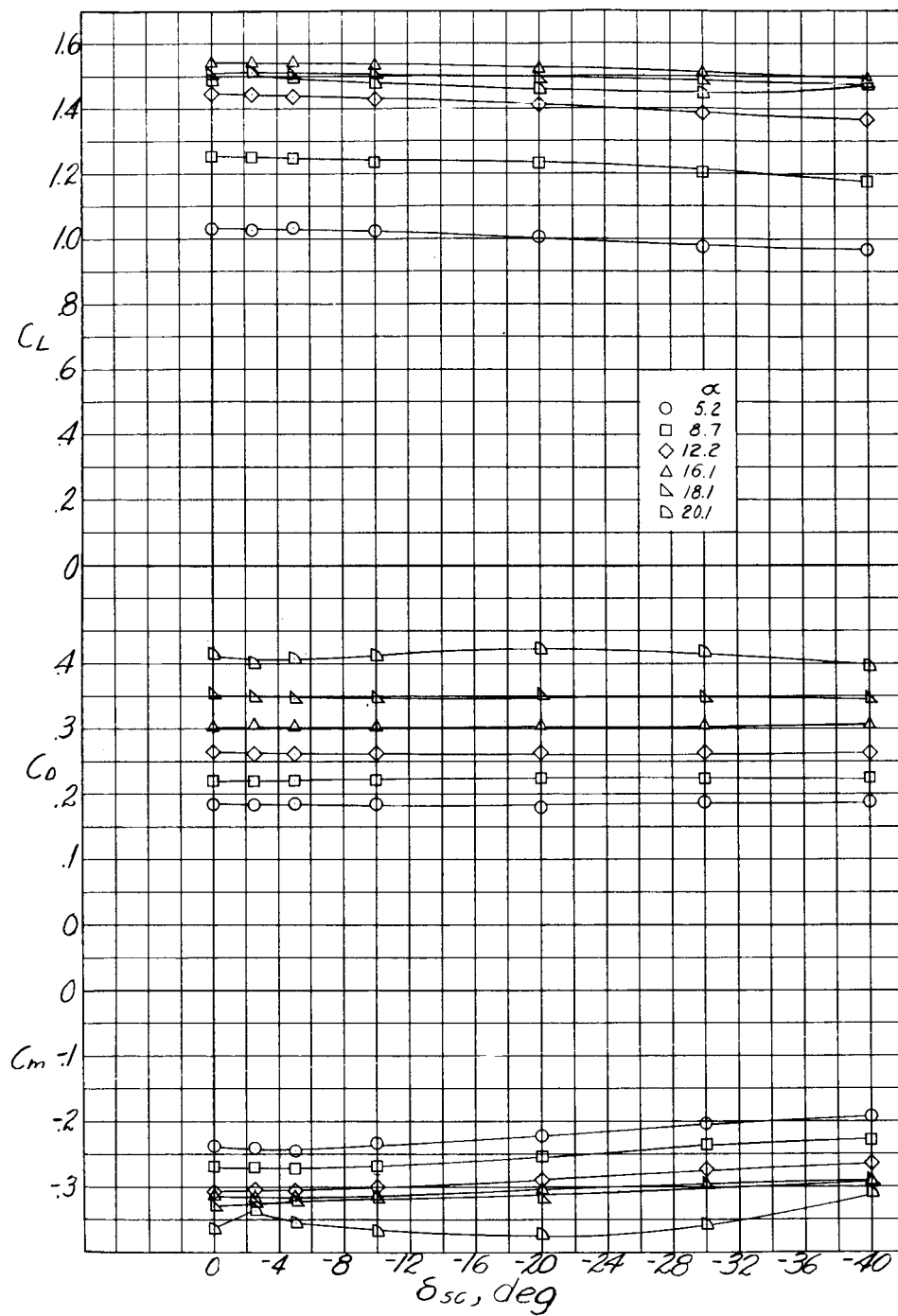


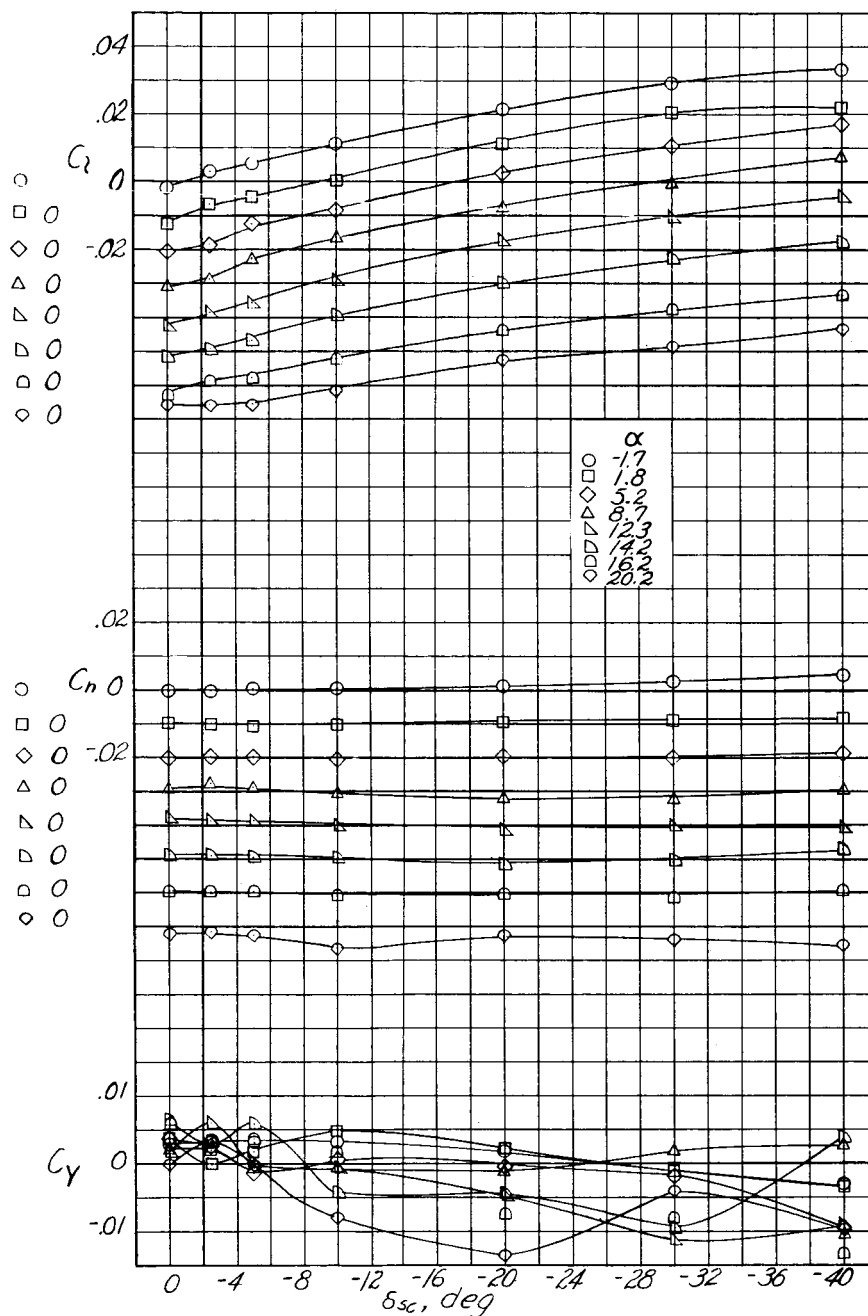
Figure 19.- Effect of spoiler-deflector deflection on the lateral and longitudinal characteristics. Spoiler with shroud (5/8-inch exit gap); outboard deflector drooped; differential motion;  $\delta_f = 45^\circ$ ;  $\delta_a = 45^\circ$ ; slats extended.





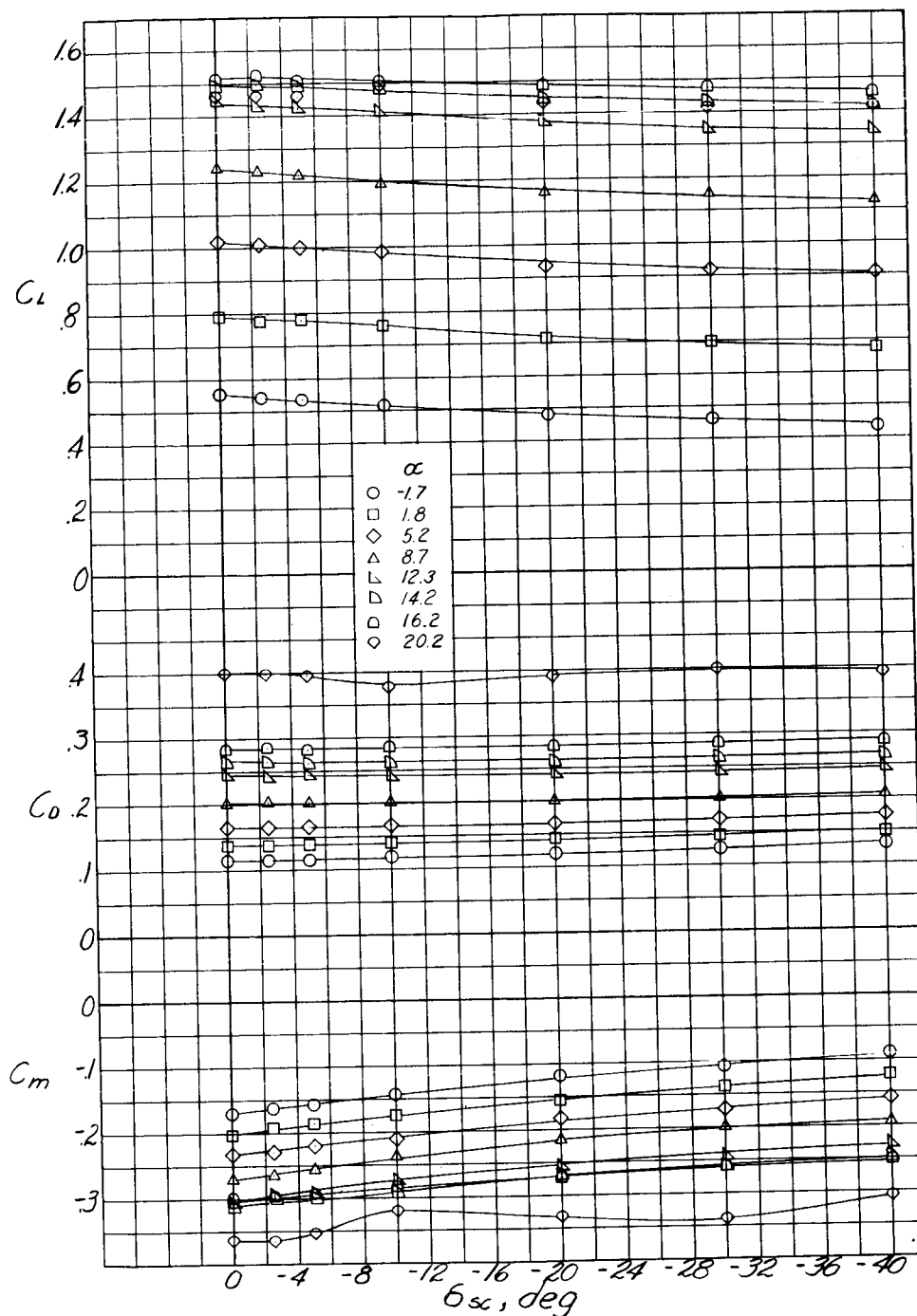
(b) Longitudinal characteristics.

Figure 19.- Concluded.



(a) Lateral characteristics.

Figure 20.- Effect of spoiler-deflector deflection on the lateral and longitudinal characteristics. Spoiler with shrouds; differential motion; modified aileron;  $\delta_f = 45^\circ$ ;  $\delta_a = 30^\circ$ ; slats extended.



(b) Longitudinal characteristics.

Figure 20.- Concluded.

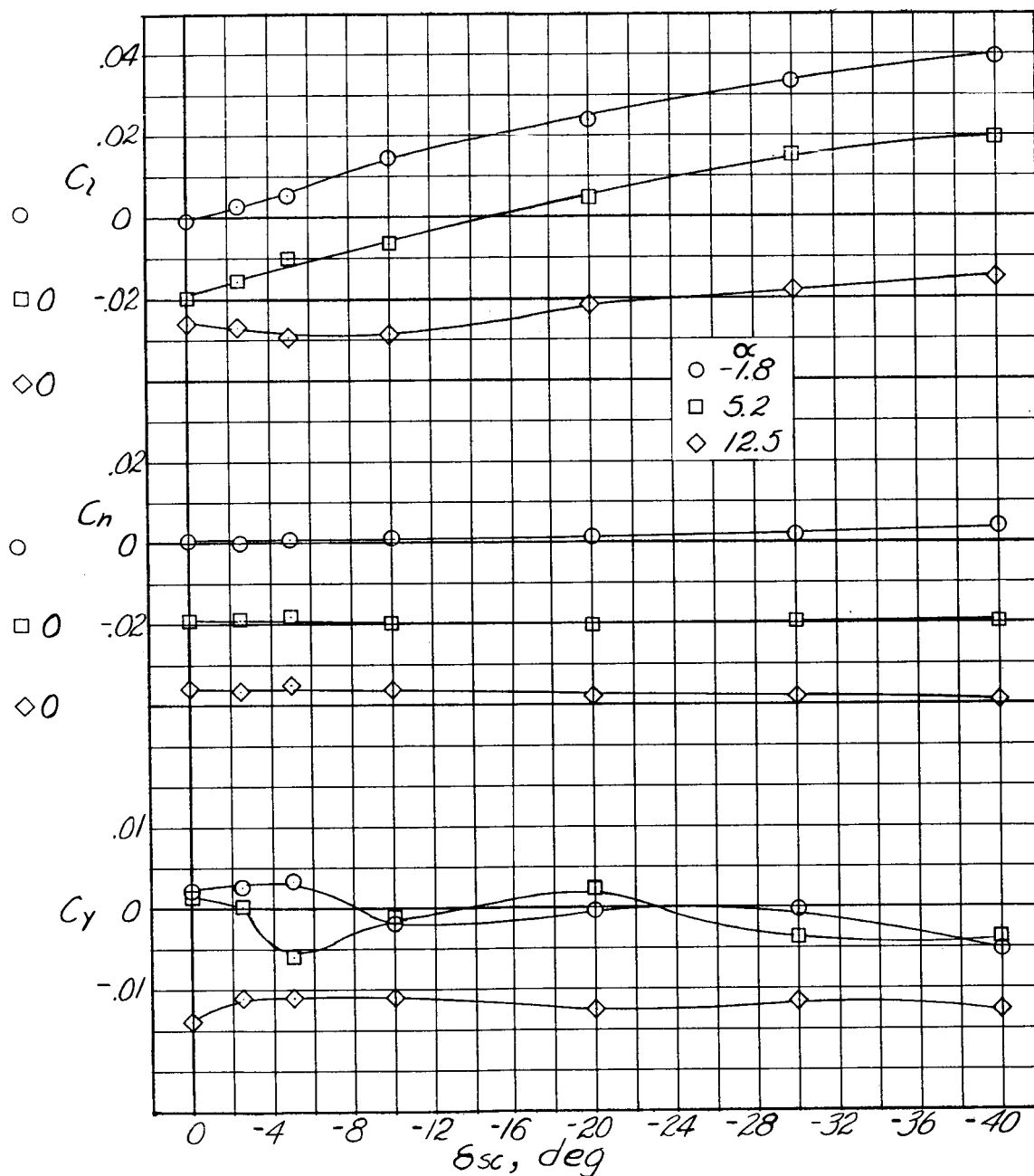
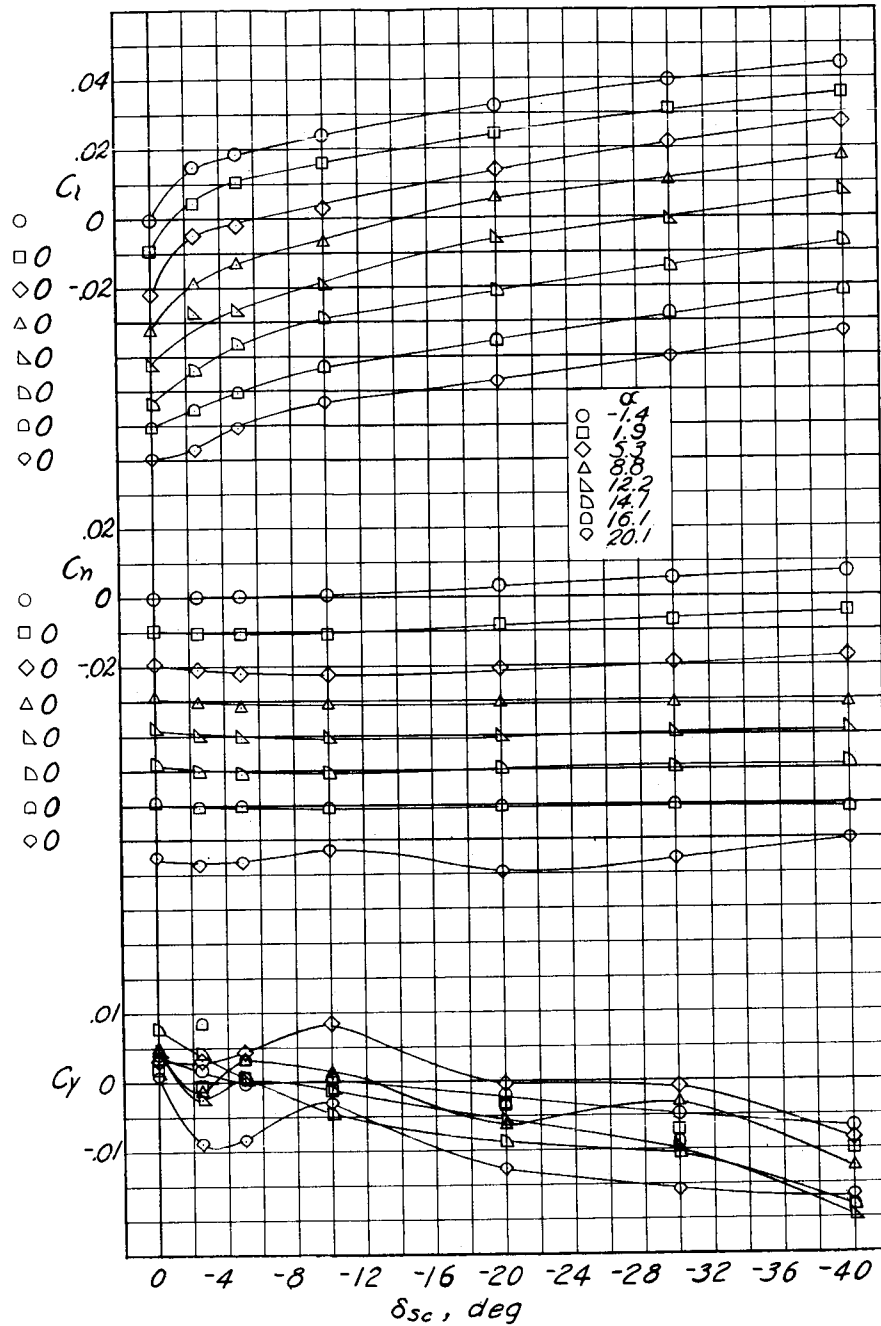
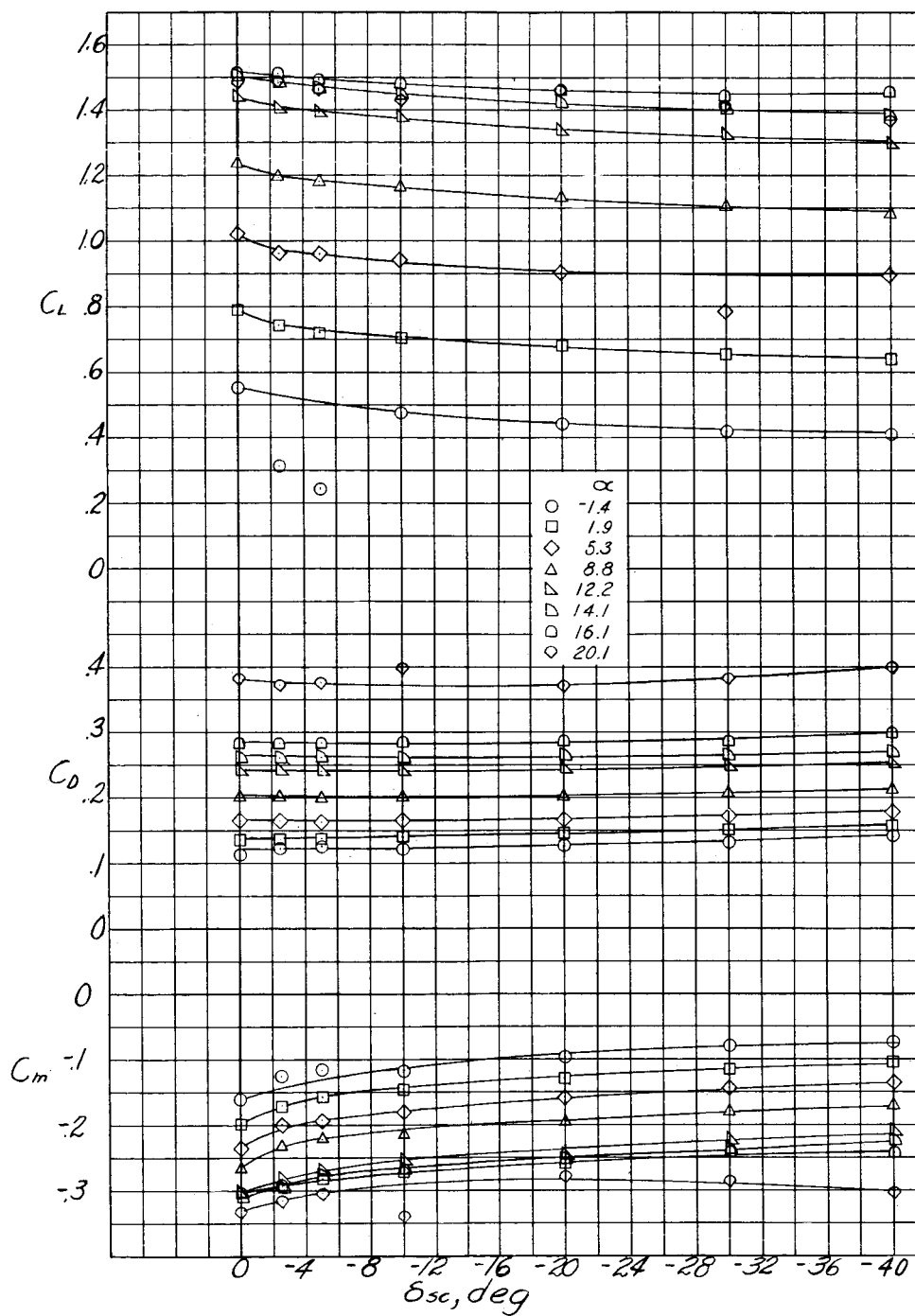


Figure 21.- Effect of spoiler-deflector deflection on the lateral characteristics with slats retracted. Spoiler with shroud; differential motion; modified aileron;  $\delta_f = 45^\circ$ ;  $\delta_a = 30^\circ$ .



(a) Lateral characteristics.

Figure 22.- Effect of spoiler-deflector deflection on the lateral and longitudinal characteristics.  $\delta_f = 45^\circ$ ;  $\delta_a = 30^\circ$ ; modified aileron; slats extended; mutual motion; shrouds on.



(b) Longitudinal characteristics.

Figure 22.- Concluded.

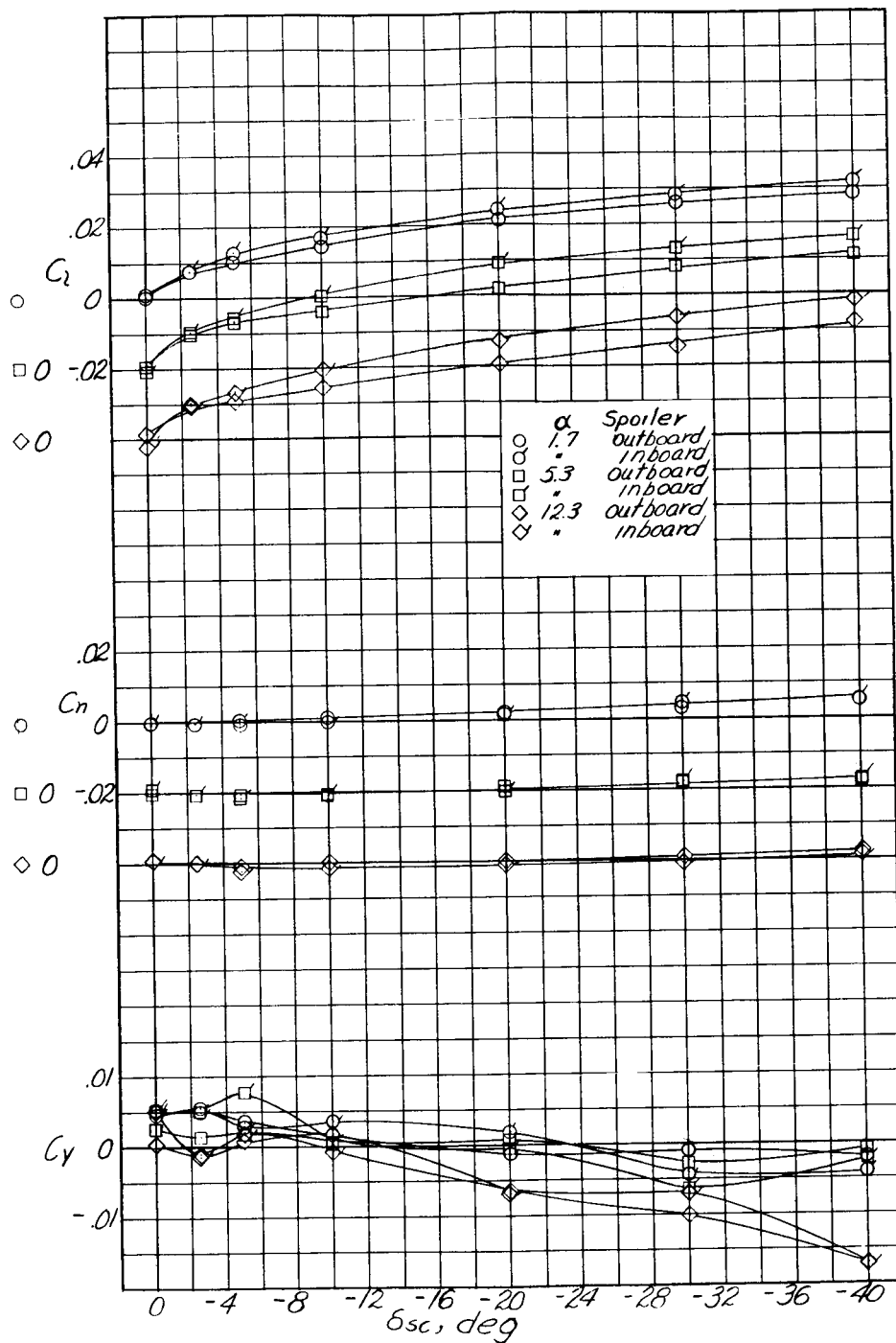


Figure 23.- Effect of spoiler-deflector deflection on the lateral characteristics at two spanwise spoiler-deflector locations. Spoiler with shroud; mutual motion;  $\delta_f = 45^\circ$ ;  $\delta_a = 30^\circ$ ; slats extended.

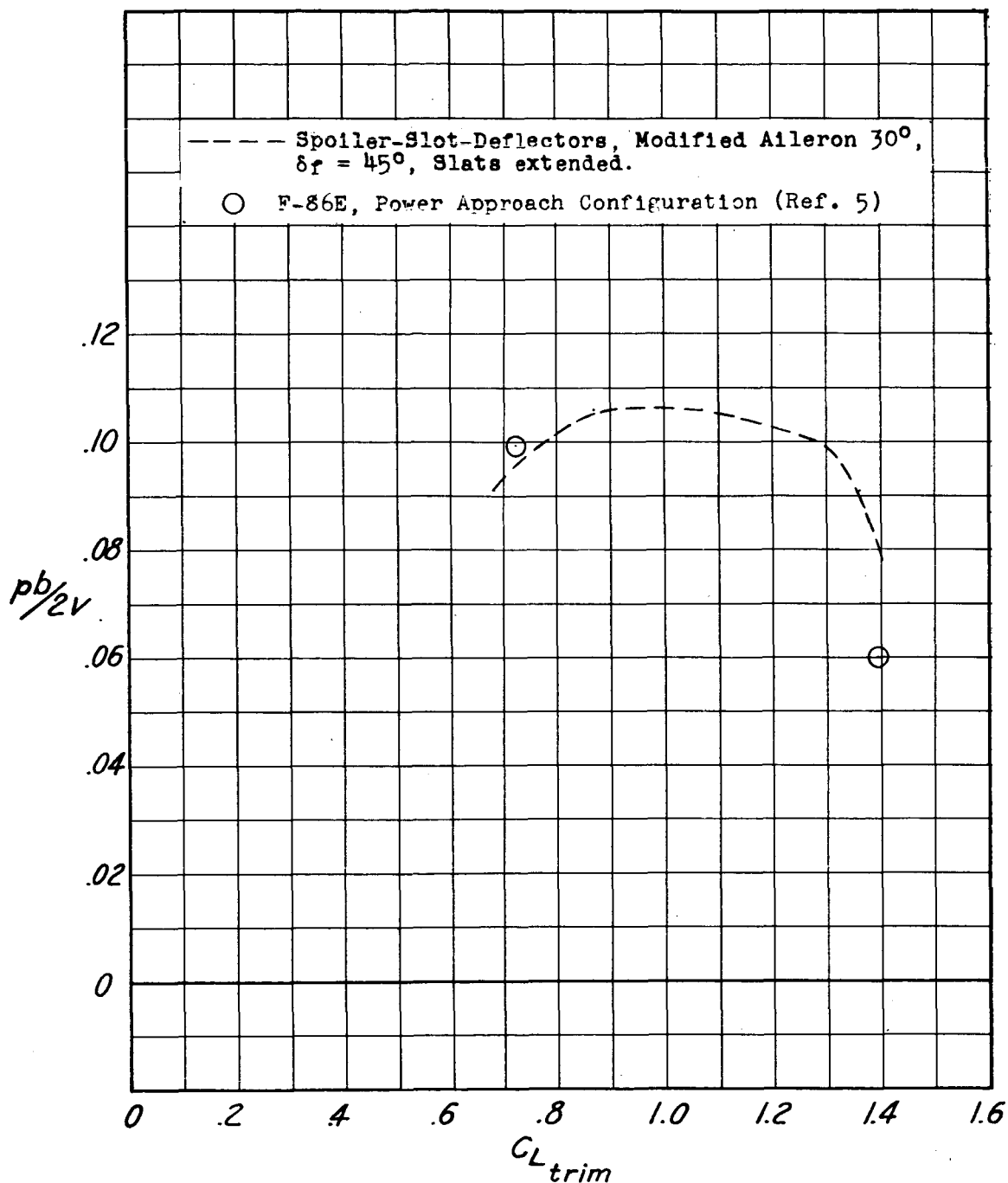
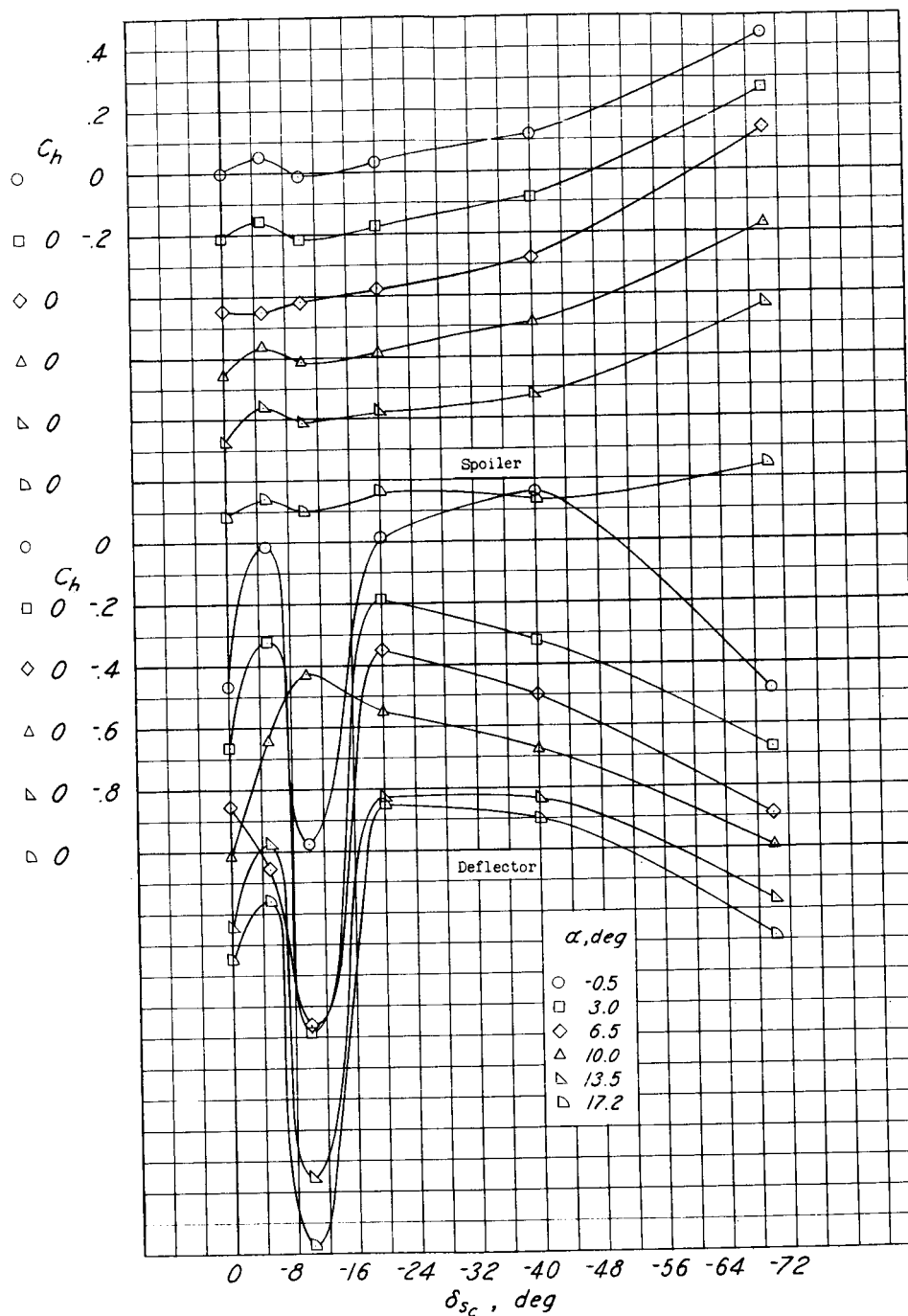


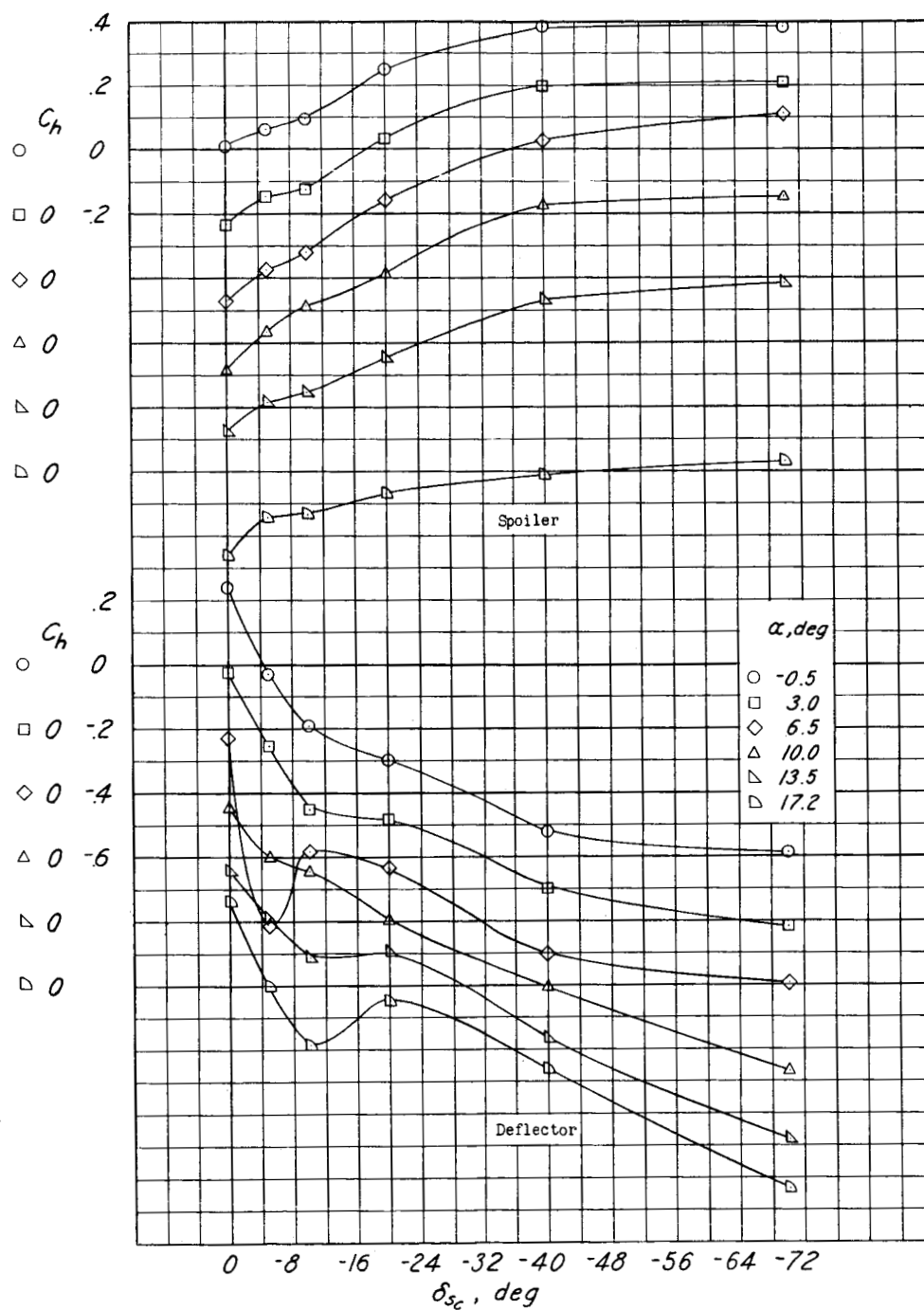
Figure 24.- Comparison of  $pb/2v$  values for the  $35^\circ$  swept-wing fighter airplane with spoiler-deflector combinations in differential motion with those for a similar airplane with conventional ailerons.





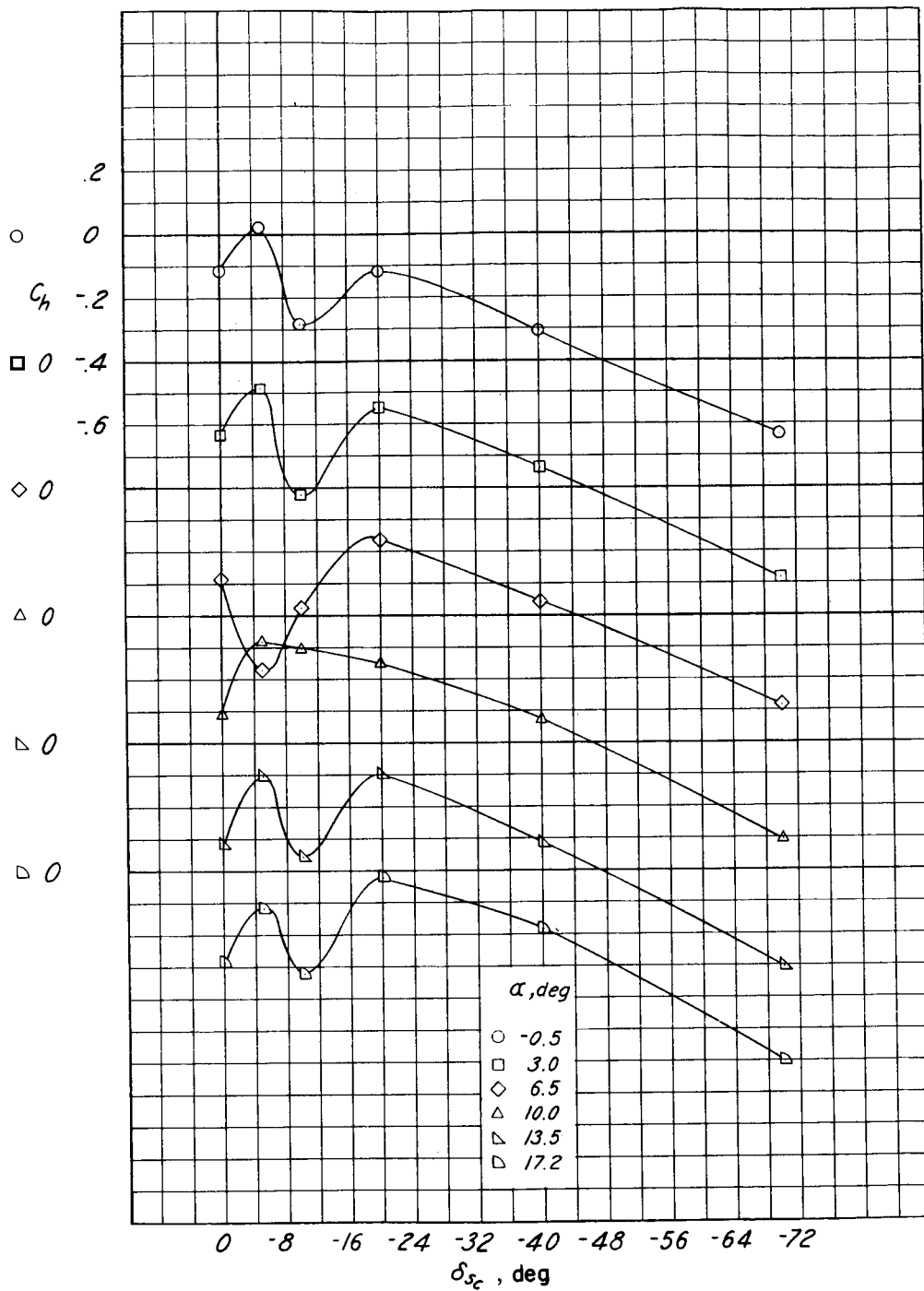
(a) Inboard spoiler and deflector.

Figure 25.- Hinge-moment characteristics of the spoilers and deflectors with the aileron neutral. Differential motion;  $\delta_f = 0^\circ$ ; slats retracted.



(b) Center spoiler and deflector.

Figure 25.- Continued.



(c) Outboard deflector.

Figure 25.- Concluded.

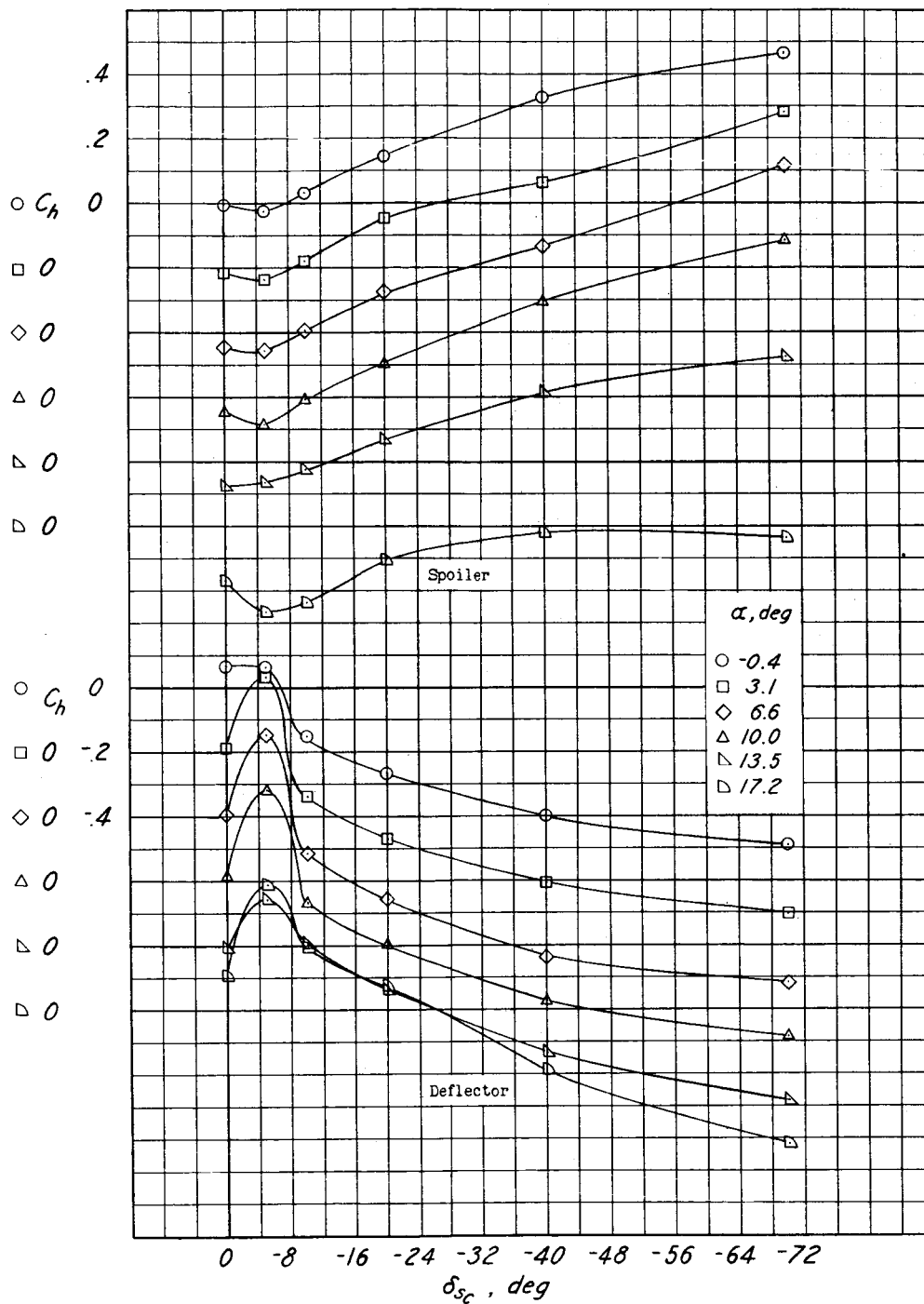


Figure 26.- Hinge-moment characteristics of the spoilers and deflectors with mutual motion.  $\delta_a = 0^\circ$ ;  $\delta_f = 0^\circ$ ; slats retracted.

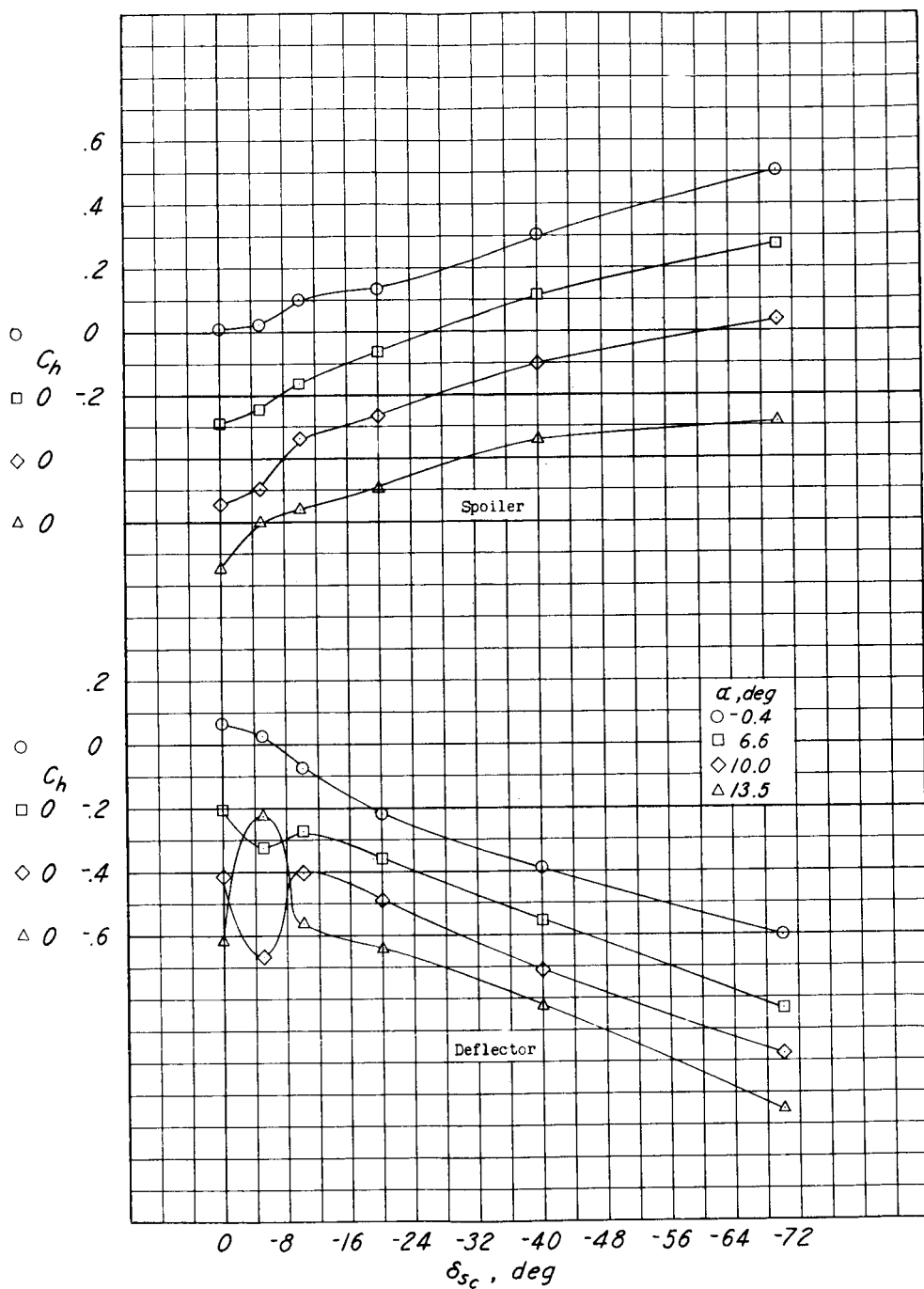
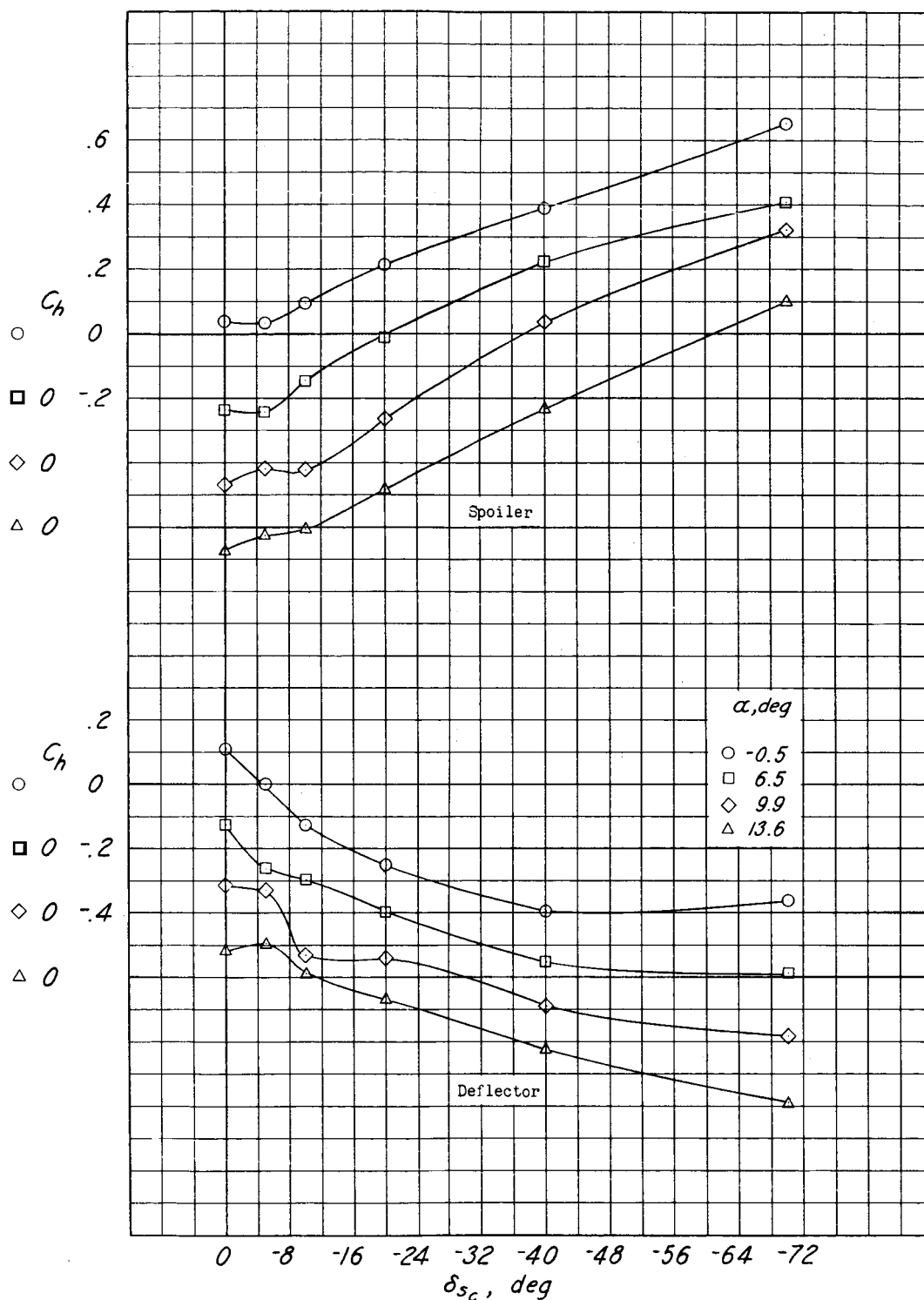
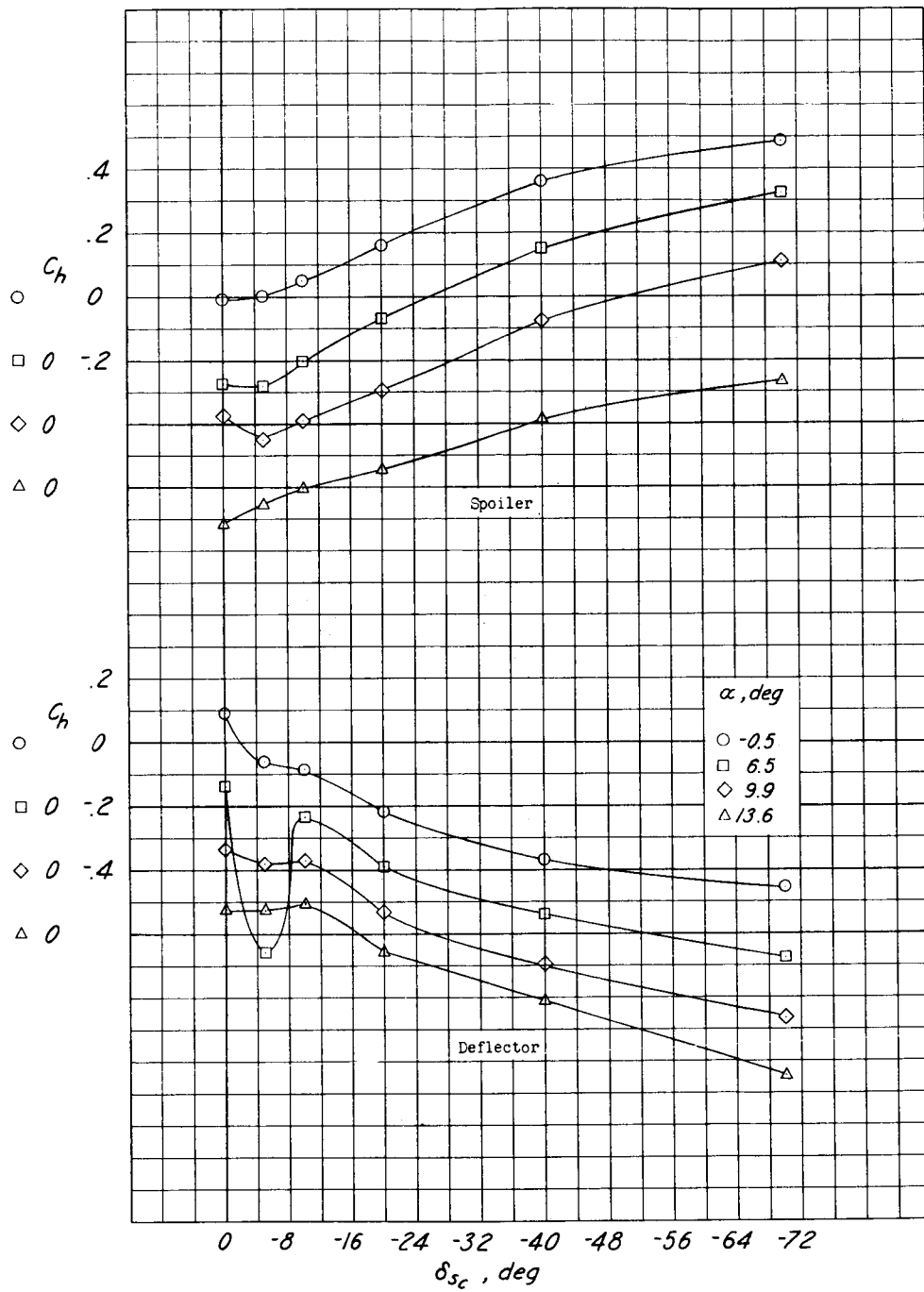


Figure 27.- Hinge-moment characteristics of the spoilers and deflectors with the spoiler hinge gaps sealed. Mutual motion;  $\delta_a = 0^\circ$ ;  $\delta_f = 0^\circ$ ; slats retracted.



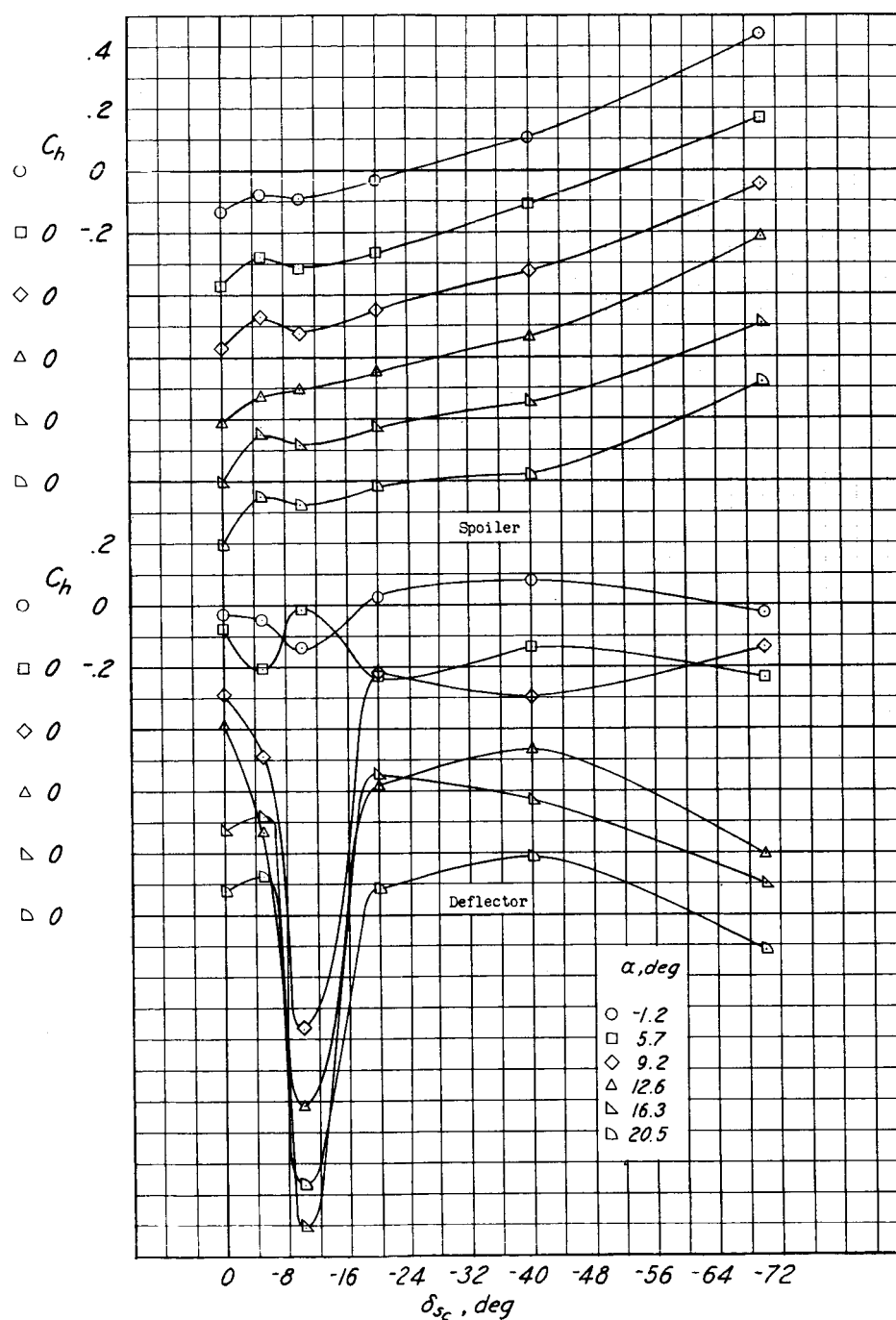
(a) Center and outboard spoilers and deflectors.

Figure 28.- Hinge-moment characteristics of partial-span spoilers and deflectors with mutual motion.  $\delta_a = 0^\circ$ ;  $\delta_f = 0^\circ$ ; slats retracted.



(b) Inboard and center spoilers and deflectors.

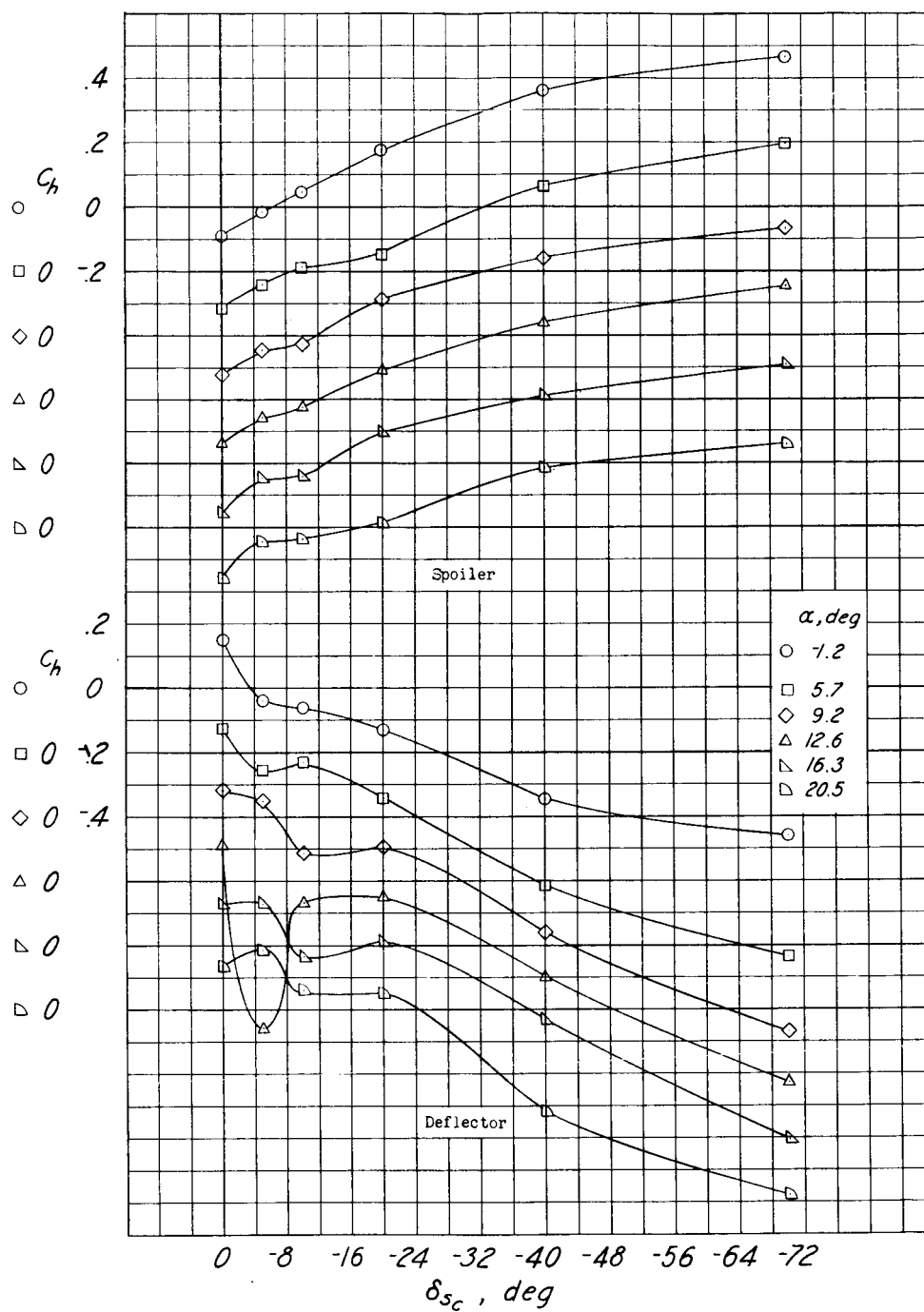
Figure 28.- Concluded.



(a) Inboard spoiler and deflector.

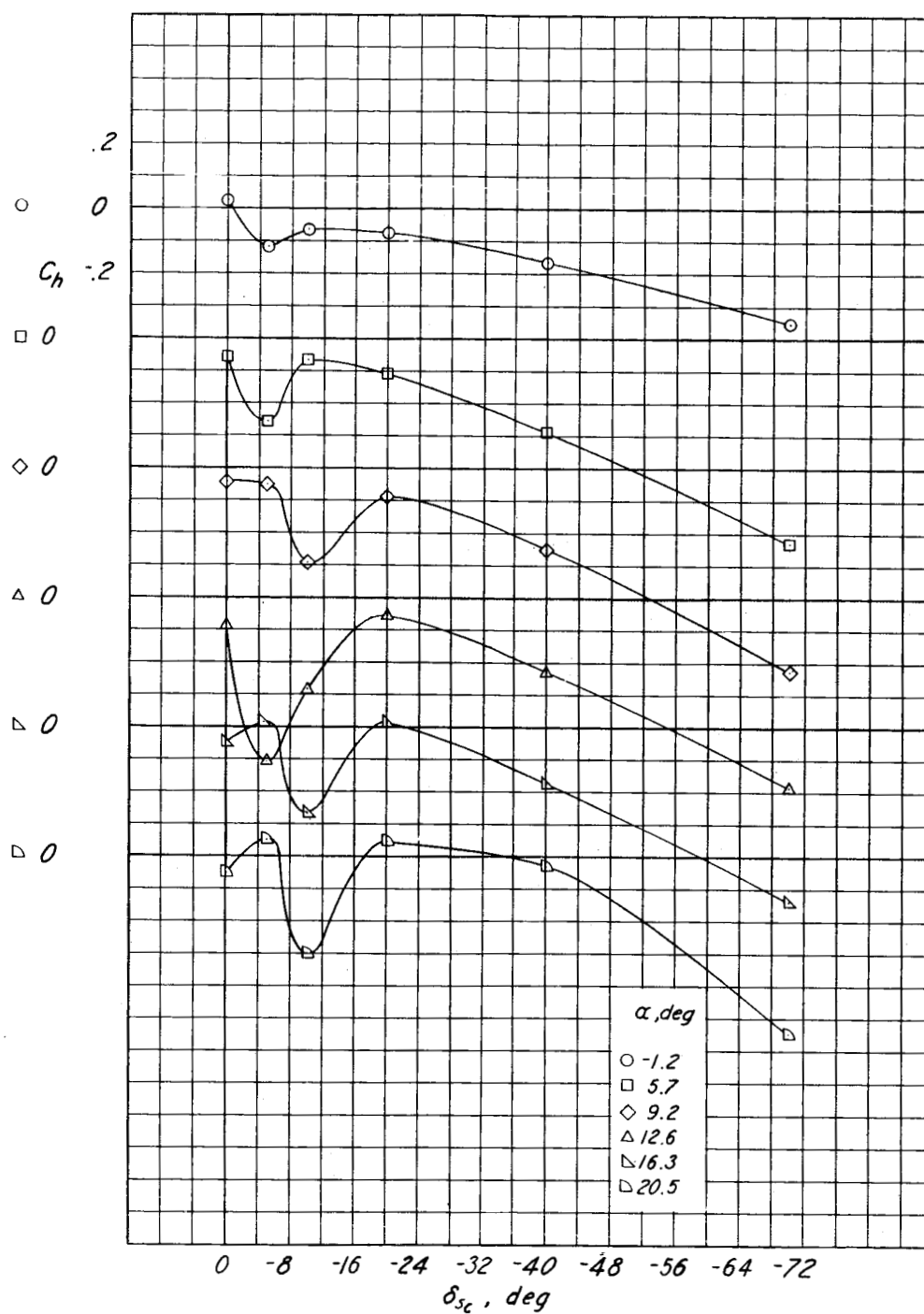
Figure 29.- Hinge-moment characteristics of the spoilers and deflectors with the aileron neutral. Differential motion;  $\delta_f = 45^\circ$ ; slats extended.





(b) Center spoiler and deflector.

Figure 29.- Continued.



(c) Outboard deflector.

Figure 29.- Concluded.

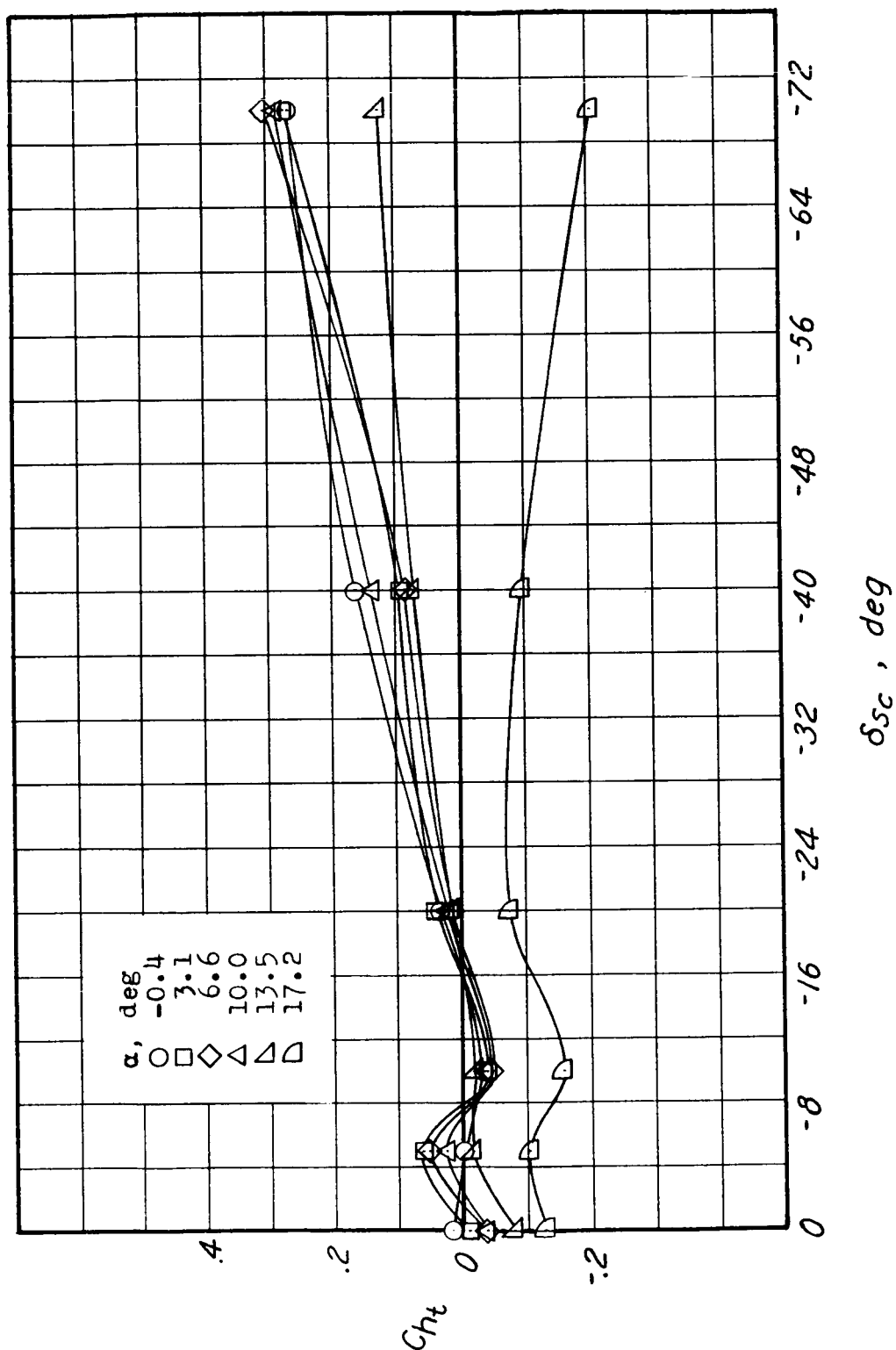
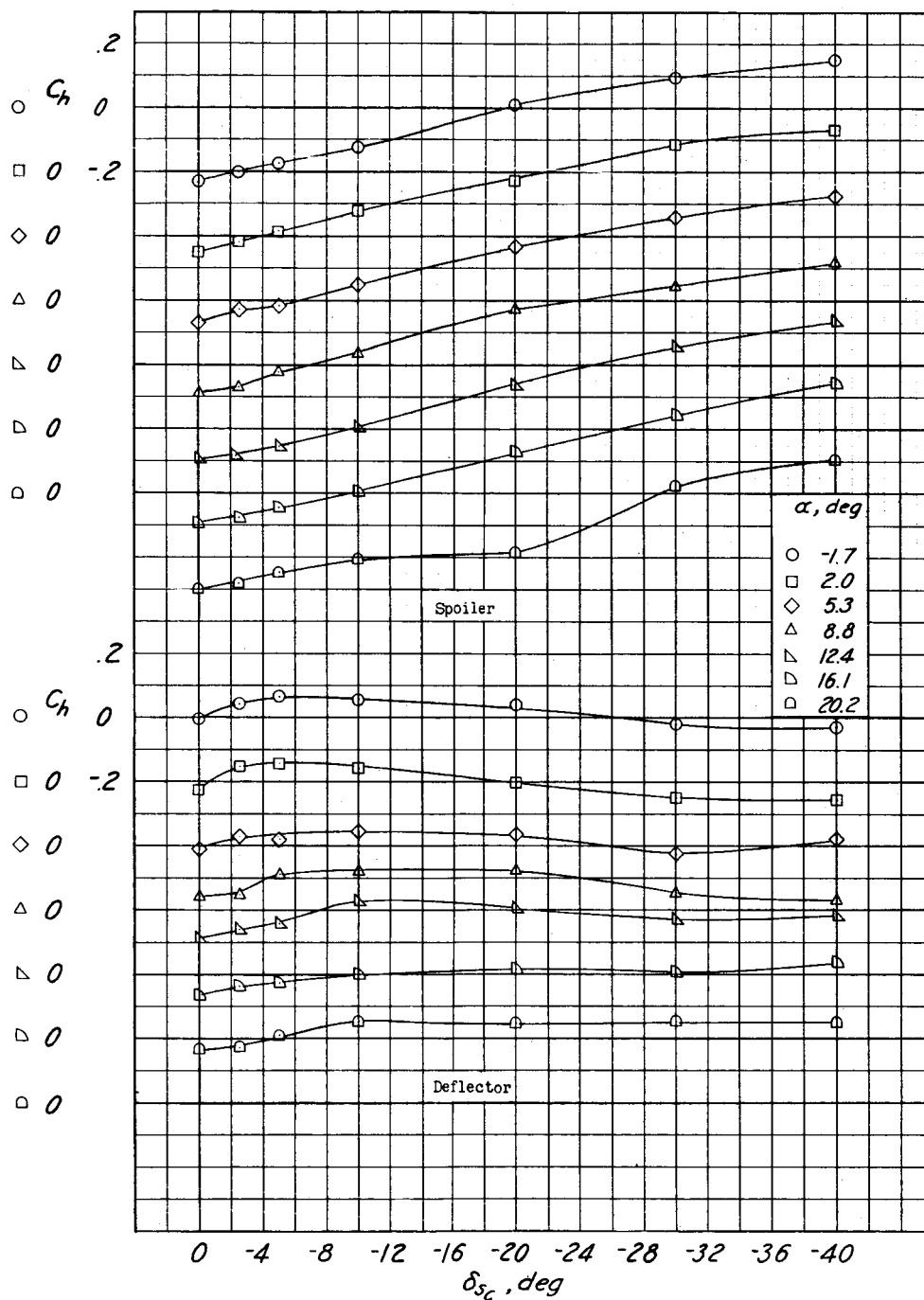
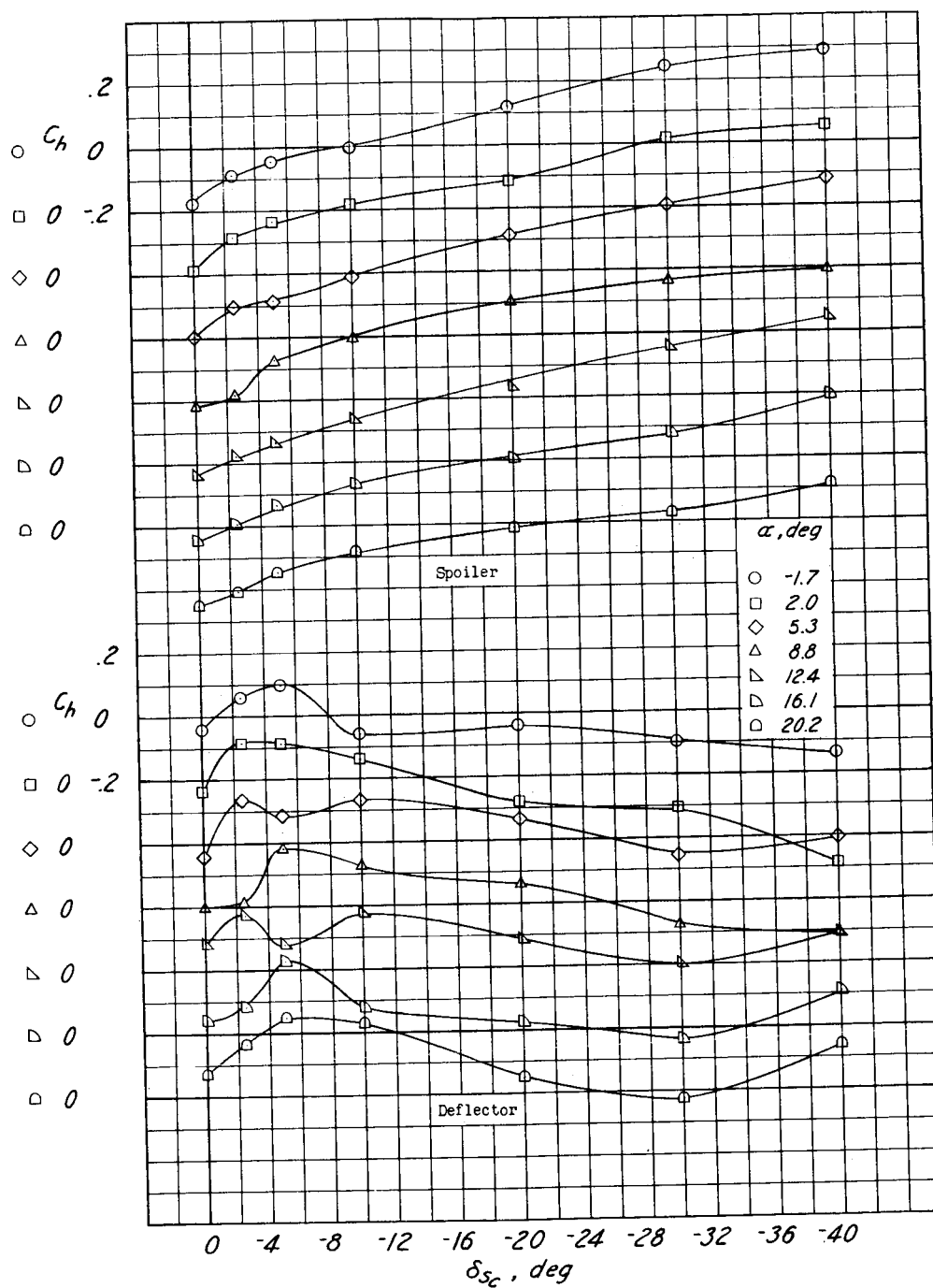


Figure 30.- Variation of total resultant hinge-moment coefficient with center spoiler deflection. Mutual motion;  $\delta_f = 0^\circ$ ;  $\delta_a = 0^\circ$ ; slats retracted.



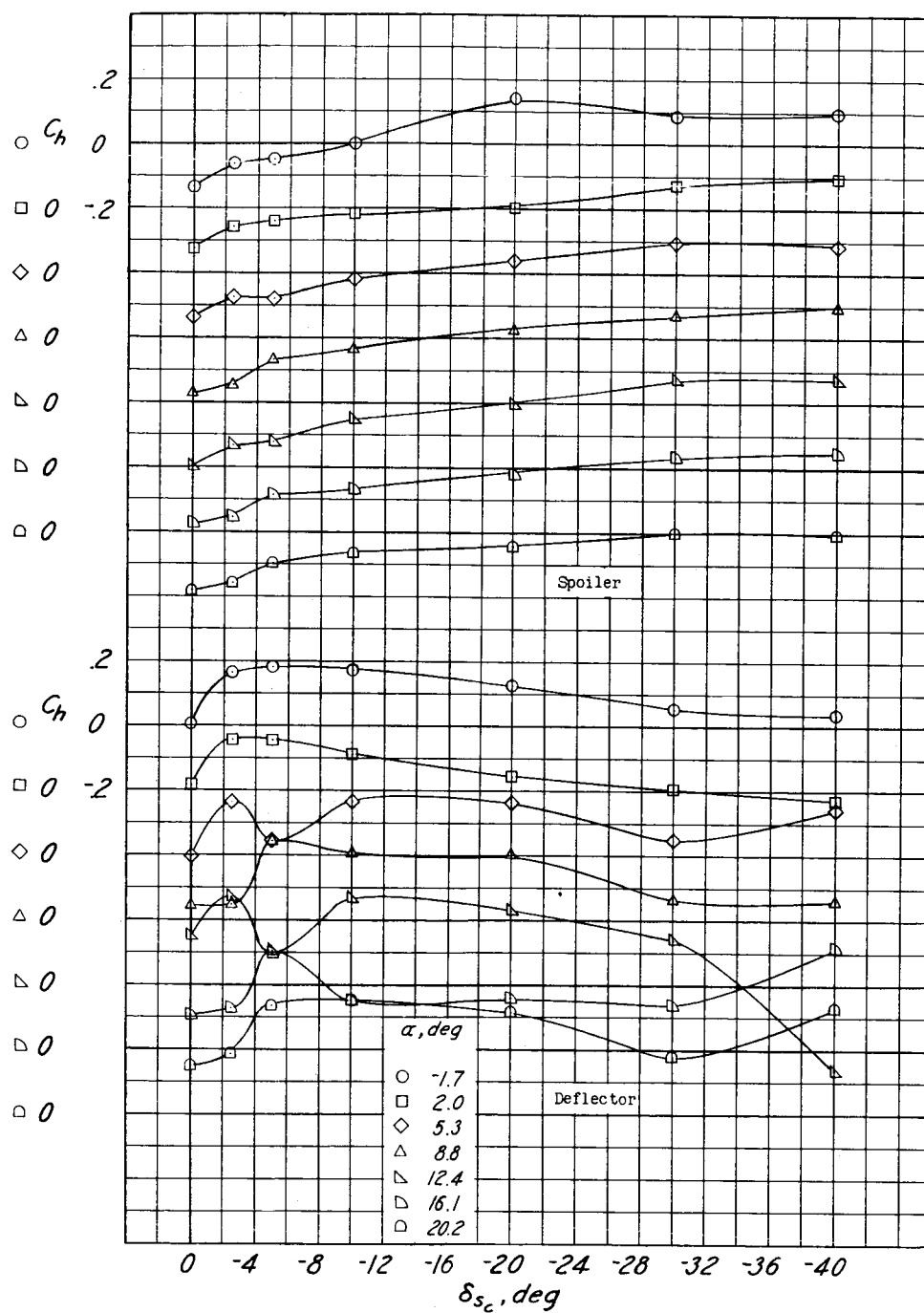
(a) Inboard spoiler and deflector.

Figure 31.- Hinge-moment characteristics of the spoilers and deflectors with differential motion.  $\delta_a = 45^\circ$ ;  $\delta_f = 45^\circ$ ; slats extended.



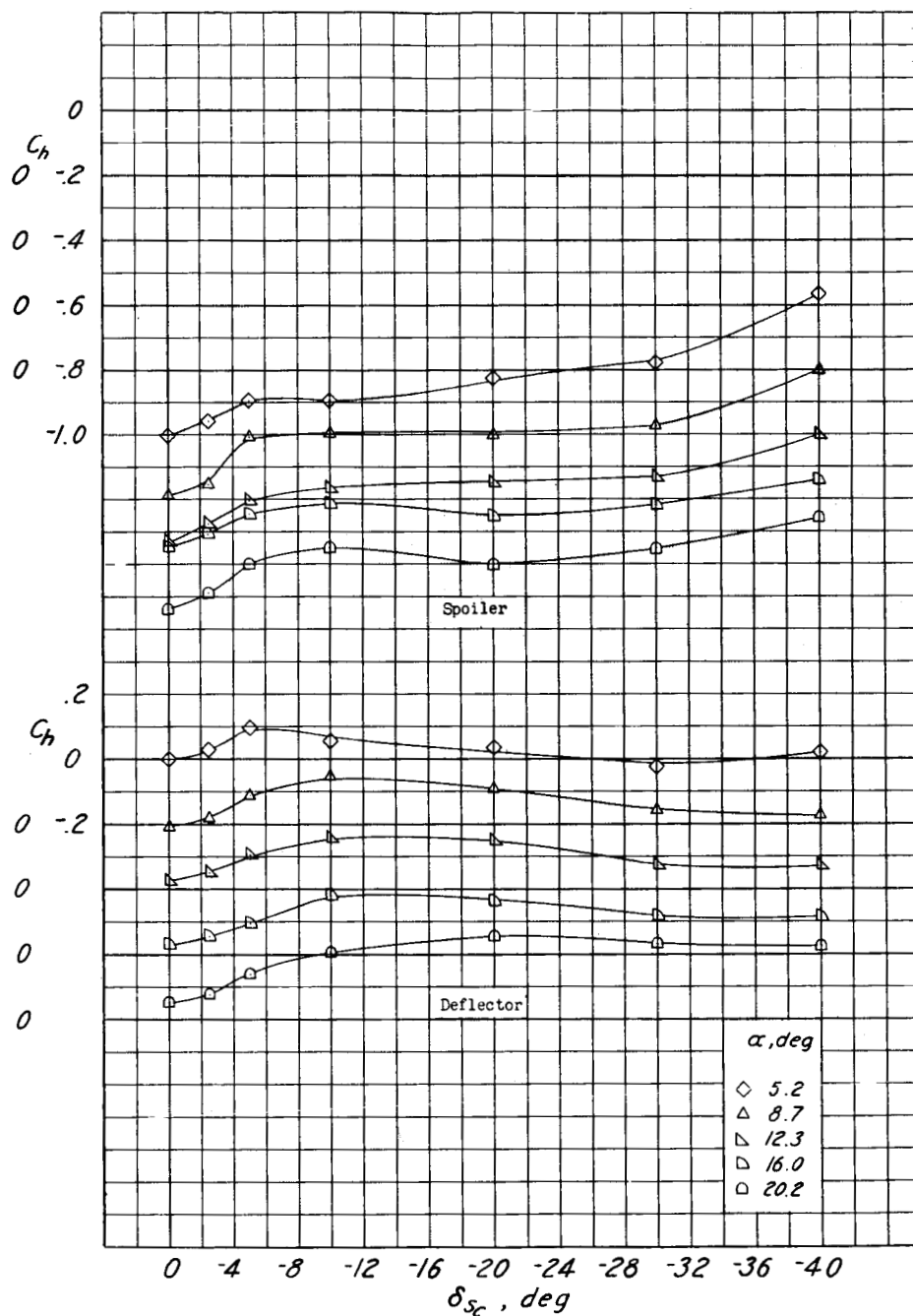
(b) Center spoiler and deflector.

Figure 31.- Continued.



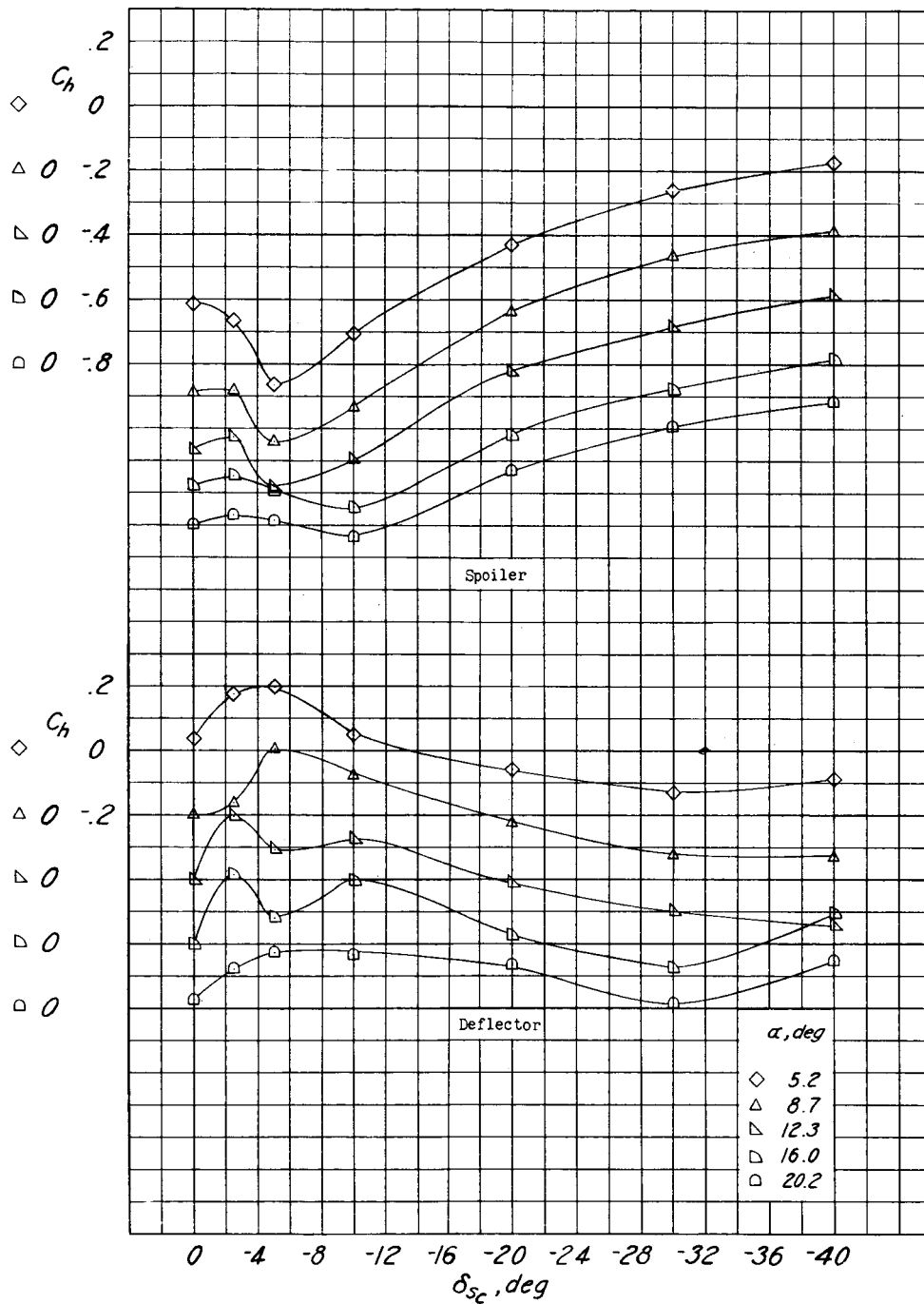
(c) Outboard spoiler and deflector.

Figure 31.- Concluded.



(a) Inboard spoiler and deflector.

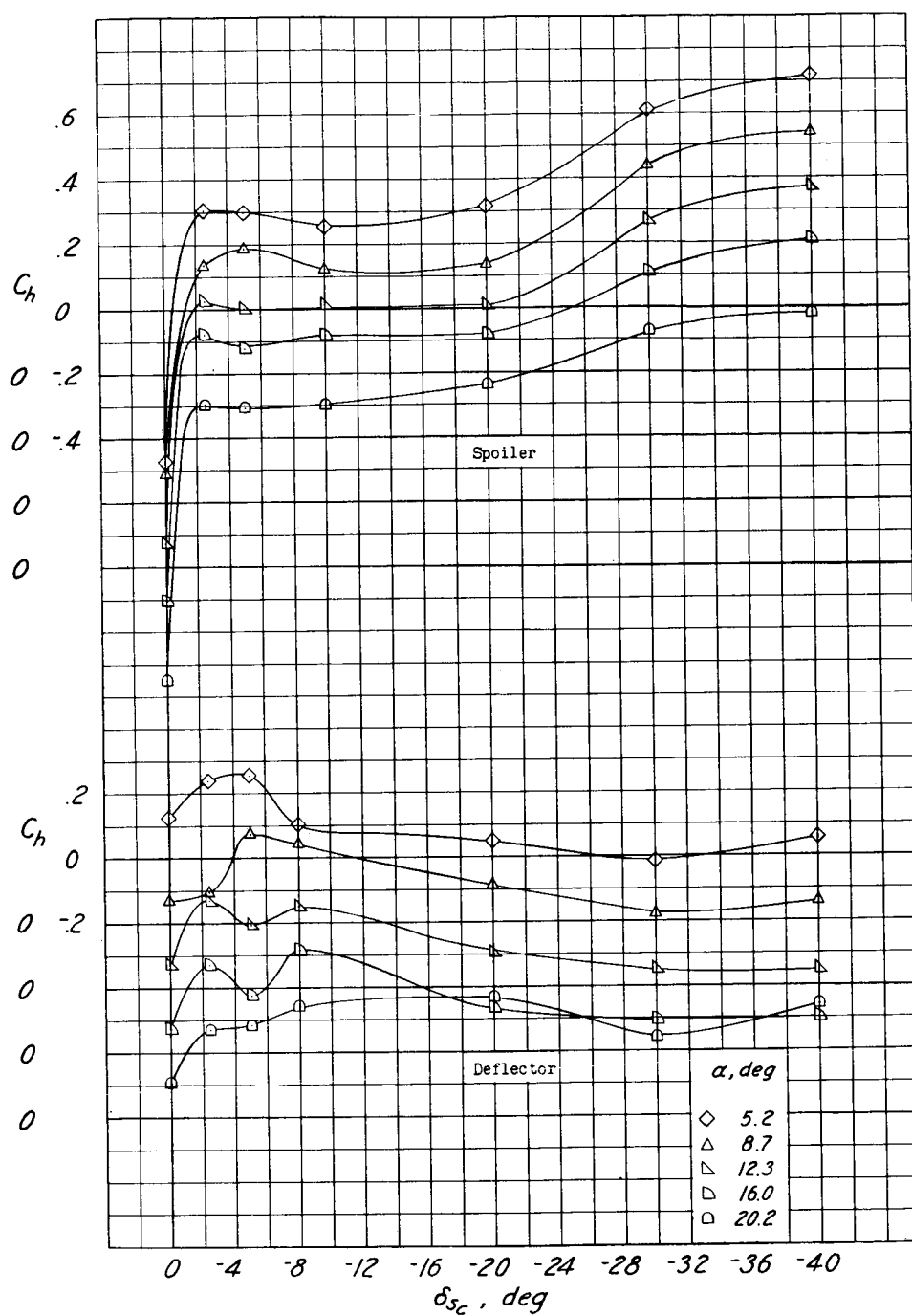
Figure 32.- Effect of shrouds on the hinge-moment characteristics of the spoilers and deflectors with differential motion. Original shrouds with constant 5/8-inch gap.  $\delta_a = 45^\circ$ ;  $\delta_f = 45^\circ$ ; slats extended.



(b) Center spoiler and deflector.

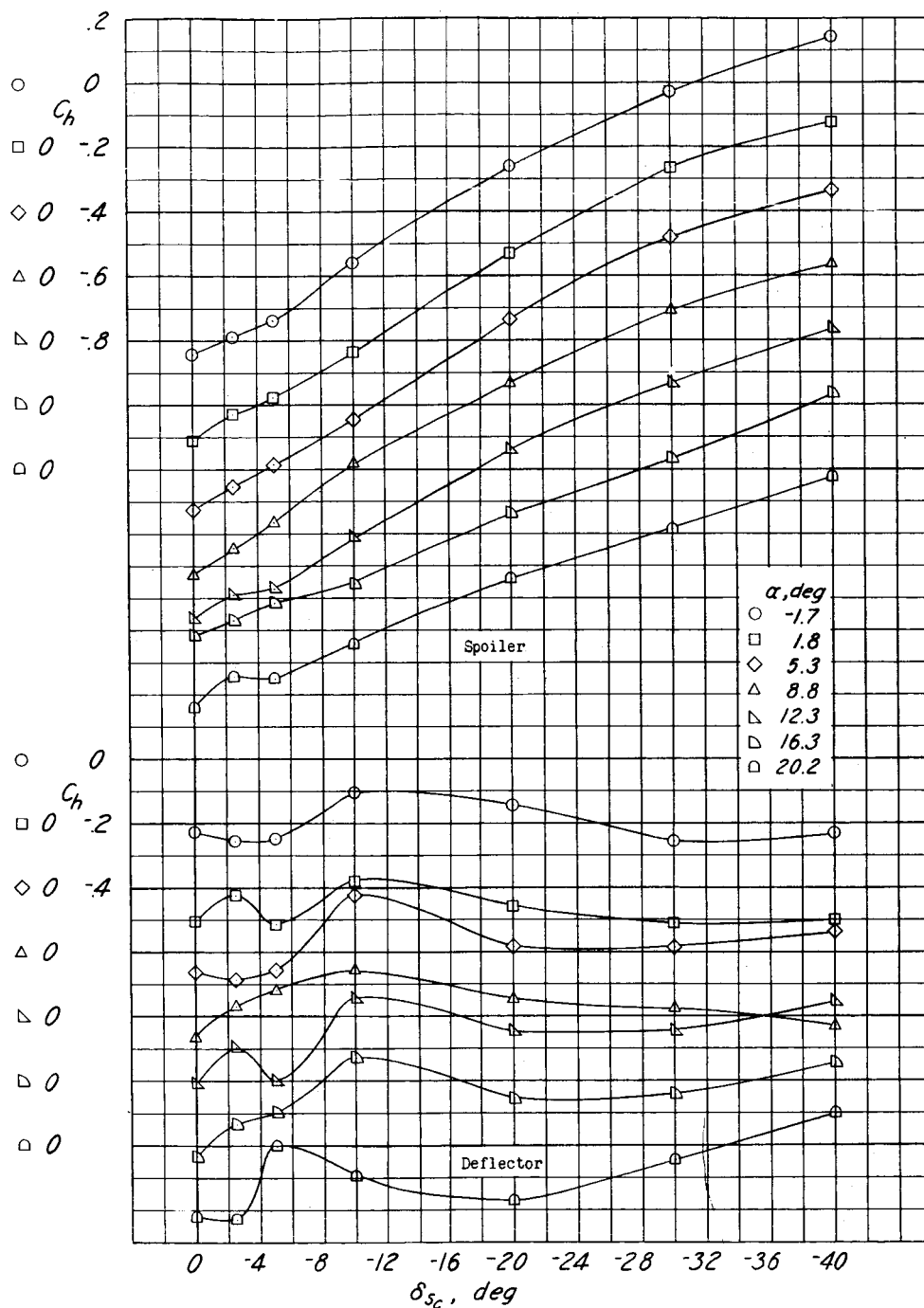
Figure 32.- Continued.





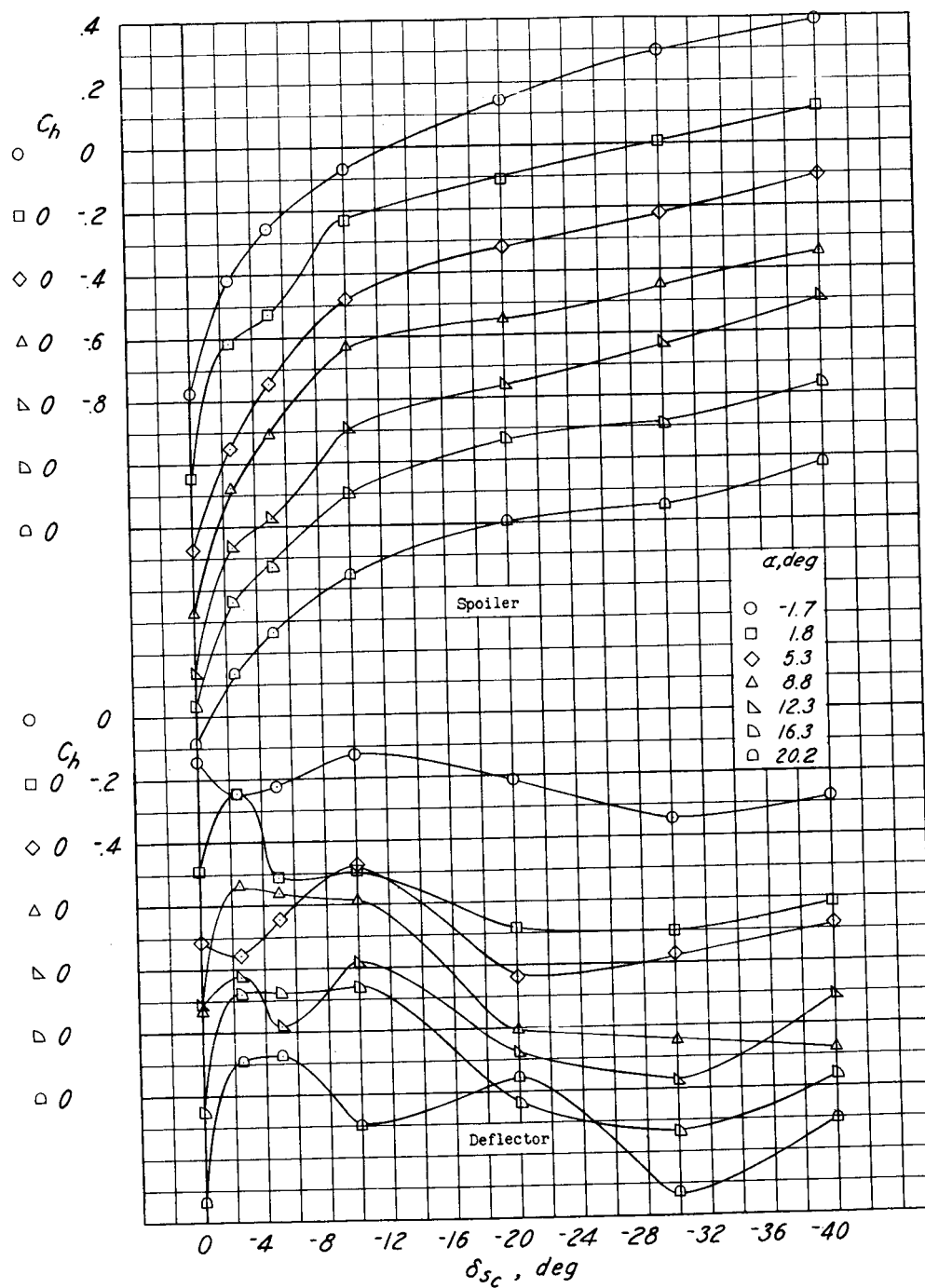
(c) Outboard spoiler and deflector.

Figure 32.- Concluded.



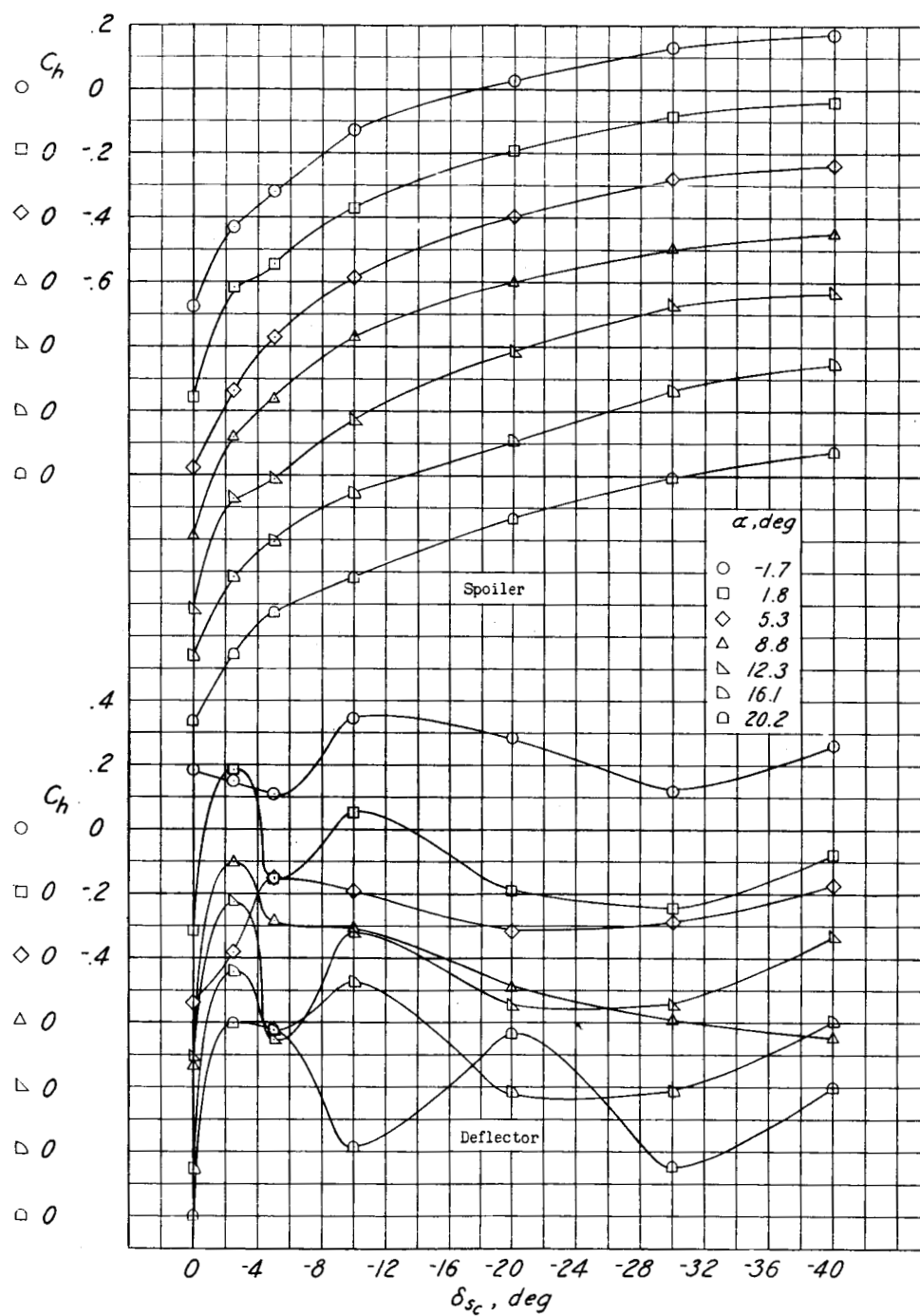
(a) Inboard spoiler and deflector.

Figure 33.- Hinge-moment characteristics of the spoilers and deflectors with original shrouds and with modified aileron contour.  $\delta_a = 30^\circ$ ;  $\delta_f = 45^\circ$ ; slats extended.



(b) Center spoiler and deflector.

Figure 33.- Continued.



(c) Outboard spoiler and deflector.

Figure 33.- Concluded.

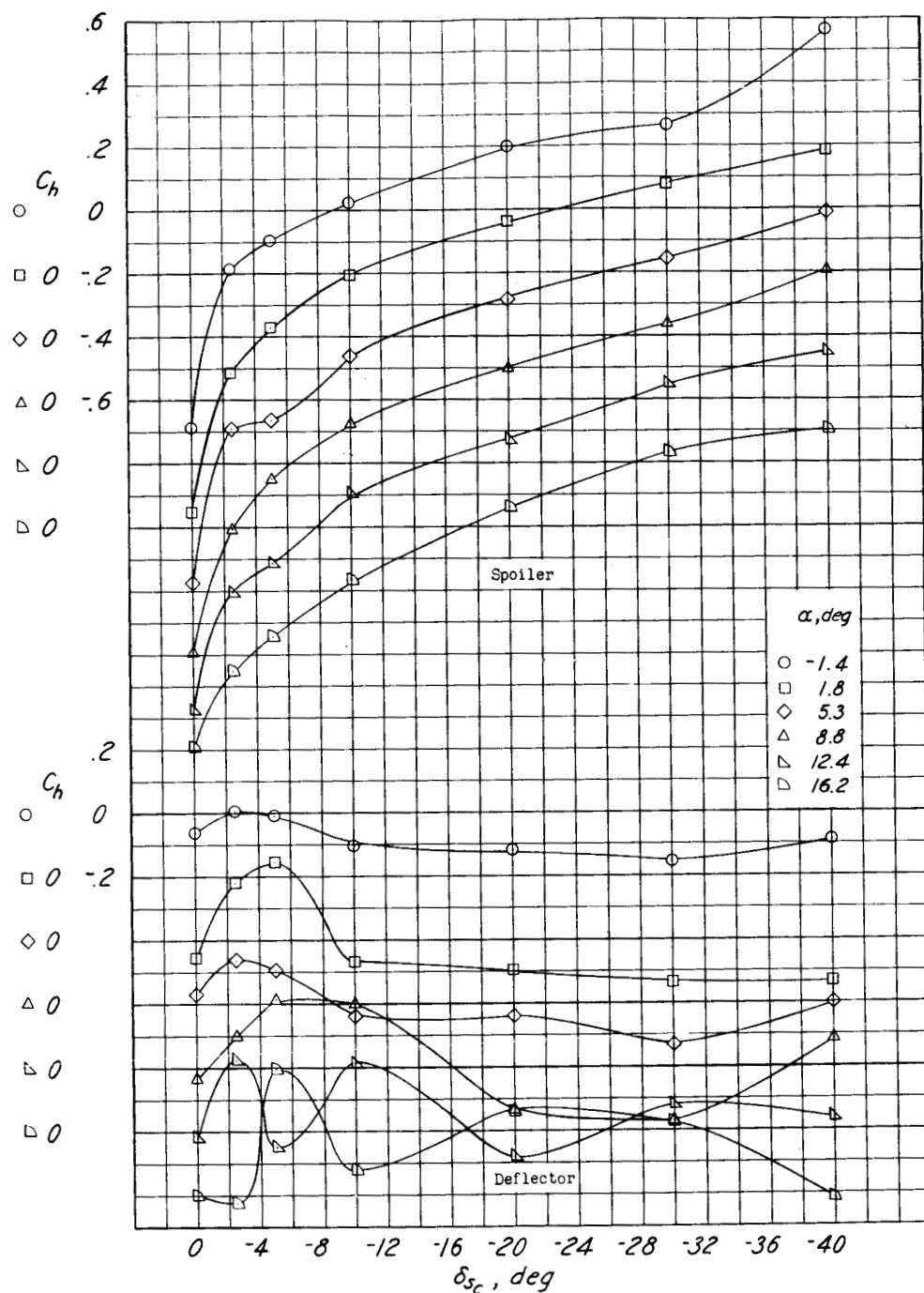


Figure 34.- Hinge-moment characteristics of the spoilers and deflectors with original shrouds and with mutual motion. Modified aileron contour;  $\delta_a = 30^\circ$ ;  $\delta_f = 45^\circ$ ; slats extended.

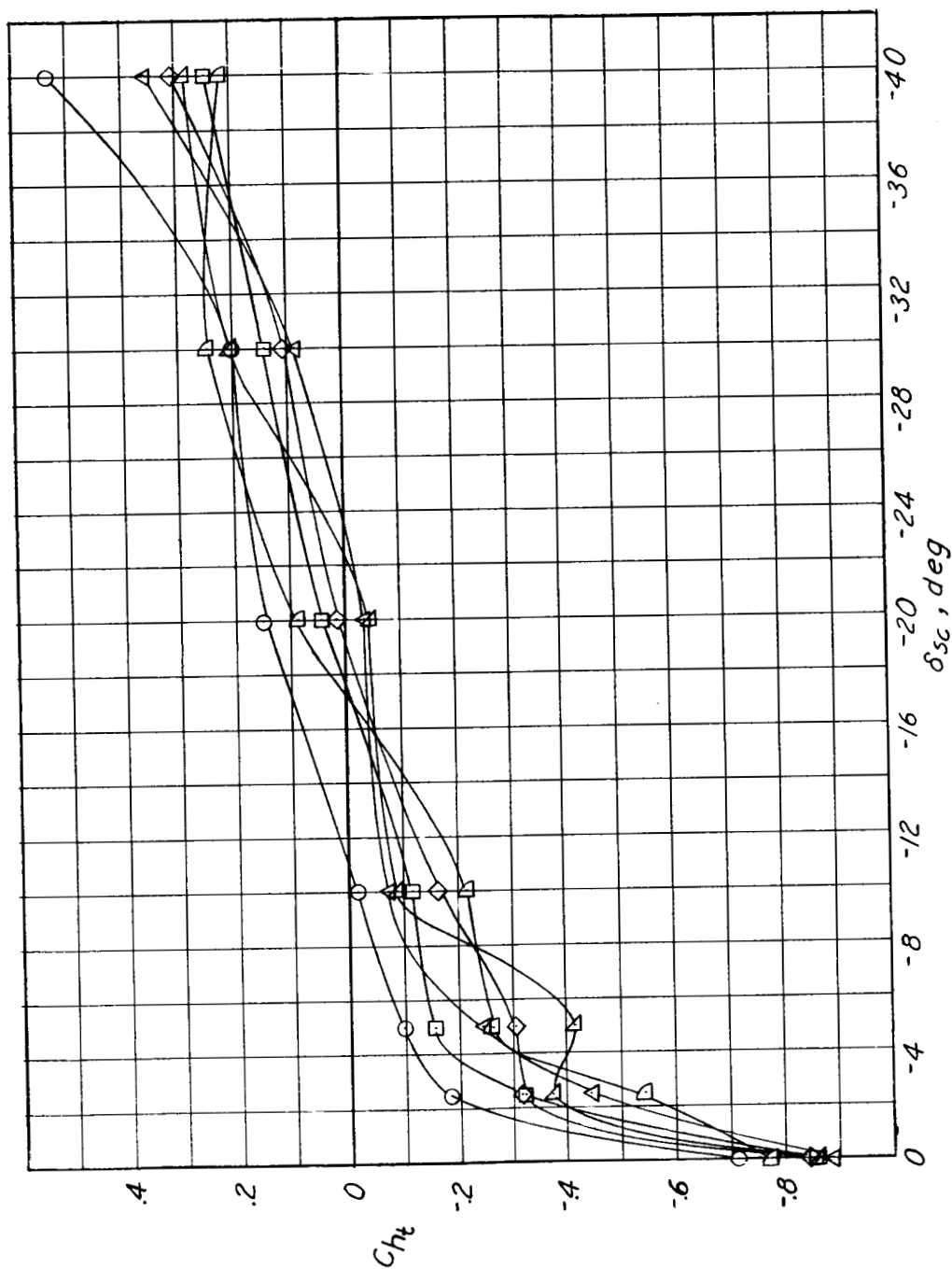


Figure 35.- Variation of total resultant hinge-moment coefficient with center spoiler deflection.  $30^\circ$  modified ailerons;  $\delta_f = 45^\circ$ ; slats extended.